AD-760 561

Holographic Optical Elements

Harris Electro-Optics Center of Radiation

prepared for

Air Force Avionics Laboratory

JANUARY 1973

Distributed By:

NTIS

National Technical Information Service
U. S. DEPARTMENT OF COMMERCE

AFAL-TR-72-409

HOLOGRAPHIC OPTICAL ELEMENTS

W. S. Colburn
R. G. Zech
L. M. Ralston

Harris Electro-Optics Center of Radiation

TECHNICAL REPORT AFAL-TR-72-409

January 1973

Approved for public release;
distribution unlimited.

Air Force Avionics Laboratory
Air Force Systems Command
Wright-Patterson Air Force Base, Ohio

NOTICE

When Government drawings, specifications, or other data are used for any purpose other than in connection with a definitely related Government procurement operation, the United States Government thereby incurs no responsibility nor any obligation whatsoever; and the fact that the government may have formulated, furnished, or in any way supplied the said drawings, specifications, or other data, is not to be regarded by implication or otherwise as in any manner licensing the holder or any other person or corporation, or conveying any rights or permission to manufacture, use, or sell any patented invention that may in any way be related thereto.

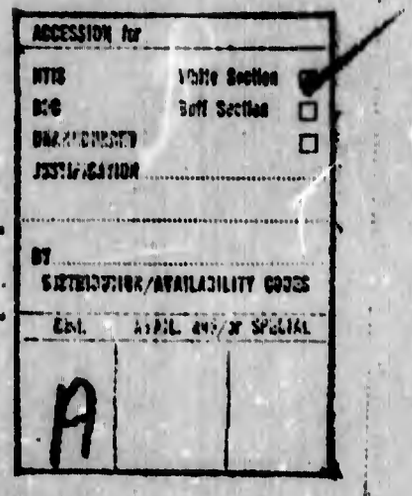

Copies of this report should not be returned unless return is required by security considerations, contractual obligations, or notice on a specific document.

Unclassified
Security Classification

DOCUMENT CONTROL DATA - R & D

(Security classification of title, body of abstract and indexing annotation must be entered when the overall report is classified)

1 ORIGINATING ACTIVITY (Corporate author)
Harris Electro-Optics Center of Radiation
P.O Box 1084
Ann Arbor, Mich. 48106

2a. REPORT SECURITY CLASSIFICATION
Unclassified

2b. GROUP
N/A

3 REPORT TITLE
HOLOGRAPHIC OPTICAL ELEMENTS

4 DESCRIPTIVE NOTES (Type of report and inclusive dates)
Final, 17 January - 17 October 1972

5 AUTHOR(S) (First name, middle initial, last name)
W. S. Colburn Lynda M. Ralston
Richard G. Zech

6 REPORT DATE
January 1972

7a. TOTAL NO. OF PAGES
~~155~~ 168

7b. NO. OF REFS
32

8a. CONTRACT OR GRANT NO
F33615-72-C-1156

b. PROJECT NO
6102-05-18

c.

d.

9a. ORIGINATOR'S REPORT NUMBER(S)
N/A

9b. OTHER REPORT NO(S) (Any other numbers that may be assigned this report)
AFAL-TR-72-409

10 DISTRIBUTION STATEMENT
Distribution of this document is unlimited

11 SUPPLEMENTARY NOTES
N/A

12 SPONSORING MILITARY ACTIVITY
Air Force Avionics Laboratory (AFAL)
Wright-Patterson AFB, Ohio

13 ABSTRACT

The significance of this research and development to the Air Force is the evaluation and characterization of possible recording materials for holographic optical elements. Seven recording materials were evaluated for use as holographic optical elements through measurement of holographic sensitometric and readout parameters and investigation of their environmental stability. The seven materials included four volume phase materials, bleached photographic emulsions, dichromated gelatin, photopolymer, and thick thermoplastics; and three thin phase materials, photoresist, iron oxide, and photoplastics. The holographic response of each material was characterized through measurements of exposure sensitivity, diffraction efficiency, signal-to-noise ratio, frequency response, and spectral variation of readout efficiency. Environmental stability was determined by monitoring the holographic parameters over a wide temperature and humidity range, under prolonged UV exposure, and by measuring the nondestructive readout intensity range. Although each material had certain outstanding characteristics, none was outstanding in all respects. Probably the most suitable material is dichromated gelatin, because of its high diffraction efficiency and signal-to-noise ratio, its moderate exposure sensitivity, and with a cover plate, its good environmental stability.

DD FORM 1 NOV 65 1473

Unclassified
Security Classification

14 KEY WORDS	LINK A		LINK B		LINK C	
	ROLE	WT	ROLE	WT	ROLE	WT
Holography						
Holographic materials						
Optical Materials						

HOLOGRAPHIC OPTICAL ELEMENTS

W. S. Colburn
R. G. Zech
L. M. Ralston

i-b

FOREWORD

This report was prepared by the Harris Electro-Optics Center of Radiation, Ann Arbor, Michigan, under Contract F33615-72-C-1156, Project Number 6102-05-18. This effort was monitored by Mr. Andrew Grandjean (AFAL/TEL). The work period covered in this report was January 1972 to October 1972.

The technical effort of the contract is directed by A. Kozma, General Manager, and A. Vander Lugt, Director of Research. The Program Manager initially was A. A. Friesem, succeeded by W. S. Colburn. Major contributors to this report are W. S. Colburn, R. G. Zech and L. M. Ralston. B. J. Chang and J. A. Losee assisted in the experimental work.

This report was submitted November 1972; it has been reviewed and is approved.

[illegible] Chief
[illegible] Br.
Electro[illegible] Div.

ABSTRACT

The significance of this research and development to the Air Force is the evaluation and characterization of possible recording materials for holographic optical elements. Seven recording materials were evaluated for use as holographic optical elements through measurement of holographic sensitometric and readout parameters and investigation of their environmental stability. The seven materials included four volume phase materials; bleached photographic emulsions, dichromated gelatin, photopolymer, and thick thermoplastics; and three thin phase materials; photoresist, iron oxide, and photoplastics. The holographic response of each material was characterized through measurements of exposure sensitivity, diffraction efficiency, signal-to-noise ratio, frequency response, and spectral variation of readout efficiency. Environmental stability was determined by monitoring the holographic parameters over a wide temperature and humidity range, under prolonged UV exposure, and by measuring the nondestructive readout intensity range. Although each material had certain outstanding characteristics, none was outstanding in all respects. Probably the most suitable material is dichromated gelatin, because of its high diffraction efficiency and signal-to-noise ratio, its moderate exposure sensitivity, and with a cover plate, its good environmental stability. Only two materials, bleached photographic emulsions and photoplastics, were sensitive to red light; these two materials show potential for sensitization to the near infrared.

TABLE OF CONTENTS

Preceding page blank

LIST OF ILLUSTRATIONS

LIST OF TABLES

SECTION I

INTRODUCTION

Holography often provides a convenient and sometimes a unique means for the fabrication of conventional and unconventional optical elements. Well known examples are diffraction gratings and Fresnel zone plates. Holographic optical elements can be synthesized on arbitrary surfaces with accurate control over their imaging properties. Furthermore, holographic elements can be easily superimposed to permit relatively complicated optical systems to be concentrated in a small space, an obvious advantage over conventional optical systems.

The aberrations of holographic elements and techniques for controlling these aberrations have been extensively investigated.[1-6] The results of these investigations demonstrate that holographic elements may be useful for monochromatic and polychromatic image formation, Fourier transformation, and spectroscopic analysis. We can reduce the disperson and chromatic aberrations of holographic element systems by using overlapping holographic elements or several holographic elements in tandem or both. In all these techniques and applications the essential components of the holographic optical element is the recording material. Although holographic recording materials have also been extensively studied in the past, the emphasis has generally been on determining their usefulness in holographic memories, optical data processing systems, and so forth. Relatively little attention had been given to the study of recording materials that show potential for use in recording holographic optical elements. In this report, we describe the results of intensive investigations of seven candidate recording materials with potential for recording holographic optical elements. These investigations included measurements of both the holographic parameters and the environmental stability of each material.

The holographic parameters we measured included exposure sensitivity, signal-to-noise ratio, (spatial) frequency response, and spectral variation of readout efficiency and transmittance. We also studied the mechanism of hologram formation in each material and, where necessary, sought to improve the ability of each material to meet the following goals:

1. Diffraction efficiency greater than 60% for plane wave gratings.
2. Good signal-to-noise ratio, with less than 2% scatter of the incident light.
3. Wavelength sensitivity from visible through 1.1 μm.
4. Good optical quality, with acceptable distortion, uniformity, and flatness.
5. Good transmission from the visible through the near infrared.

We investigated the effects of temperature and humidity as well as exposure to UV radiation on each material. In particular we measured the performance of the materials under the following environmental conditions:

1. 20 to 90% relative humidity.
2. -40° to 140°F temperature range.
3. Exposure to direct solar illumination
4. Exposure to high intensity laser illumination.

In certain cases we investigated techniques to improve the resistance of materials to environmental degradation.

The seven recording materials we tested are phase materials. Four that record volume phase holograms are bleached photographic emulsions, dichromated gelatin, photopolymer, and thick thermoplastics. The remaining three, photoresist, iron oxide, and photoplastic, record thin phase holograms.

We obtained mixed results with the various materials; each material had certain advantages, but none was outstanding in all respects. Four materials, dichromated gelatin, photopolymer, thick thermoplastics, and blazed photoresist, recorded plane wave gratings with better than 60% diffraction efficiency. Most materials recorded holograms with excellent signal-to-noise ratio, and only bleached photographic emulsions (and perhaps photoplastics) were limited by light scattering. The spectral sensitivities of most of the materials was limited to the UV and blue regions of the spectrum, with only bleached photographic emulsions and photoplastic sensitive to red light. None of the materials was sensitive to near infrared radiation. All the materials had good optical quality, which in general was a function of the care taken in preparation. The transmission of the different materials varied, as we will show in detail.

Only one material, iron oxide, was completely unaffected by the environmental tests. Most of the materials were affected to some degree by the combination of high temperature and humidity. Dichromated gelatin holograms are so sensitive to humidity that they can be considered practical only with a protective overcoating that seals the gelatin layer. Subzero temperatures did not appear to affect the materials, but those materials sensitive to high humidity were harmed by frost that condensed on the hologram surface. Holograms in several of the materials, bleached photographic emulsions, photopolymer, and photoresist, were degraded by exposure to UV radiation. We found a range of nondestructive readout intensities for the various materials, with the highest intensities occurring for photoresist and dichromated gelatin holograms.

In the next section we describe the experimental procedure we used to measure the holographic parameters and environmental stability of candidate recording materials. In the following section, we outline the mechanism of hologram formation, describe the method of use, and present tabular and graphical data for each of the seven materials. Finally we summarize and compare the performance of the materials, and present an assessment of the potential of each material.

SECTION II

EXPERIMENTAL PROCEDURE

The major effort of work on this contract was the characterization of the holographic sensitometric and readout parameters and the investigation of the environmental integrity of each material. Some effort was concentrated on improving the holographic response of certain materials and in providing increased protection against degradation caused by environmental changes. In the paragraphs that follow, we describe the basic experimental procedure that was common to all of the materials.

2.1 Holographic Parameters

We measured exposure sensitivity, diffraction efficiency, signal-to-noise ratio, bandwidth, and spectral readout efficiency for each material. The basic experimental configuration is shown in Figure 1. We determined exposure sensitivity, diffraction efficiency, frequency response, and spectral readout efficiency from measurements made on simple plane wave gratings recorded in each material. These were recorded with the geometry shown in Figure 1 but with the signal removed. We recorded a series of plane wave gratings with varying exposures and reference-to-signal beam, or K ratios in each material. We then determined exposure sensitivity and diffraction efficiency from curves of diffraction efficiency plotted as a function of exposure. The frequency response was measured by recording a series of plane wave gratings with varying offset angles between the reference and signal beams. A curve of diffraction efficiency of the gratings plotted as a function of the spatial frequency of their interference patterns then gives the frequency response of the material. We measured the spectral readout variation by recording a plane wave grating at one wavelength, and measuring the diffraction efficiency at various

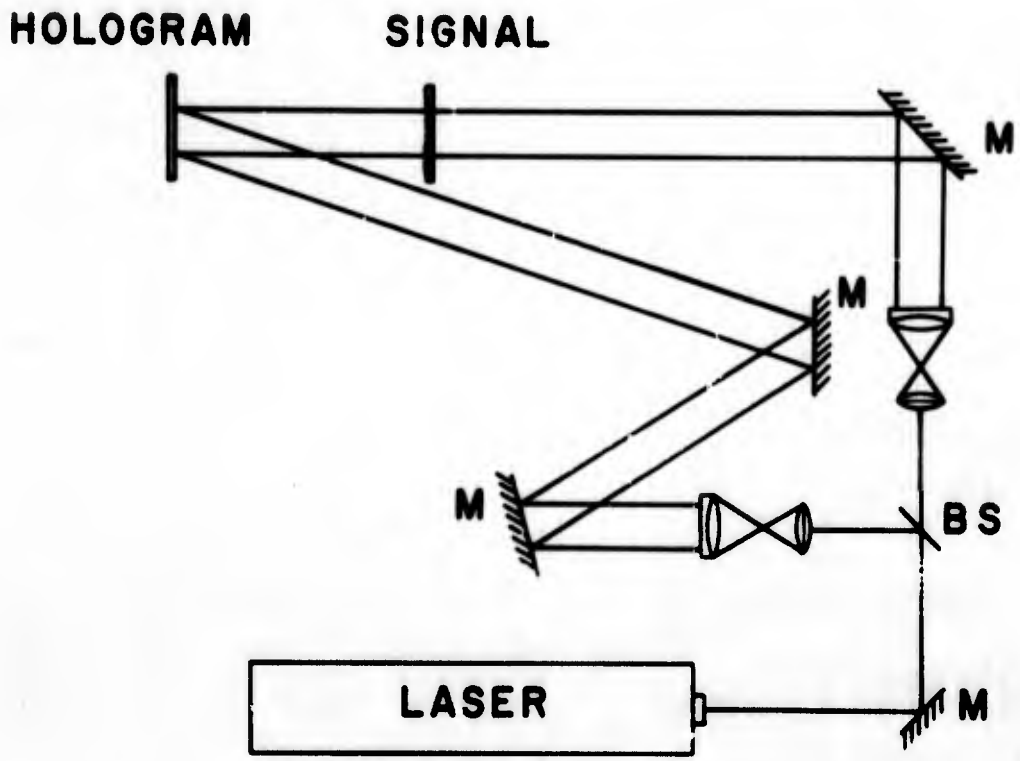

Figure 1

Recording Configuration

wavelengths. These readout wavelengths included the dominant wavelengths of the krypton laser, 476 nm (blue), 521 nm (green), 568 (yellow), and 647 nm (red), and the near infrared wavelength of the He-Ne laser, 1150 nm. We determined the noise characteristics of the materials by recording holograms with a complex signal and measuring the signal-to-noise ratio (SNR) and diffraction efficiency of these holograms. The results are shown in curves of diffraction efficiency and SNR plotted as functions of exposure and the K-ratio.

Holograms were read out in a geometry similar to the recording geometry; the holograms could be rotated if necessary to offset any thickness changes that may have occurred in processing. Diffraction efficiency was computed as the fraction of the incident light diffracted into the first order by the hologram. In some cases, losses due to reflection by the substrate were subtracted from the incident light. As we show later, since the exposure sensitivity is determined from curves of diffraction efficiency as a function of exposure, it must often be chosen in a rather arbitrary manner, depending somewhat on the application. Similarly, the diffraction efficiency depends not only on the exposure and K-ratio, but also on the signal. The diffraction efficiency of plane wave gratings is generally higher than that of holograms recorded with complex signals.

Signal-to-noise ratio measurements were made on holograms recorded with the signal shown in Figure 2. This is a 2 cm ground glass square with a 1 cm opaque square in the center. The distance between the signal and hologram was 17.5 cm, giving an information packing density at the hologram on the order of 10^6 bits/cm^2. Diffraction efficiency of these holograms was measured as with the plane wave gratings except that a lens was introduced into the diffracted beam to collect the diffracted light. We measured the SNR by scanning a reconstructed real image with a photomultiplier tube. The SNR was computed as the ratio of the average

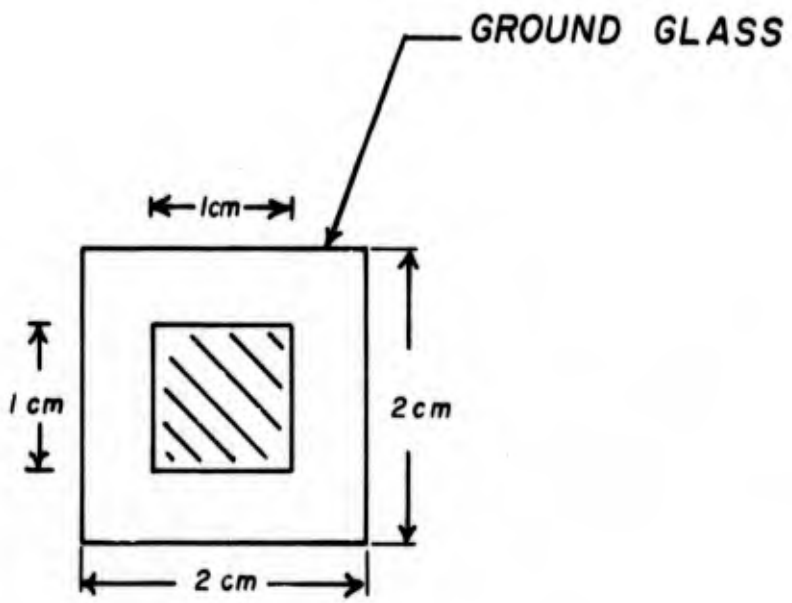

Figure 2

Diffuse Signal

intensity in the bright portion of the image to the average intensity in the dark center. It will be seen later that there is a tradeoff between SNR and diffraction efficiency for the materials we tested, so that it is difficult to determine an absolute SNR for each material. Nevertheless, a comparison of SNR and diffraction efficiency curves gives a relative indication of the noise characteristics of each material.

2.2 Environmental Tests

We tested the resistance of each material to temperature, humidity, and UV radiation, and determined the nondestructive laser readout intensity. Temperature and humidity testing were carried out in a Tenney TH Jr. environmental chamber as shown in Figure 3.

A readout laser beam was introduced through a port in the side of the test chamber and reflected by a mirror onto the hologram. The hologram was located near a large window in the front of the chamber so that both the transmitted and diffracted light could be measured from outside the chamber. The hologram could be rotated remotely about the vertical axis to compensate for any thickness changes that might occur at elevated temperatures or humidity. We could vary the temperature from -40°F to 140°F and the humidity from 20 to 95 percent (for wet bulb temperatures above 35°F). In general, holograms were read out in situ at the various conditions of temperature and humidity. At high temperature and humidity, condensation of water vapor often prevented measurements. Similarly, at subzero temperatures, the formation of frost prevented in situ measurements. In these cases, measurements were made before and after the holograms were cycled through the environmental condition.

We exposed holograms recorded in each material to UV light from a Black Light Eastern model B-100 UV lamp. This simulated exposure to solar radiation, since the destructive nature of solar radiation lies in the UV portion of the

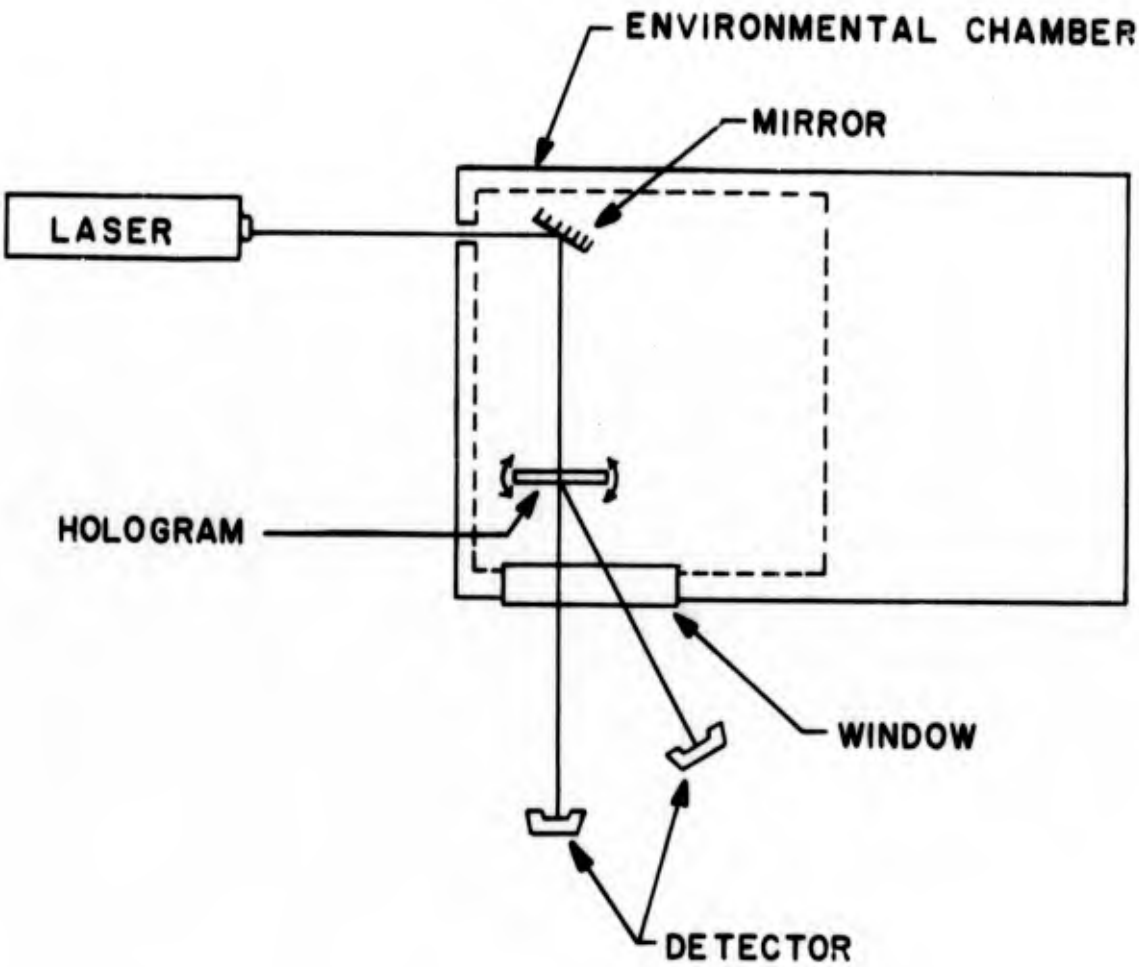

Figure 3

Configuration of Environmental Testing

solar spectrum. Holograms were placed several centimeters from the lamp and irradiated for periods of 25 to 80 hours. Transmittance and diffraction efficiency were measured before and after the UV exposure.

The nondestructive laser readout intensity limit was determined with 488 nm light from an argon laser focused to an intense spot. Since destructive readout intensity is a function of the readout time, we took measurements to generate curves of laser intensity as a function of the readout time required to destroy the hologram. The destructive limit for continuous readout can be estimated from the tail of the curves at long readout times. The laser intensity was varied by changing the spot size of the focused beam; the area of the damaged region was determined from measurements made with a microscope.

Finally, we exposed selected holograms recorded on each material to direct solar illumination in an out-of-doors environment (during the month of June). The holograms were kept in this environment for a total accumulated time of about 50 hours. The diffraction efficiency of each hologram was measured before and after the exposure. In general the results were rather poor with most materials degrading due either to the UV radiation or to the humidity. We will show curves of diffraction efficiency as a function of readout wavelength measured before and after the test.

SECTION III
MATERIALS INVESTIGATIONS

We evaluated seven phase materials for holographic optical elements. The materials tested include the following:

Bleached photographic emulsions
Dichromated gelatin
Photopolymer
Thick thermoplastics
Photoresist
Iron oxide
Photoplastics

We chose to investigate these materials because they showed the most promise of immediately satisfying many of the specified requirements. In particular the first four materials were attractive because of their ability to form thick phase holograms, with diffraction efficiencies exceeding 90% in some cases. The last three materials form thin phase materials which are limited, in general, to diffraction efficiencies below 30%. We chose to investigate these thin phase materials because of their specialized attributes for some applications. In particular we have developed techniques for coating and subsequently etching iron oxide films to the point where they can now be used for recording good quality holographic elements. After development and proper curing, these films are essentially impervious to adverse environmental conditions. We have also developed techniques for fabricating photoplastic devices for holographic recordings. We find that with careful selection of sensitizers we are able to record high quality holograms at 647.1 nm. The results are sufficiently encouraging to suggest that these photoplastic materials may be suitable for holographic recording with near infrared light. In special cases holograms with very high diffraction efficiency, as high as 80%, can be recorded in photoresist. These high efficiencies, apparently due to a blazing effect, make photoresist holograms attractive for some applications.

3.1 Bleached Photographic Emulsions

High resolution photographic emulsions are the most commonly used holographic recording material. These emulsions have very high · ing power, relatively high exposure sensitivity, and broad spectra· ·e. Holograms are formed in photographic emulsions as spatial distributions of finely divided elemental silver. These absorption holograms are limited to diffraction efficiencies of only several percent.

Bleaching the photographic emulsions changes the absorption holograms into phase holograms, with high potential diffraction efficiencies. The bleaching process converts the opaque silver grains into a transparent silver salt such as silver bromide. The silver salt particles have a high refractive index relative to the gelatin, so that there is a differential in the net refractive index where there is a differential in the concentration of the silver salt. This variation in refractive index forms the phase hologram.

3.1.1 Mechanism of Hologram Formation. — Diffraction of light by holograms in bleached photographic emulsions is due to the difference in index of refraction between silver halide crystals and gelatin. Typically, the index of refraction of gelatin is about 1.52 while that of the silver halides is 2.253, 2.071, and 2.21 for bromide, chloride, and iodide, respectively. Chang and George[7] have modeled bleached photographic emulsions in terms of lossy dielectric particles (silver halide crystals) in a lossless dielectric matrix (the gelatin). By assuming various shape factors for the silver halide crystals, we can apply Lorenz-Lorentz theory to derive an expression for the relative permittivity as a (spatial) function of the hologram exposure. Analysis yields expressions for an effective Δn and an absorption coefficient; these are functions of both the silver halide and gelatin indices of refraction and the mean volume density of silver halide crystals (which is related to the average hologram exposure).

Further insight into the nature of the hologram recording mechanism is obtained by recalling that for lossy dielectric holograms the general expression for diffraction efficiency is given by

$$DE = \exp[-f(\varepsilon'')] \sin^2 [g(\varepsilon')]$$

where $\varepsilon_1 = \varepsilon' + i\varepsilon''$ is the change in dielectric constant induced by the hologram recording processing, and $f(\varepsilon'')$ and $g(\varepsilon')$ are real, positive, known functions of ε'' and ε', respectively. The parameters ε', ε'' are determined from the properties of a dielectric layer of silver halide particles suspended in a gelatin matrix as previously discussed. For lossless dielectrics $\varepsilon'' = f(\varepsilon'') = 0$ and 100 percent diffraction efficiency is possible. In general, $f(\varepsilon'')$ is not zero, and hence, the maximum experimentally measured efficiency is typically on the order of 50%. It is not uncommon for more than 25 percent of the incident laser energy to be absorbed. Thus, a bleached silver halide emulsion must be considered as a lossy dielectric. A main objective of our experimental investigations was to make ε'' as small as possible. The data in Table 1 illustrates the magnitude of absorption losses for plane wave gratings recorded on Kodak High Resolution plates at 488 nm with a reference-to-signal beam ratio of 10 and for high (D19), medium (D165) and low (POTA) contrast developers.

	Developer		
Energy Summary	D19	D165	POTA
Diffracted	17%	11%	4%
Transmitted	22%	44%	65%
Reflected	12%	12%	12%
Scattered	1%	1%	1%
	52%	68%	82%
"Absorbed"	48%	32%	18%

TABLE 1. Absorption losses in a bleached photographic emulsion for various developers

The absorption mechanisms which generate ε'' are not all known or understood. Available evidence suggests that ε' and ε'' (and also $f(\varepsilon'')$ and $g(\varepsilon')$) are not independent. The situation is analogous to light-induced phenomena in photochromic materials where hologram recording induces not only spatial variations of absorption but also corresponding spatial variations of the index of refraction. These effects correspond to the creation of an ε'' and an ε', respectively, and are related by means of the Kronig-Kramers relations.

At present a number of possible absorption mechanisms are suggested by experimental work or by theoretical considerations. They are as follows:

1) Gelatin stain due to oxidation products formed during the development process. The stain is tan colored, absorbs in proportion to prebleach density, and does not appear to be removable by any known chemical processing. The stain can be easily observed by fixing a bleached hologram of high initial density. It appears that the stain not only accounts for some absorption but also may act as a sensitizer for subsequent darkening of the hologram.

2) Multiple internal scattering. Some of the incident laser light is trapped within the volume of the hologram due to intergrain scattering and total internal reflection. The amount of light energy lost due to this effect is not known, but clearly depends on prebleach density.

3) Internal lattice irregularities. Point defects such as ion vacancies or interstitial silver atoms can create absorption phenomena different than that due to the inherent absorption bands of silver halide.

3.1.2 Method of Use. — Photographic plates are purchased from the manufacturer or supplier in ready to use form. Although Lippmann-type emulsions of high quality suitable for holography can be made in the

laboratory, the time and cost required, as well as the technical problems, make this approach unattractive.

The primary suppliers of photographic plates suitable for holography are Eastman Kodak and Agfa Gevaert. Kodak produces the panchromatic 649F plate (17 and 35 μm thick) and the orthochromatic 649GH and High Resolution plates (6 μm thick). In addition, Kodak has made available a special holographic emulsion for the red part of the spectrum which is designated as type 120-02. All of these plates have a resolving power in excess of 3,000 lines/mm. Typical exposure requirements are 0.05-0.25 mJ/cm^2.

The equivalent Agfa emulsions are designated as the Scientia series. Agfa 8E75 is similar to 649F and 8E56 is similar to 649GH High Resolution plates. Also, 10E75 and 10E56 plates are available which have lower resolving power (approximately 2500 lines/mm) but have 20 to 30 times increased exposure sensitivity. All Agfa plates have a dry coating thickness of 6 μm. Greater thicknesses are available on special order.

Photographic emulsions are generally the most light-sensitive hologram recording media. Kodak 649F plates are panchromatic[8] and must be used in total darkness. Kodak High Resolution plates are orthochromatic[8] which permits the use of a deep red safelight. Agfa Scientia emulsions have code numbers of 70 and 75 for panchromatic emulsions and the code number 56 for orthochromatic emulsions.

Photographic plates are quite stable. They can be stored at room temperature for at least 6 months and in cold storage indefinitely. However, environmental conditions do modify the characteristics of most emulsions. Extreme high temperatures cause fogging while low temperatures reduce exposure sensitivity; excessive humidity causes swelling and hypersensitization. It is recommended that for recording holograms the temperature and relative humidity be maintained in the ranges of 60-80°F and 30-60 percent, respectively.

Pre-exposure processing of photographic plates is generally unnecessary; they can be used without modification as received from the manufacturer. In some instances, however, hypersensitization may be required. Bathing the plates in dilute solutions of either ammonia or triethanolamine gives possible speed gains of two to four. Stress relief is occasionally required to obtain optimum hologram quality. This can be accomplished by soaking the plate in distilled water for 15 minutes followed by slow drying.

Index-matching of photographic plates is required to produce the highest quality holograms. Since the emulsion of photographic plates is not affected by most organic chemicals, convenient, volatile solvents can be used for index matching. Ethyl benzoil acetate (n = 1.523), for example, is almost a perfect match for Kodak 649F plates.

The processing of photographic plates to obtain bleached holograms involves a number of straightforward steps. We have summarized in Table 2 and 3 the order and nature of each step. The first step, development, is the only really critical operation. For consistent, repeatable results development time and temperature must be carefully controlled. Each of the other steps permit variation in time of the order of 20 percent. It is important, however, to maintain the temperature of each bath at the same temperature to within a few degrees to avoid gelatin reticulation.

We have recommended Kodak D19 for development. Kodak D165 and Agfa Metinal U are also excellent developers. Kodak D8 and HRP developer are specifically not recommended because of their staining properties.

Steps 9 through 12 can be skipped in order to measure the reconstruction parameters of the unbleached holograms. Further processing can begin later at step 9 after first soaking the emulsion in distilled water for 15 minutes.

TABLE 2

CHEMICAL PROCESSING OF PHOTOGRAPHIC EMULSIONS

FOR BLEACHED HOLOGRAMS

1. Develop: D19, 5 minutes @72°F
2. Stop: Kodak Indicator, 20 seconds
3. Fix: Kodak Rapid Fixer, 10 minutes
4. Rinse: 10 minutes
5. Hardener: Kodak SH1, 3 minutes
6. Rinse: 30 seconds
7. Fix: Kodak Rapid Fixer, 3 minutes
8. Rinse: 10 minutes
9. Bleach: 10 minutes
10. Rinse: 5 minutes
11. Clear: 5 minutes
12. Rinse: 10 minutes
13. Dry: 50% methanol, 5 minutes
14. Dry: 3 minutes, 100% methanol, 3 minutes
15. Free Air Dry: minimum 1 hour @50% RH

— Keep all bath temperatures at 72°F —

TABLE 3

PREPARATION OF BLEACH AND CLEARING BATH

Bleach

1. Dissolve 25 gm of $FeCl_3$ in 500 ml of distilled water.
2. Add and dissolve 25 gm of $CuBr_2$.
3. Carefully add 10 ml of concentrated H_2SO_4 while stirring slowly.
4. If the color of the solution is a brilliant emerald green, add distilled water to make 1 liter of solution. If not the right color, add up to 10 ml more of concentrated H_2SO_4 and then add the distilled water.
5. Filter the solution (a paper towel can be used as the filter).
6. Discard the bleach solution following its use; i.e., do not return used bleach solution to the original container.

Clearing Bath

Solution A: Dissolve 5 gm of potassium permanganate (KM_nO_4) in 1 liter of distilled water.

Solution B:
1. Dissolve 50 gm of potassium bromide (KBr) in 500 ml of distilled water.
2. Carefully add 10 ml of concentrated H_2SO_4.
3. Add distilled water to make 1 liter of solution.

Just before use, add one part of Solution A to ten parts of Solution B. Discard after use.

3.1.3 Experimental Results. — The emulsions we tested included Kodak High Resolution Plates and 649F Spectrographic plates. Nominal emulsion thicknesses were 6 μm for High Resolution Plates, and both 17 and 35 μm for 649F Plates. The spectral sensitivity of the High Resolution Plates is limited to the blue-green region of the visible spectrum while the 649F plates are panchromatic. We measured in detail the holographic response of High Resolution Plates at 488 nm and of 649F plates at both 488 nm and 633 nm.

3.1.3.1 Holographic Parameters. — The plates were exposed in a normal manner without preprocessing. After exposure, the plates were processed with the steps and solutions given in Tables 2 and 3. We measured the diffraction efficiency in some cases before bleaching the holograms, in order to determine the effect of the bleaching process. Figure 4 shows the diffraction efficiency as a function of exposure for plane wave gratings recorded in High Resolution Plates with K-ratios of 1, 4, 10, and 50. These measurements were made on the holograms before they were bleached; a peak diffraction efficiency of about 5% was reached with K = 1 at an exposure of 40 $\mu J/cm^2$. Similar data produced curves of slightly different shape for 649F plates (17 μm emulsion) at 633 nm as shown in Figure 5. Here the peak diffraction efficiency is about 4% for K = 1 at an exposure of 100 $\mu J/cm^2$.

After bleaching, the curves appear as shown in Figures 6 (High Resolution Plates) and 7 (649F). In Figure 6 the peak diffraction efficiency reached is 38% at K = 1, occurring at an exposure of 80 $\mu J/cm^2$. The efficiency decreases at higher exposures because of the increased absorption and scattering losses caused by the high concentration of silver halide particles.

Figure 7 shows that the diffraction efficiency of holograms recorded in bleached 649F emulsions (17 μm thick) reach a peak of about 45% for K = 1 at an exposure of 600 $\mu J/cm^2$. Note that there is only a small increase in

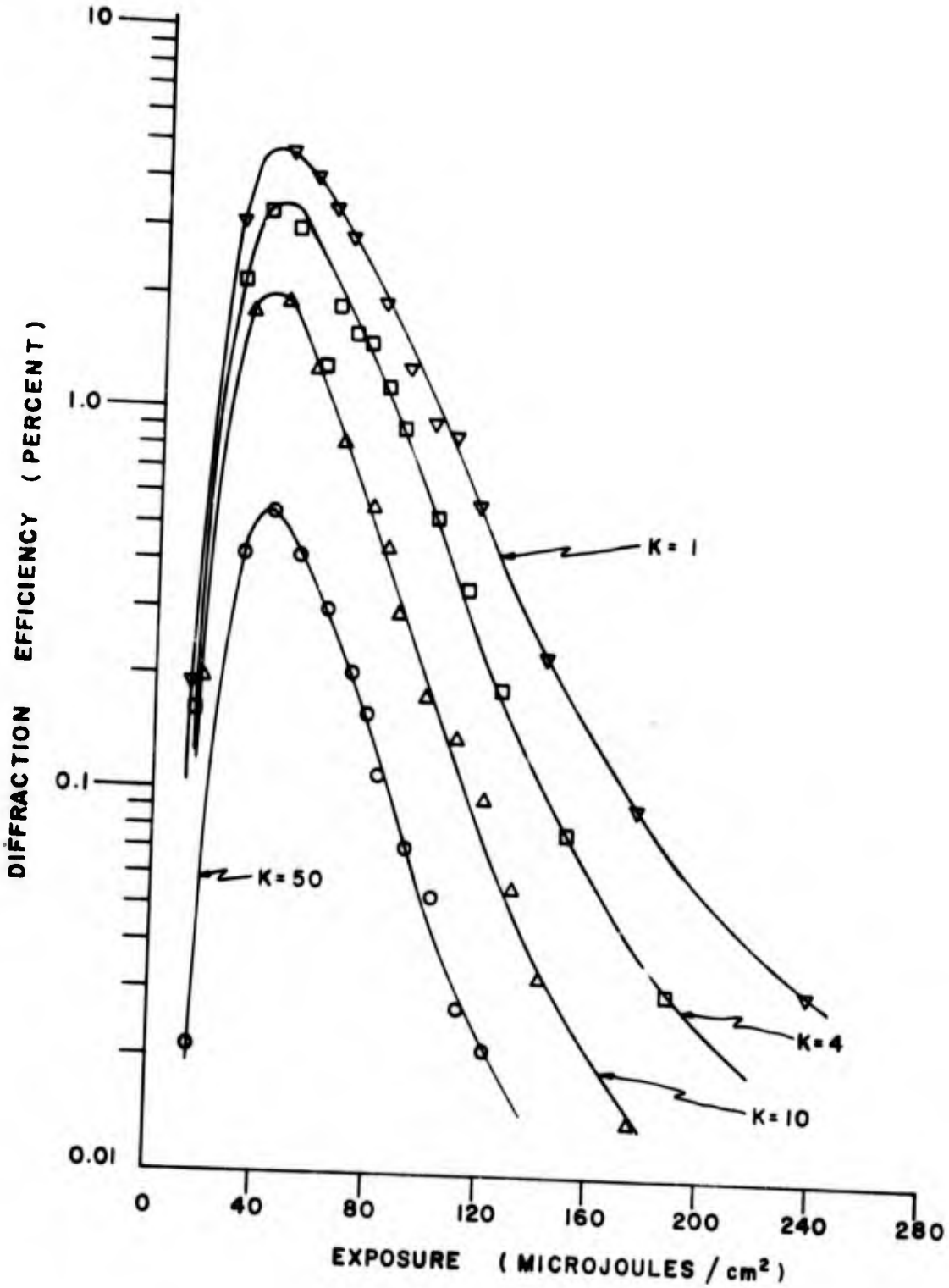

Figure 4

Diffraction efficiency as a function of exposure for plane wave grating recorded in unbleached High Resolution Plates at 488 nm.

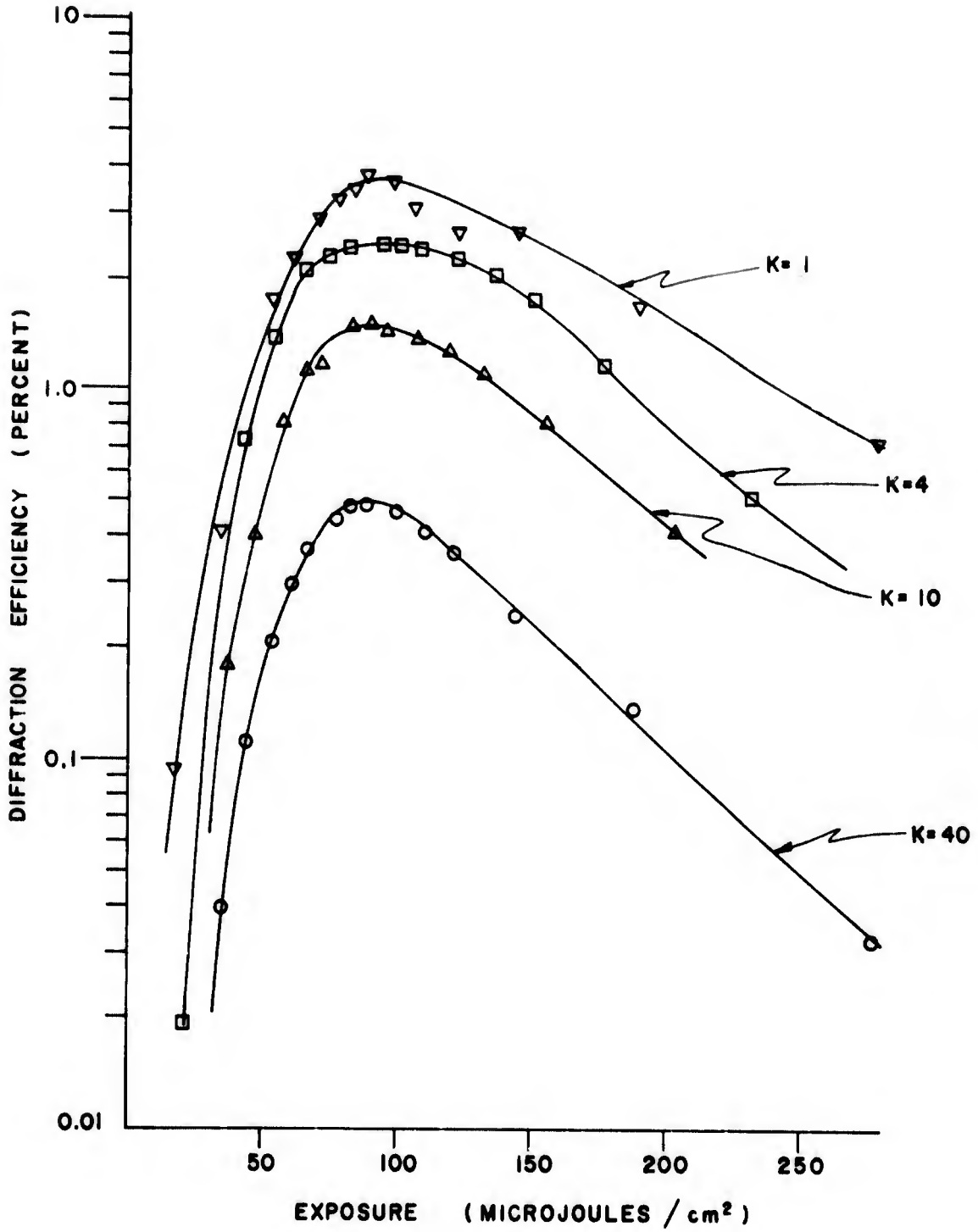

Figure 5

Diffraction efficiency as a function of exposure for plane wave gratings recorded in unbleached 649F plates (17μm thick) at 633 nm.

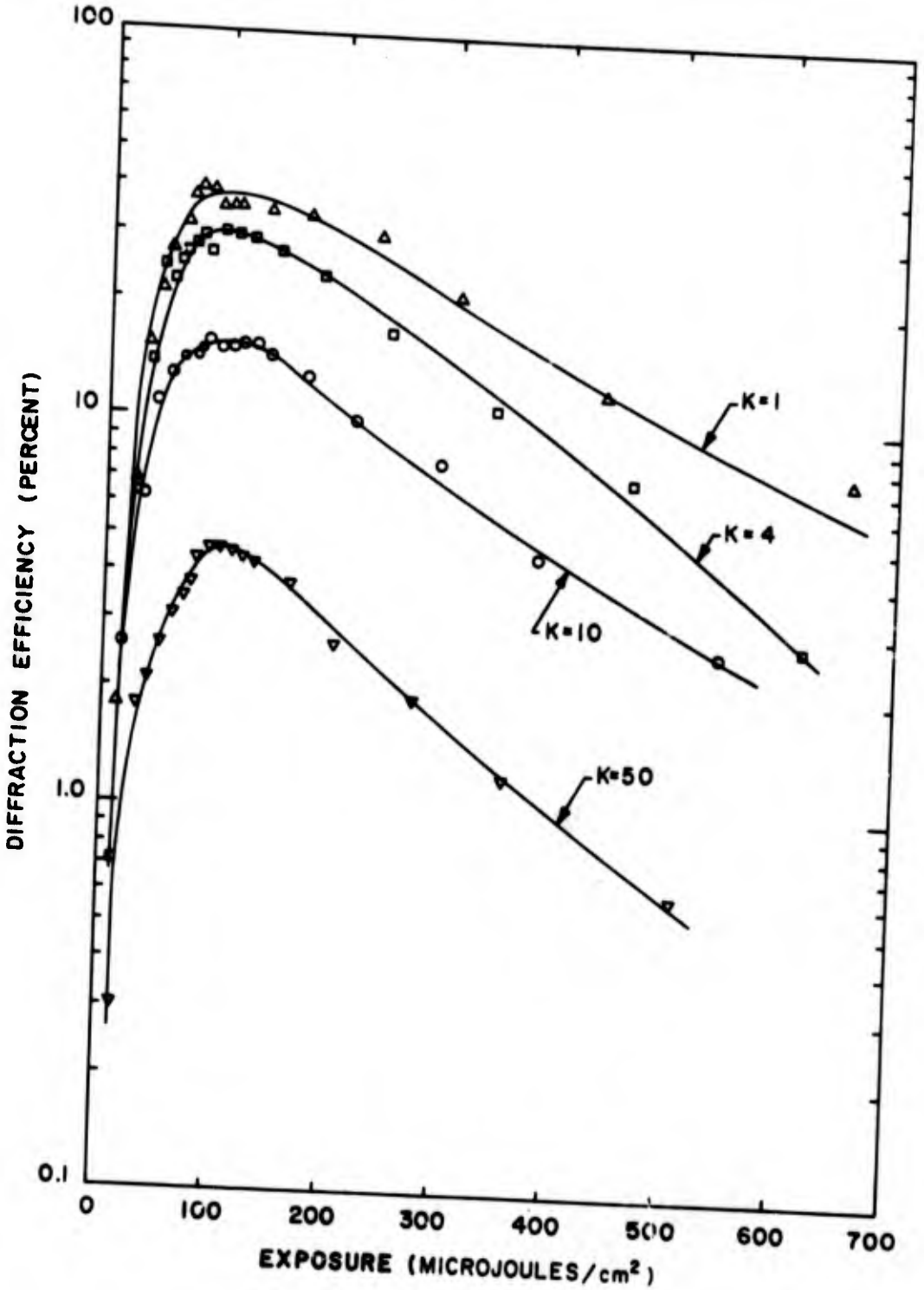

Figure 6

Diffraction efficiency of plane wave gratings recorded in bleached High Resolution Plates at 488 nm.

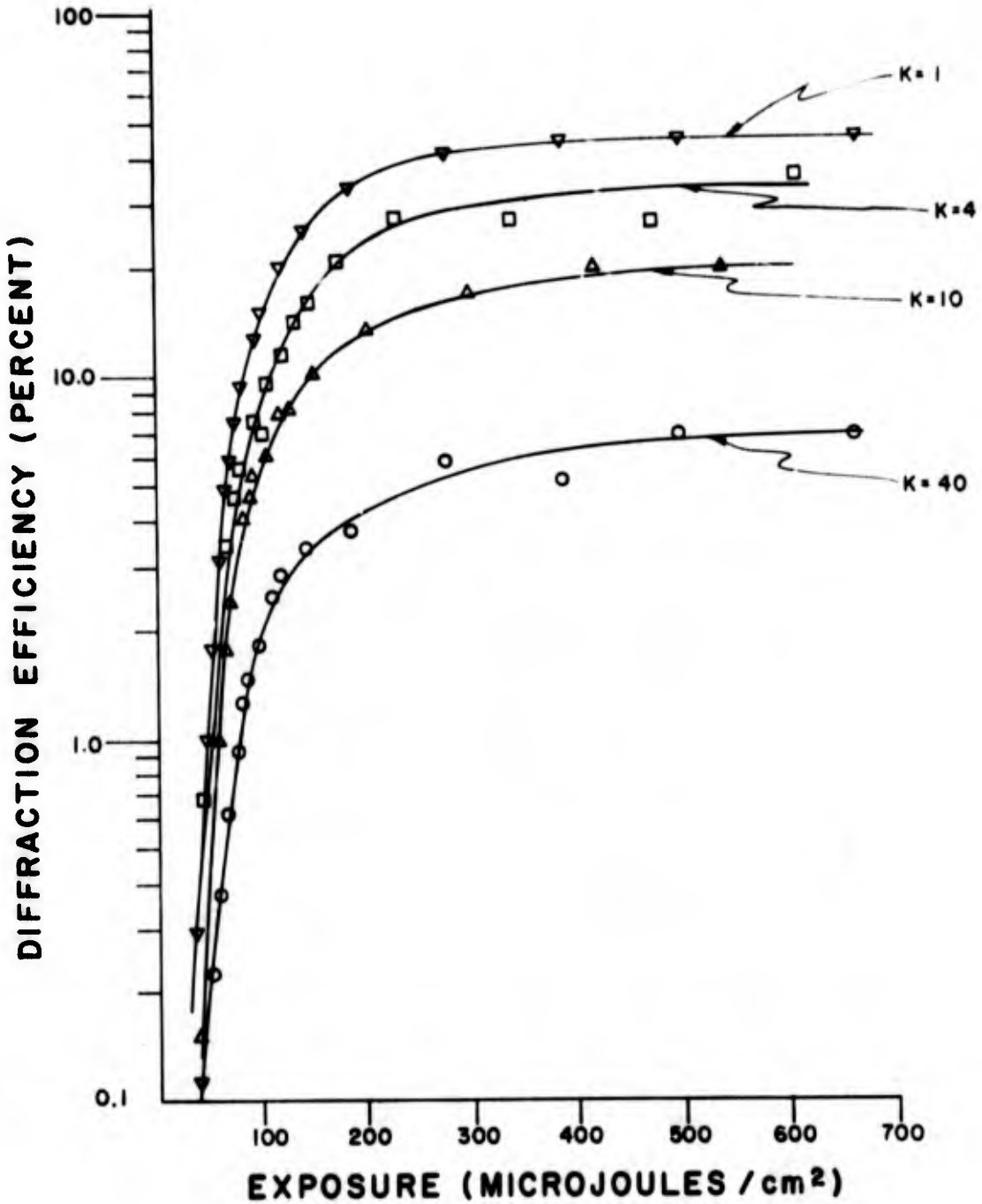

Figure 7

Diffraction efficiency of plane wave gratings recorded in bleached 649F plates (17μm thick) at 633 nm.

diffraction efficiency for exposures greater than 250 $\mu J/cm^2$. This exposure is still considerably greater than the 100 $\mu J/cm^2$ determined for the unbleached plates, indicating that the highest efficiencies are obtained from holograms that are relatively dense before bleaching. Figure 8 shows the variation of diffraction efficiency with exposure for plane wave gratings recorded in bleached 649F plates (17 μm thick emulsions) at a wavelength of 488 nm. Here the peak diffraction efficiency is about 35% for K = 1. This reduced efficiency of holograms recorded with blue light is typical for 649F plates, and is due to increased scattering and absorption at the shorter wavelength. As with the High Resolution Plates, the efficiency decreases at high exposures because of increased scattering by the more heavily exposed holograms. Figure 9 shows diffraction efficiency as a function of exposure for plane wave gratings recorded at 633 nm in bleached 649F plates with 35 μm thick emulsions. The results are similar to those obtained with 17 μm thick emulsions except that diffraction efficiencies are lower for gratings in the thicker emulsion.

The results obtained with the complex signal were considerably different from those of plane wave gratings. The diffraction efficiency of the holograms was significantly reduced, and the variation of SNR with the K-ratio was opposite to the variation of diffraction efficiency with K. Figures 10 through 13 show the variation of SNR and diffraction efficiency with exposure for K = 1 (Figure 10), K = 4 (Figure 11), K = 10 (Figure 12), and K = 40 (Figure 13). These data were taken from bleached 649F plates (17 μm emulsion) at 633 nm. As with the plane wave gratings, the diffraction efficiency decreases with increasing K-ratio. The SNR increases, however, with increasing K-ratio. This is shown more clearly in Figure 14 where the SNR is shown as a function of exposure for all four K-ratios. The previous SNR and diffraction efficiency curves also show a general tendency for the SNR to decrease while the diffraction efficiency increases. This

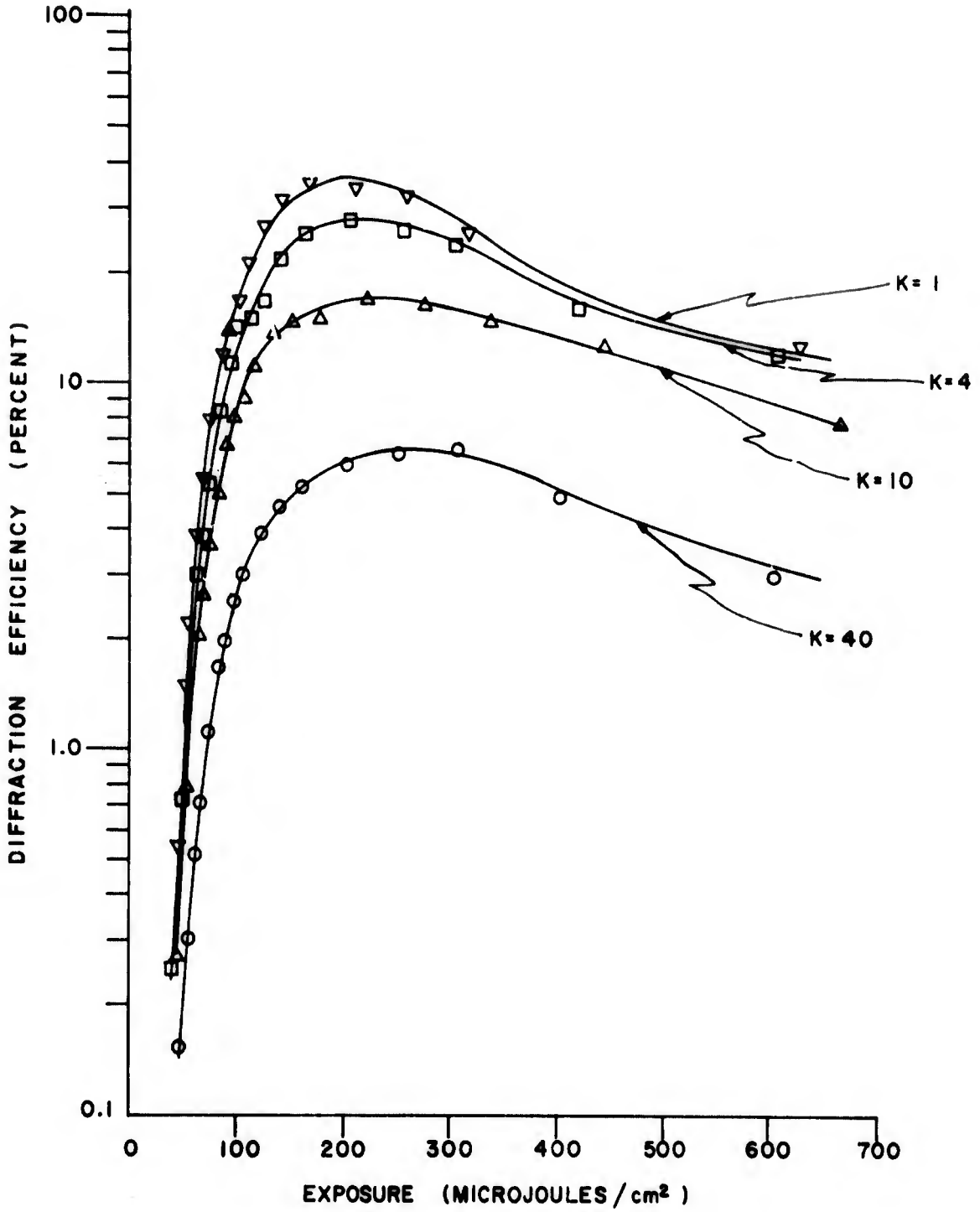

Figure 8

Diffraction efficiency of plane wave gratings recorded in bleached 649F plates (17μm thick) at 488 nm.

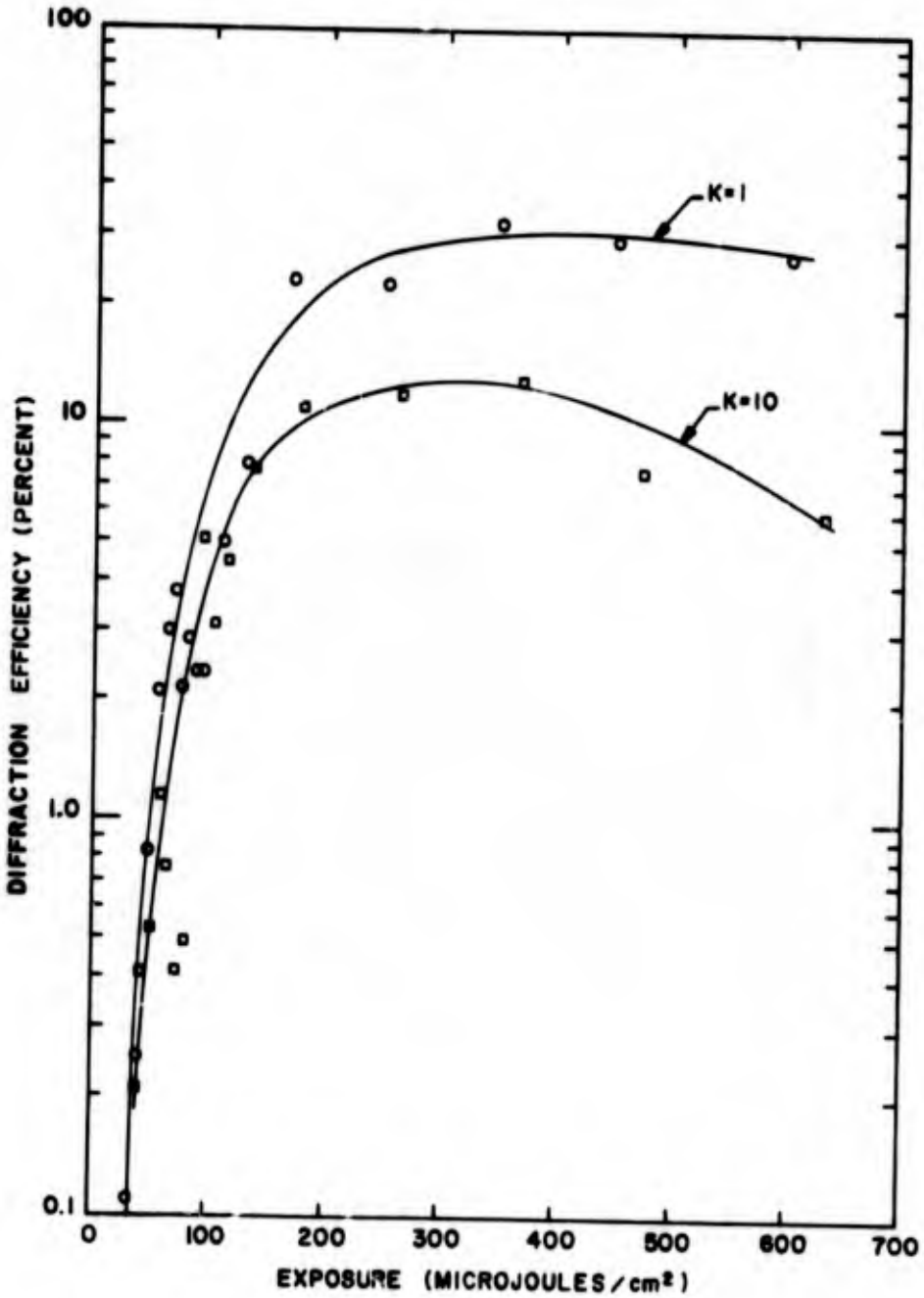

Figure 9

Diffraction efficiency of plane wave gratings recorded in bleached 64%F plates (35μm thick) at 633 nm.

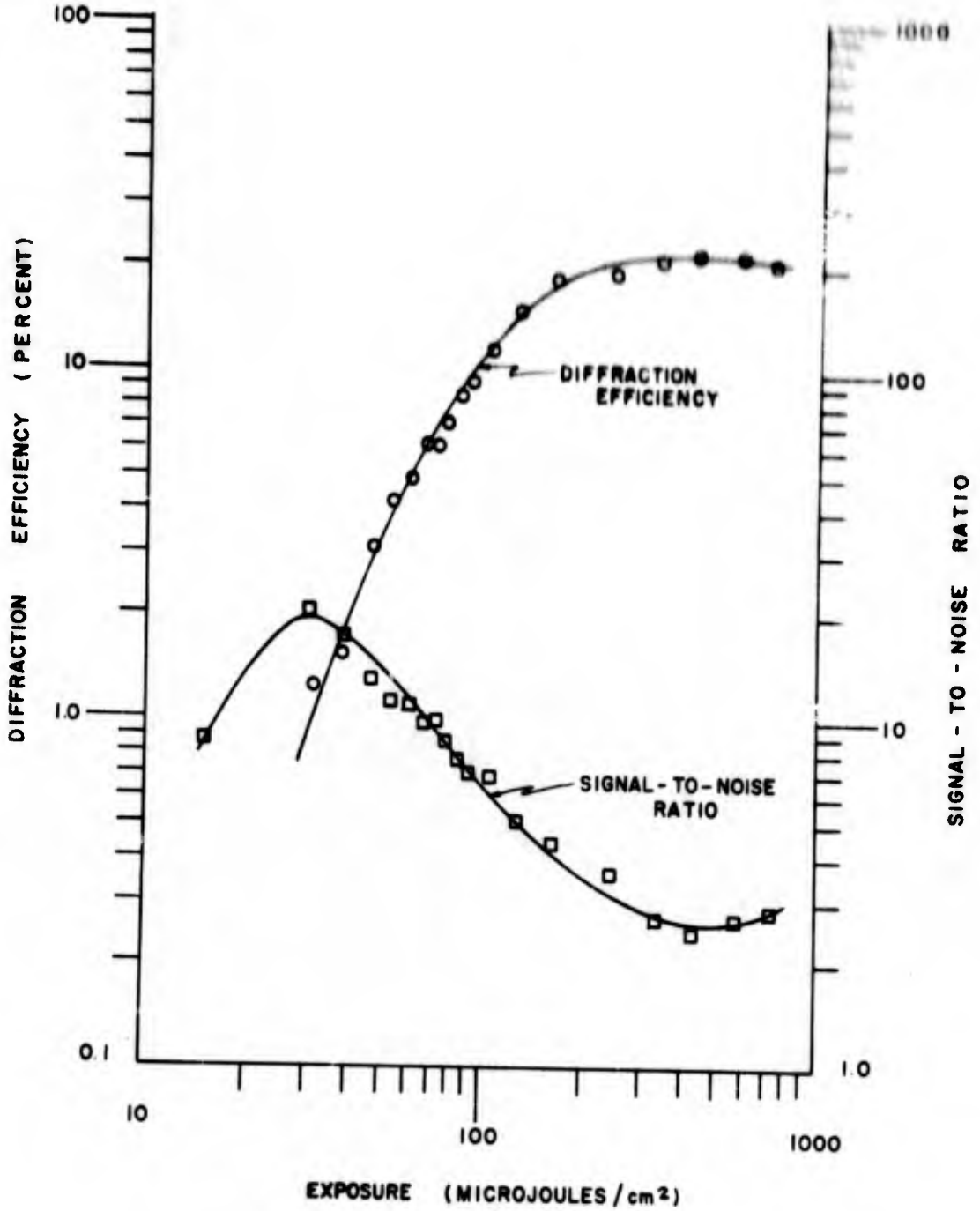

Figure 10

Diffraction efficiency and SNR as functions of exposure for holograms recorded in bleached 649F (17μm thick) at 633 nm, K=1.

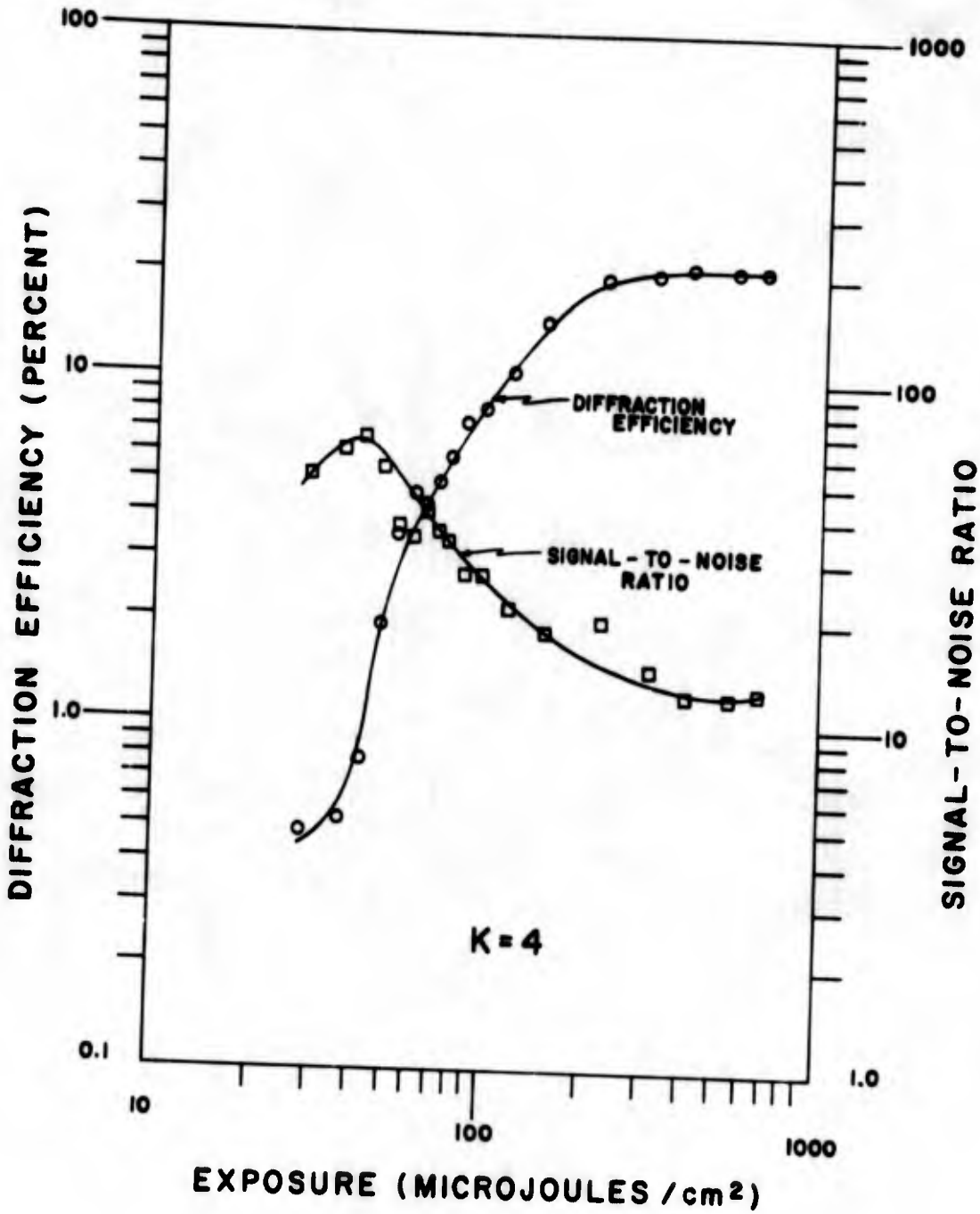

Figure 11

Diffraction efficiency and SNR of holograms recorded in bleached 649F (17μm thick) at 633 nm, K = 4.

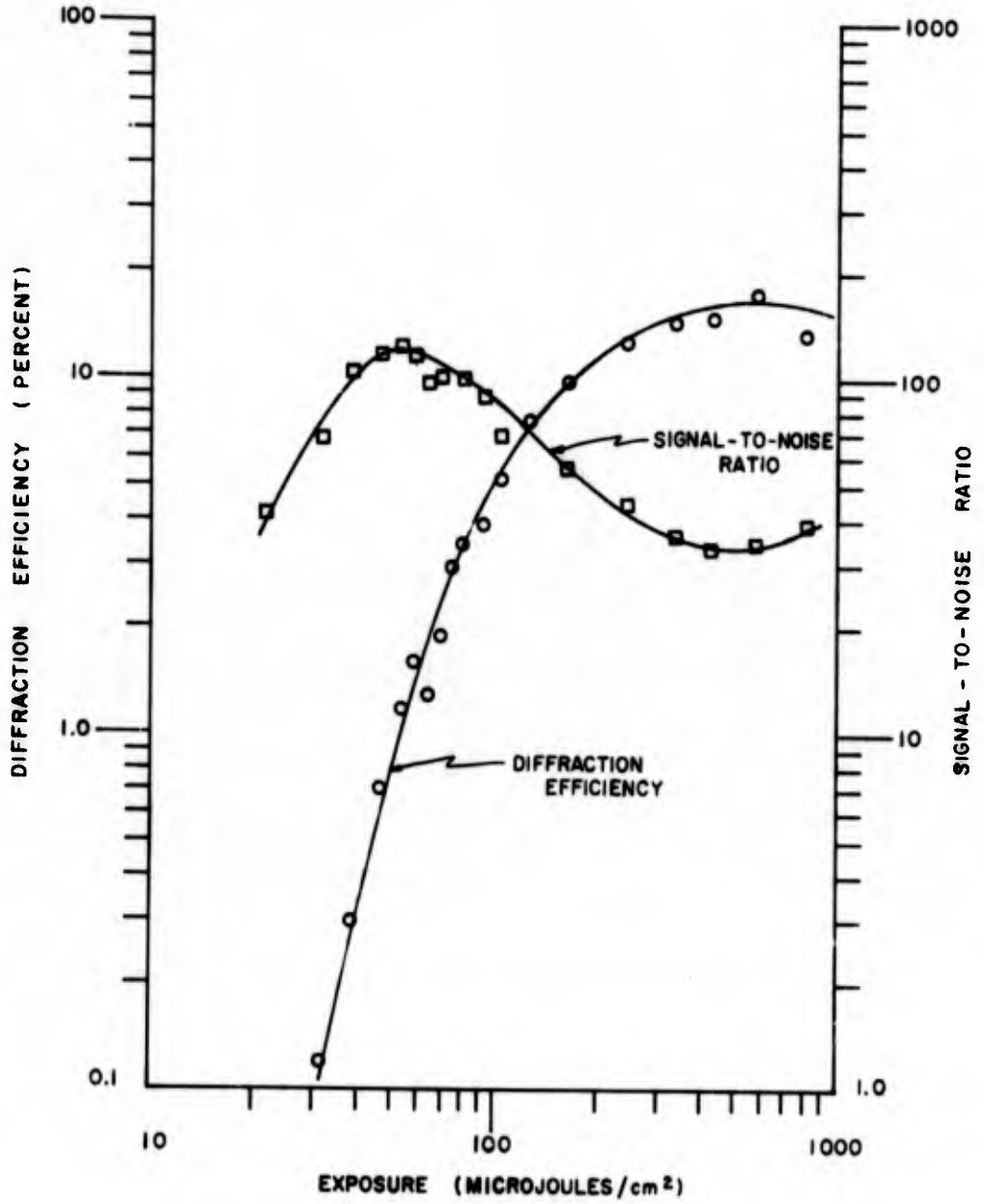

Figure 12

Diffraction efficiency and S/N ratio holograms recorded in bleached 649F (17μm thick) at 633 nm, V = 10.

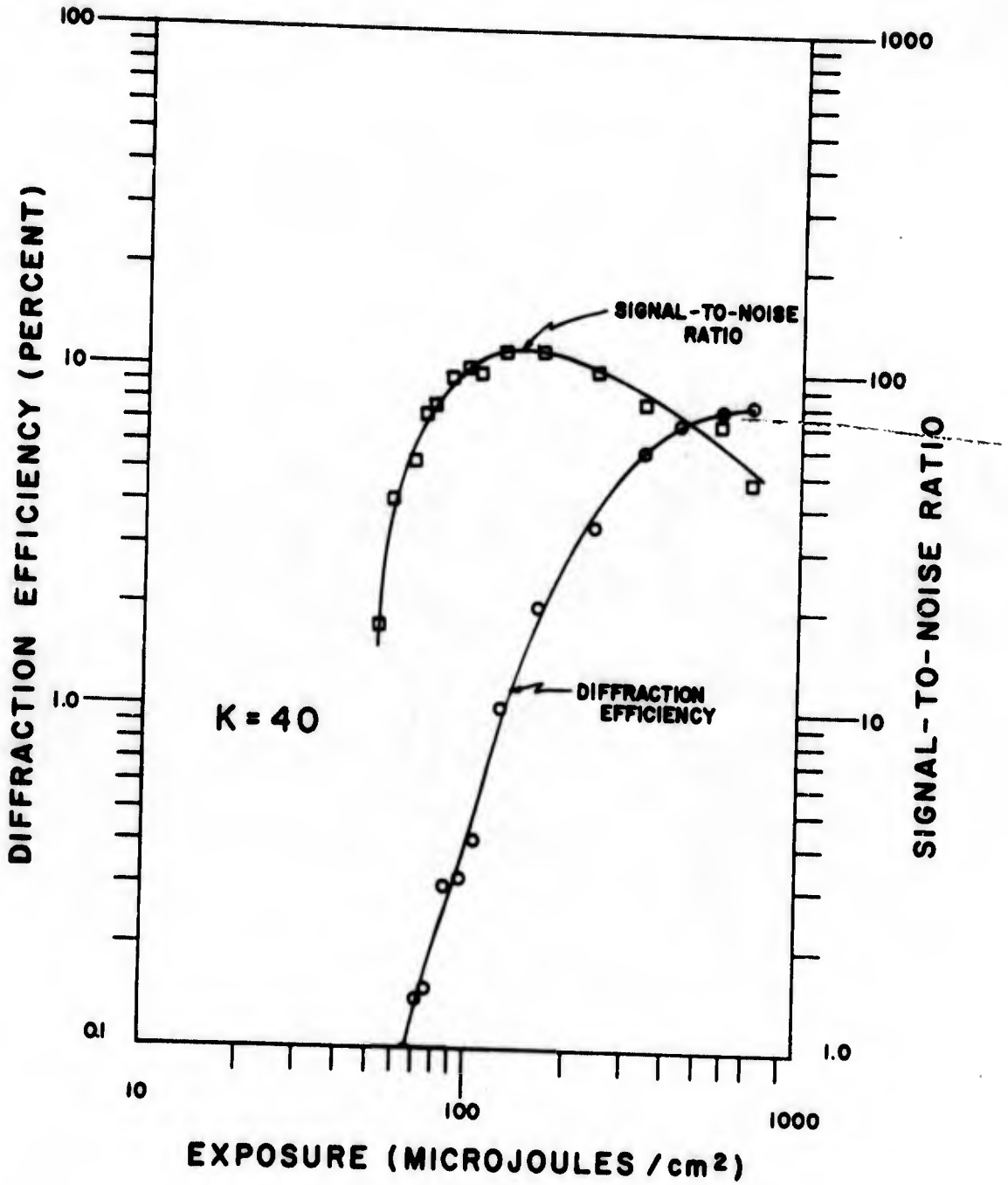

Figure 13

Diffraction efficiency and SNR of holograms recorded in bleached 649F (17μm thick) at 633 nm, K=40.

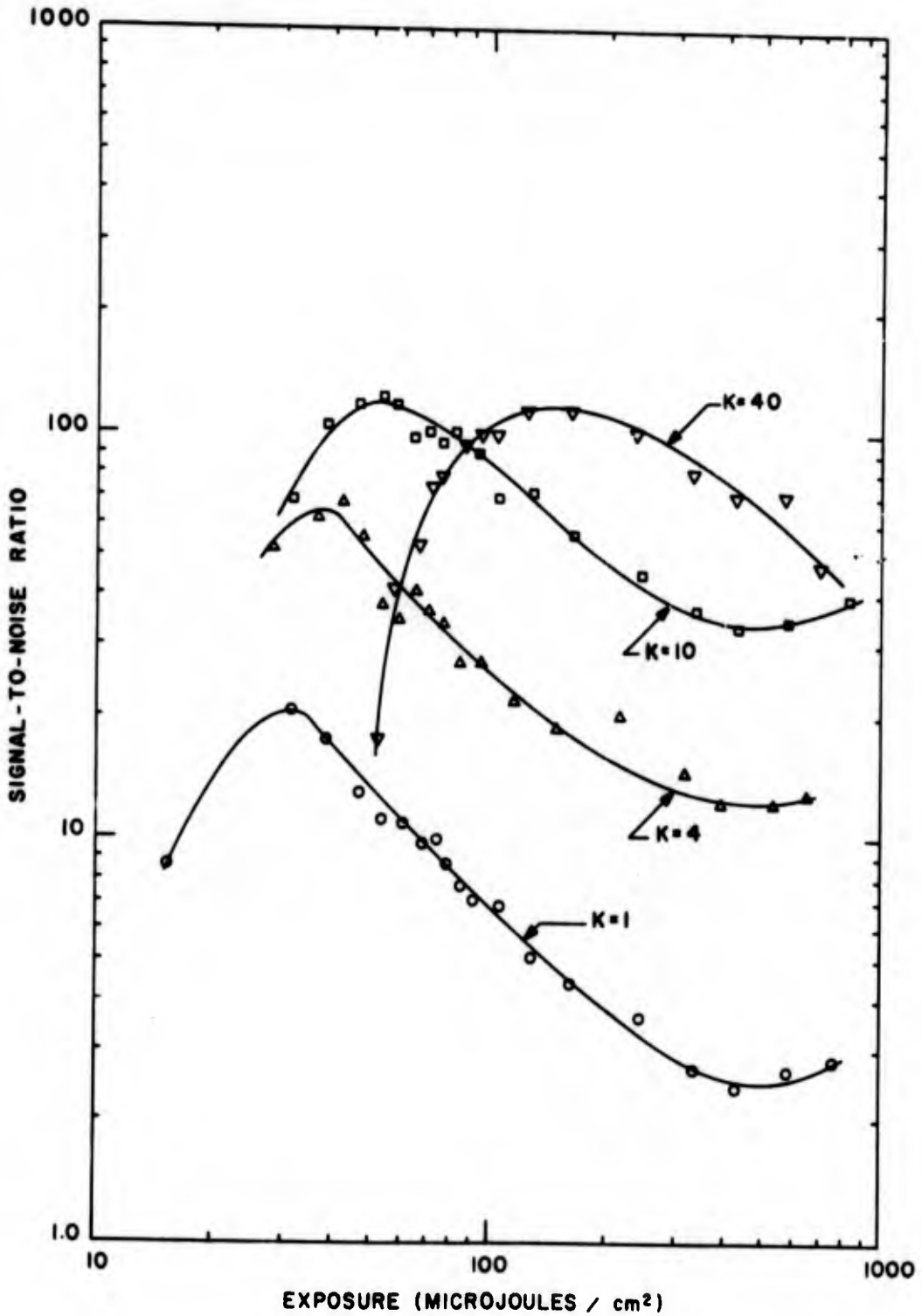

Figure 14

R as a function of exposure for holograms recorded in bleached 649F (17μm thick) at 633 nm.

tradeoff between diffraction efficiency and SNR was generally evident for all the materials we tested. We attribute this decrease in SNR with increasing diffraction efficiency to intermodulation distortion that results from nonlinearities of both the phase recording process and the materials themselves. In addition, increased scattering at heavy exposures contributes to the decrease in SNR of the bleached photographic emulsions. The best SNR that we measured was about 120 or 21 dB, which occurred at K-ratios of both 10 and 40. The diffraction efficiency at the peak SNR was only 0.9% for K = 10 and 1.3% for K = 40. At the peak diffraction efficiency of 20%, the best SNR that we measured was 15, or 12 dB, at K = 4. Perhaps the best compromise is a SNR of 57, or nearly 18 dB, at a diffraction efficiency of 10%; these quantities occurred at K = 10. The slight upturn in the SNR curves at high exposure appears to be similar to that reported by Upatnieks and Leonard.[9]

As might be expected from our results with plane wave gratings, the SNR we measured at 488 nm was not as good as at 633 nm. This is illustrated by Figure 15, showing SNR and diffraction efficiency for holograms recorded in bleached 649F plates (17 μm thick emulsions) with a K-ratio of ten. This figure should be compared to Figure 12. The peak SNR at 488 nm was 76, or 19 dB; this is 2 dB less than at 633 nm. At a diffraction efficiency of 10%, the SNR is 40, or 16 dB, compared to 17-1/2 dB for 10% diffraction efficiency at 633 nm.

Figure 16 shows the SNR and diffraction efficiency as a function of exposure for holograms recorded in bleached 35 μm thick 649F emulsions. These holograms were recorded at 488 nm with K = 10. Both SNR and diffraction efficiency are significantly lower than for 17 μm thick 649F. The peak SNR is only 15, or 12 dB, and the peak diffraction efficiency is less than 6%. We believe these low figures are caused by increased scattering due to the extra thickness of the emulsion.

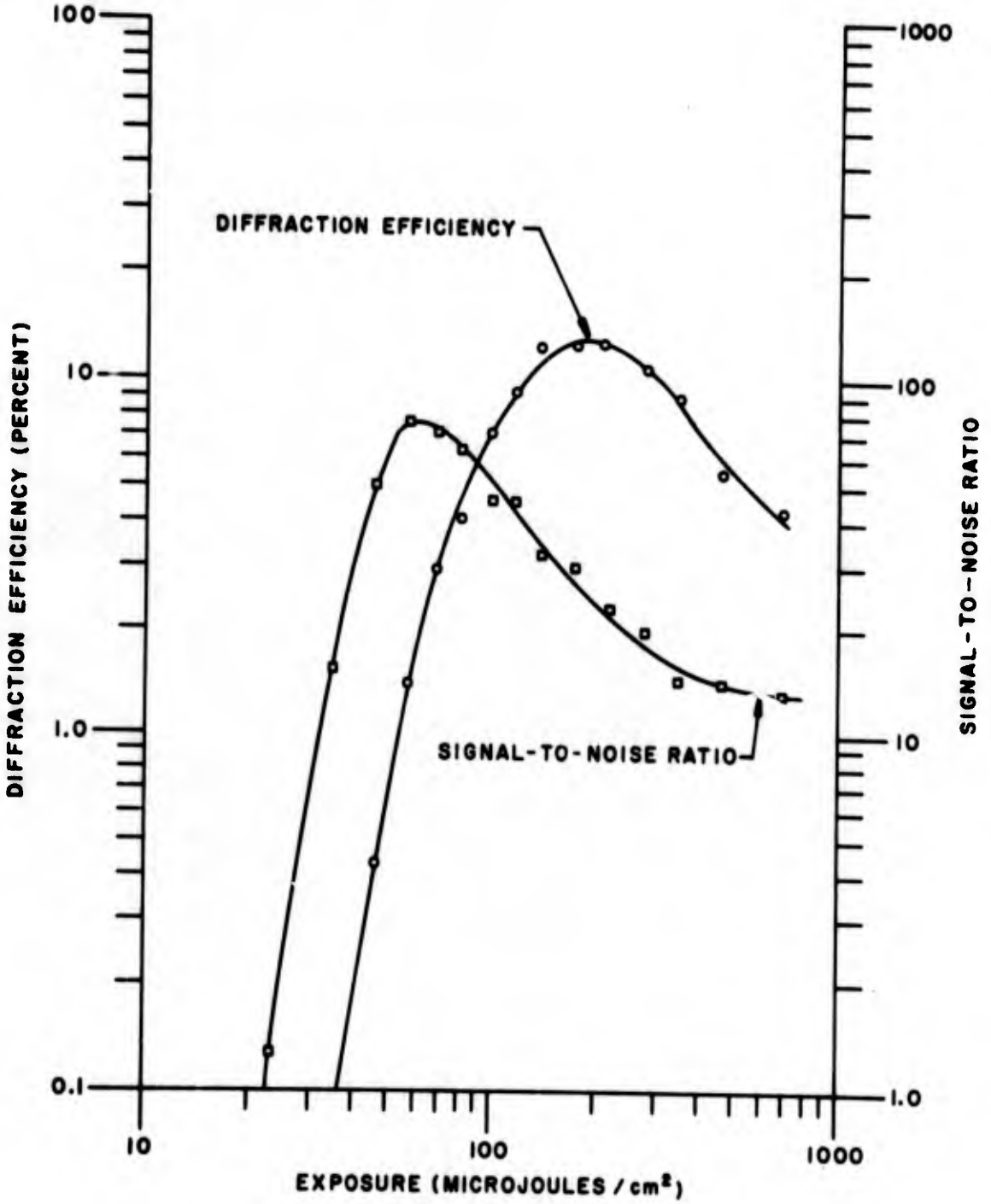

Figure 15

Diffraction efficiency and S/N of [illegible] recorded [illegible] beam in 649F (17 μm thick) at 488 nm.

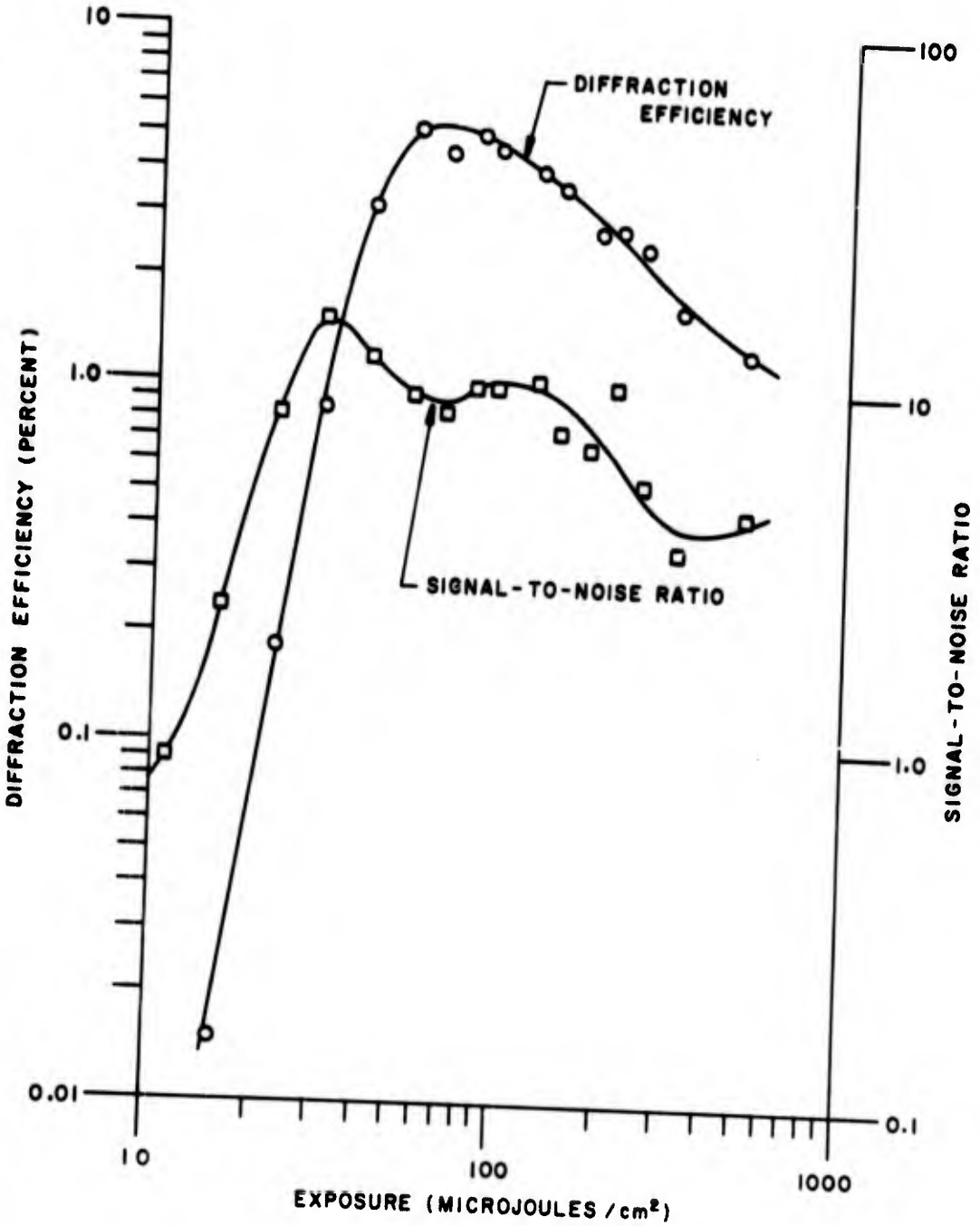

Figure 16

Diffraction efficiency and SNR of holograms recorded in bleached 649F (35μm thick) at 488 nm, Y = 10.

The response of High Resolution Plates was similar to that of the 17 μm thick 649F emulsions. At 488 nm with K = 10, we measured a peak SNR of 86, or 19 dB, at 3.5% diffraction efficiency.

We did not measure the frequency response of the photographic emulsions since it is well known to be flat to 2000 lines/mm[10] and to be capable of response to at least 4000 lines/mm.

We measured the diffraction efficiency as a function of readout wavelength for bleached plane wave gratings in each of the three emulsions. We found that the variation of readout efficiency with wavelength depended on the exposure of the hologram read out. This is illustrated by the curves shown in Figures 17 (649F, 17 μm thick emulsion), 18 (649F, 35 μm thick emulsion), and 19 (High Resolution Plates). In each case the curves represent data taken from plane wave gratings recorded at 488 nm with K = 10. In order to avoid imaginary readout angles at 1150 nm, we recorded these holograms with the low offset angle of 15°. Kogelnik[11] derived an expression relating diffraction efficiency and wavelength in volume phase gratings as follows:

$$\text{Diffraction Efficiency} = \exp\left[-\frac{\alpha(\lambda)t}{\cos\theta}\right] \sin^2\left[\frac{\pi(\delta n)}{\lambda\cos\theta}\right],$$

where the symbols are defined as follows:

$\alpha(\lambda)$ = absorption coefficient of the material

λ = wavelength

t = thickness of the material

θ = angle of incidence

δn = refractive index modulation.

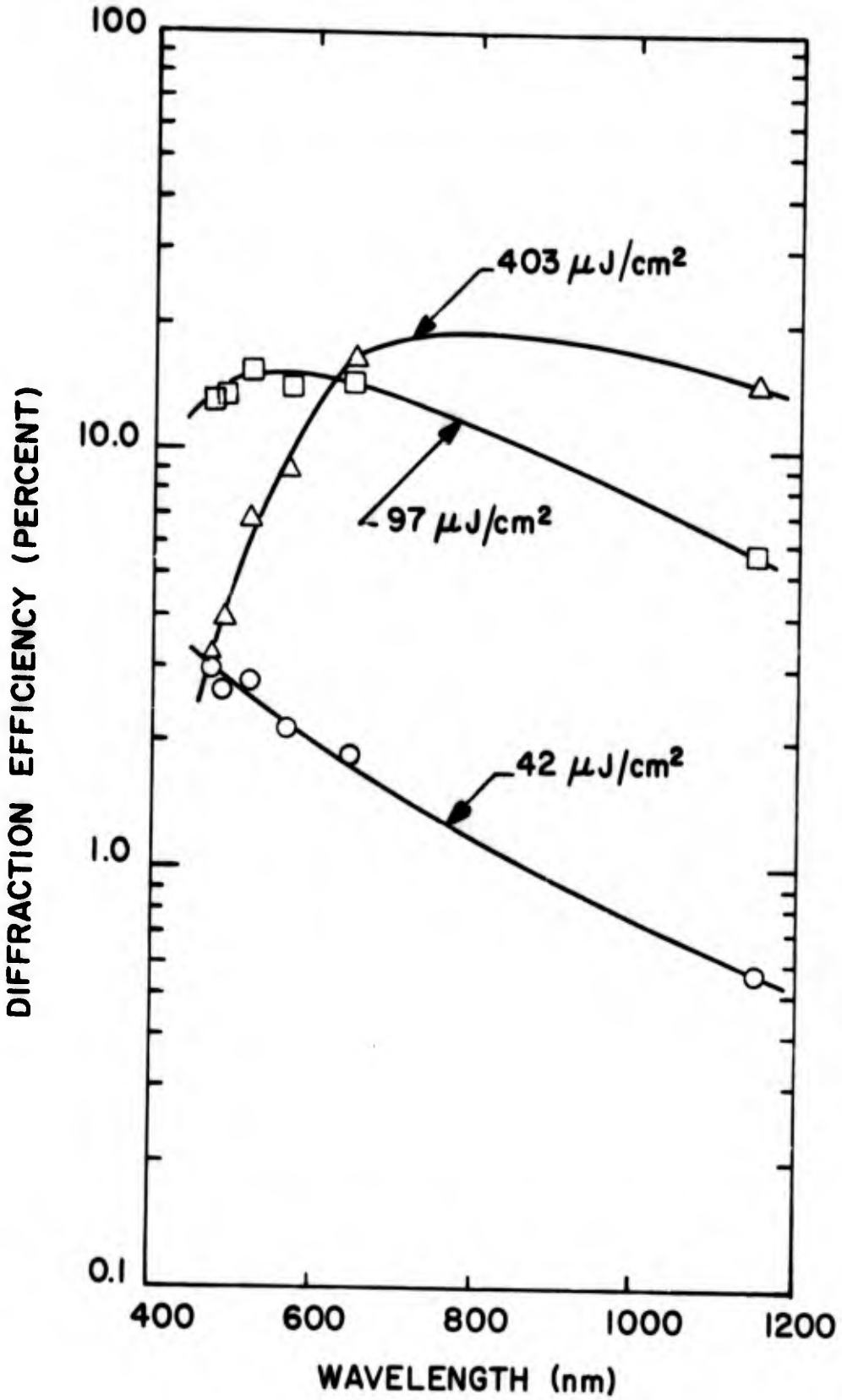

Figure 17

Spectral variation of readout efficiency for gratings recorded in bleached 649F (17μm thick).

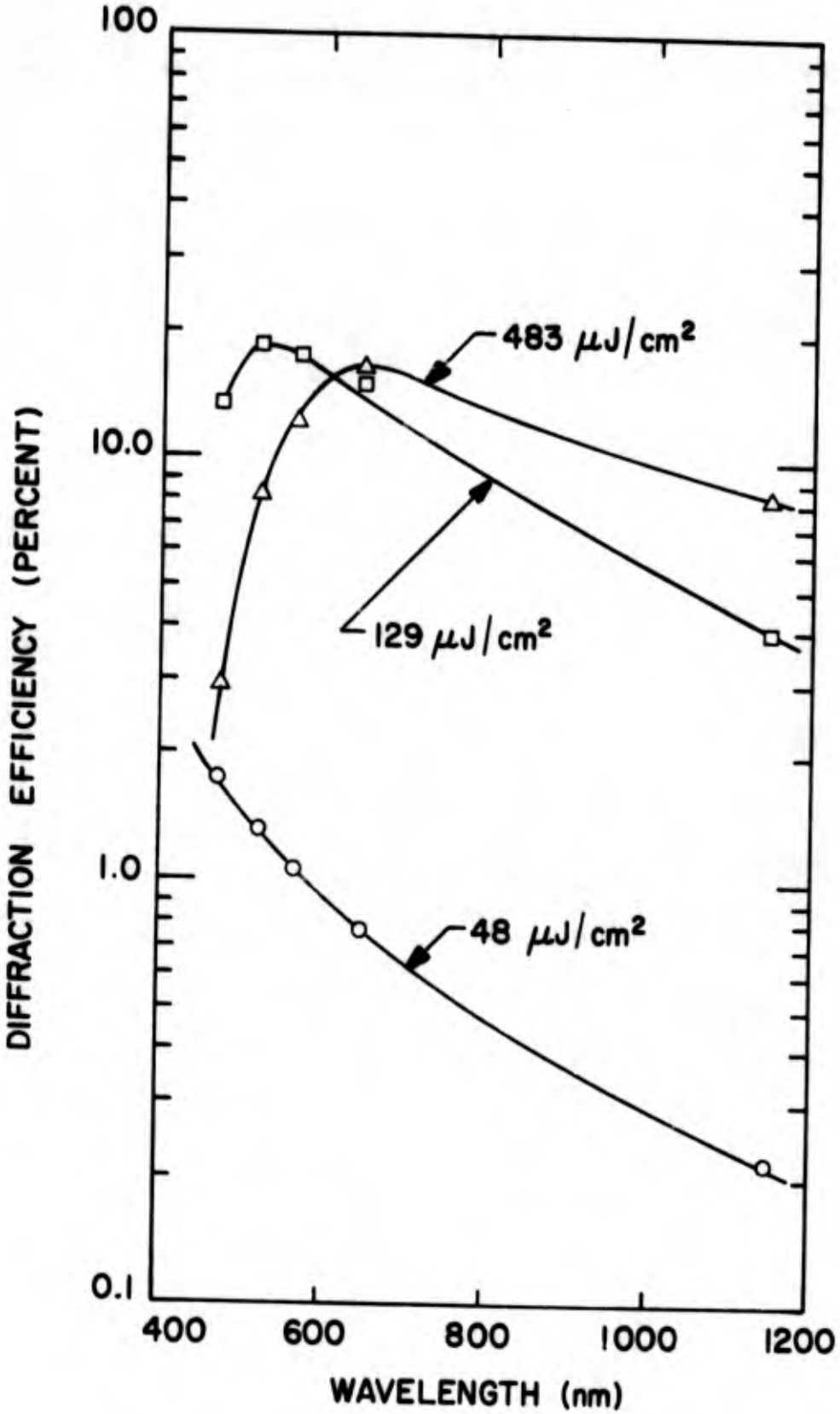

Figure 18

Spectral variation of readout efficiency for gratings recorded in bleached 649F (35μm thick).

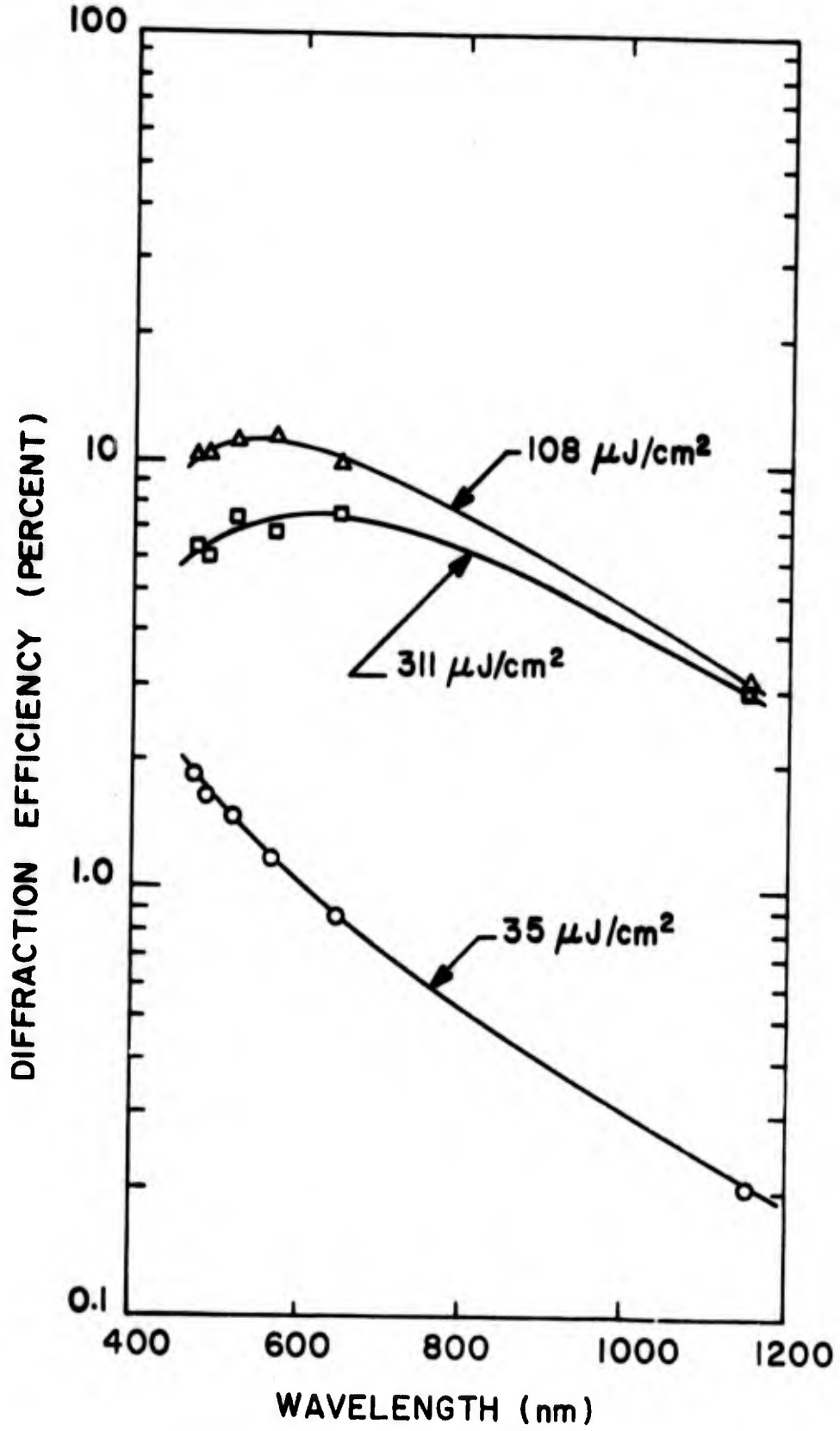

Figure 19

Spectral variation of readout efficiency for gratings recorded in bleached High Resolution Plates

If the absorption coefficient $\alpha(\lambda)$ and the refractive index modulation δn remain constant, the λ^{-1} dependence of the argument of the sin function will cause a reduction in diffraction efficiency as λ increases. In Figures 17, 18, and 19, most of the curves show a decrease in diffraction efficiency with increasing wavelength. The diffraction efficiency of gratings that were recorded with heavy exposures decreases with decreasing wavelength because relatively heavy concentrations of silver halide particles in those gratings scatter and absorb more of the short wavelength light. This is shown more explicitly by the curves in Figure 20. These show the spectral variation of both readout efficiency and transmittance, where the transmittance is defined as follows:

$$\text{Transmittance} = \frac{I_t + I_d}{I_{inc}} ,$$

and where I_t = transmitted zero order intensity
I_d = diffracted intensity
I_{inc} = incident intensity

(For most materials the transmittance is measured in a region where there is no hologram. With photographic emulsions, all silver halide grains are removed from the unexposed areas; consequently significant light scattering and absorption occurs only in exposed regions. For this reason we measured transmittance as defined above). The decrease in transmittance at short wavelengths is due primarily to increased light scattering and absorption by the silver halide grains; in other words, the absorption coefficient $\alpha(\lambda)$ increases as λ decreases.

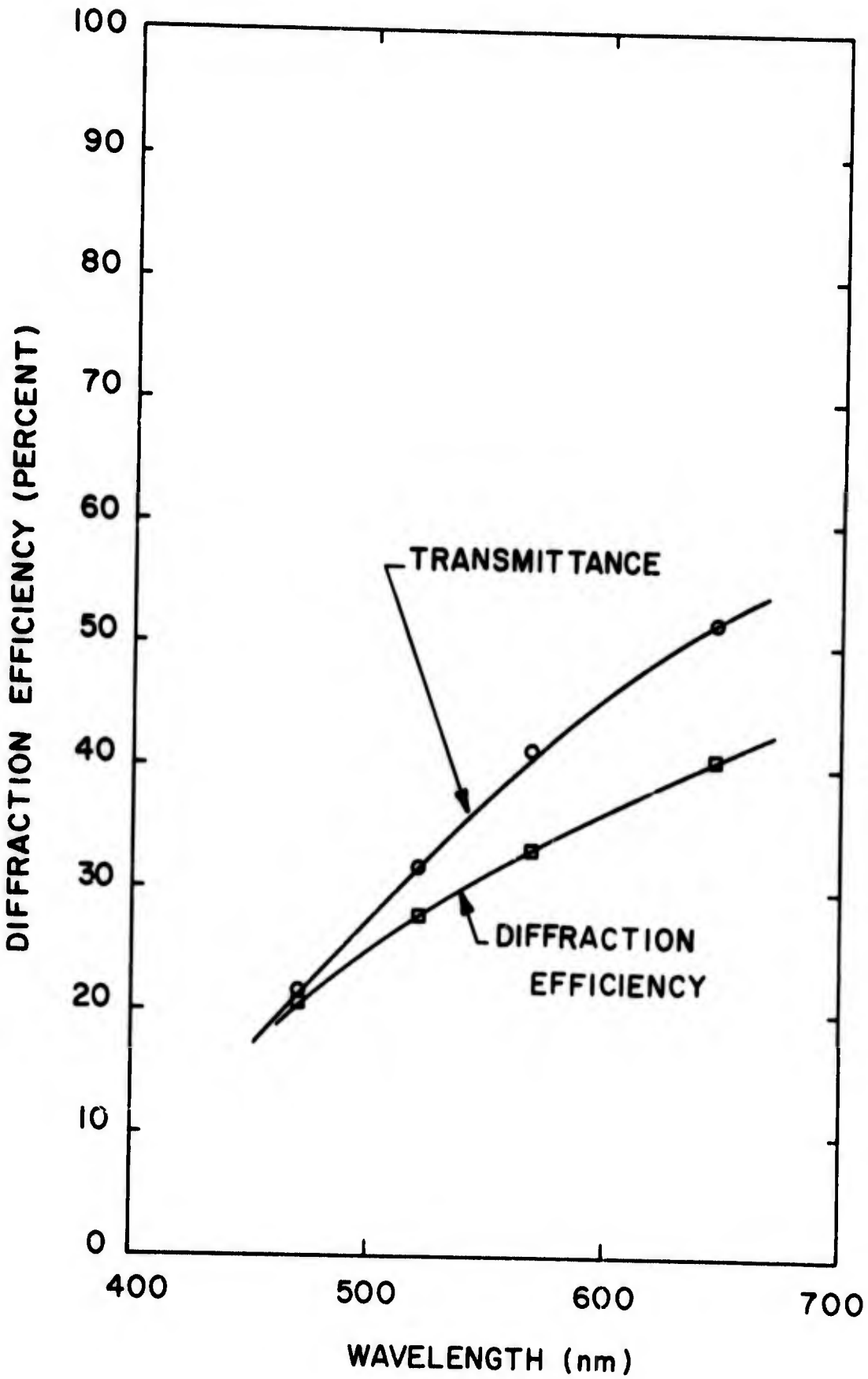

Figure 20

Spectral variation of transmittance and readout efficiency for a grating recorded in bleached 649F (17 μm thick).

3.1.3.2 Environmental Testing. — Figure 21 shows the diffraction efficiency of bleached High Resolution Plates as a function of relative humidity for several elevated temperatures. These curves represent the diffraction efficiency of a single hologram that was cycled through the 10 to 90% relative humidity range at increasingly higher temperatures. The dashed lines show the change in efficiency that occurred while the humidity was decreased. The hologram was rotated slightly at high relative humidity to compensate for emulsion swelling. The curves show that irreversible degradation occurs at high humidity; the deterioration is aggravated at elevated temperatures. Results were similar for bleached 649F holograms as shown in Figure 22. We observed increased emulsion swelling at high relative humidity with the 649F plates which we attribute to the greater emulsion thickness. At elevated temperatures and 90% relative humidity, the emulsions swelled so much that the Bragg angle shifted beyond the four degree rotation capacity of our apparatus. At low humidity the photographic emulsions were relatively unaffected by temperature variations over the entire range from -40 to 140°F. The worst case was at both high temperature and high humidity. At subfreezing temperatures, frost tended to form on the holograms and cause degradation, probably upon melting as the holograms returned to room temperature. This degradation did not occur when frost was kept from the actual hologram surface. Finally, we should note that A. J. Chenoweth[12] reported that the effect of humidity on bleached 649F plates depends on the particular bleach that is used. He observed that reversible changes occur with R-10 bleach, and that irreversible decreases in diffraction efficiency occur with potassium ferricyanide bleach.

We found that 25 hours exposure to UV radiation caused the bleached emulsions to darken. The diffraction efficiency of plane wave gratings in High Resolution Plates decreased by 7 to 20%, with an average decrease of about 12%. The UV radiation affected bleached 649F emulsions even more strongly, causing reductions in diffraction efficiency of 30 to 60%.

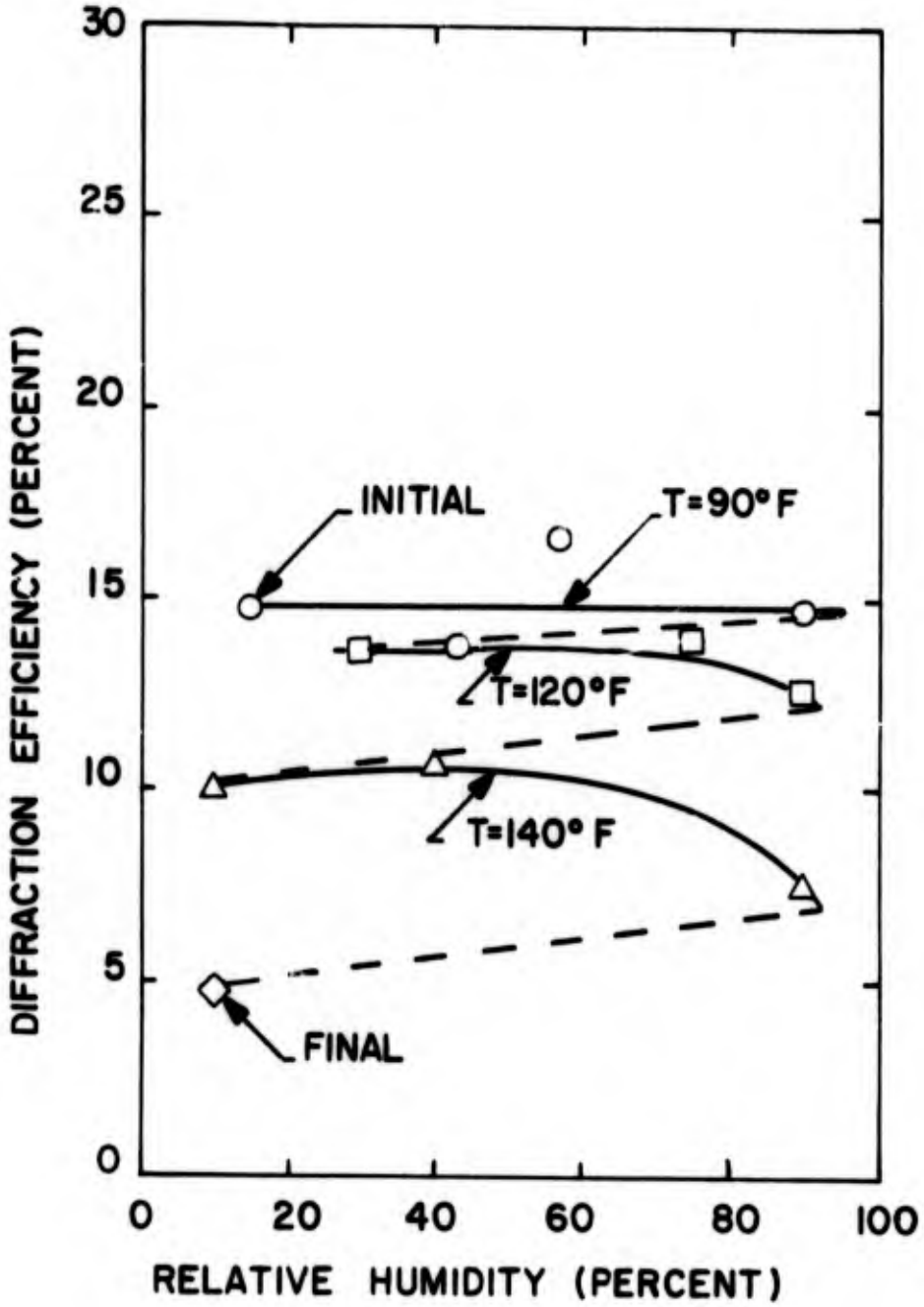

Figure 21

Diffraction efficiency as a function of relative humidity for gratings recorded in bleached High Resolution Plates.

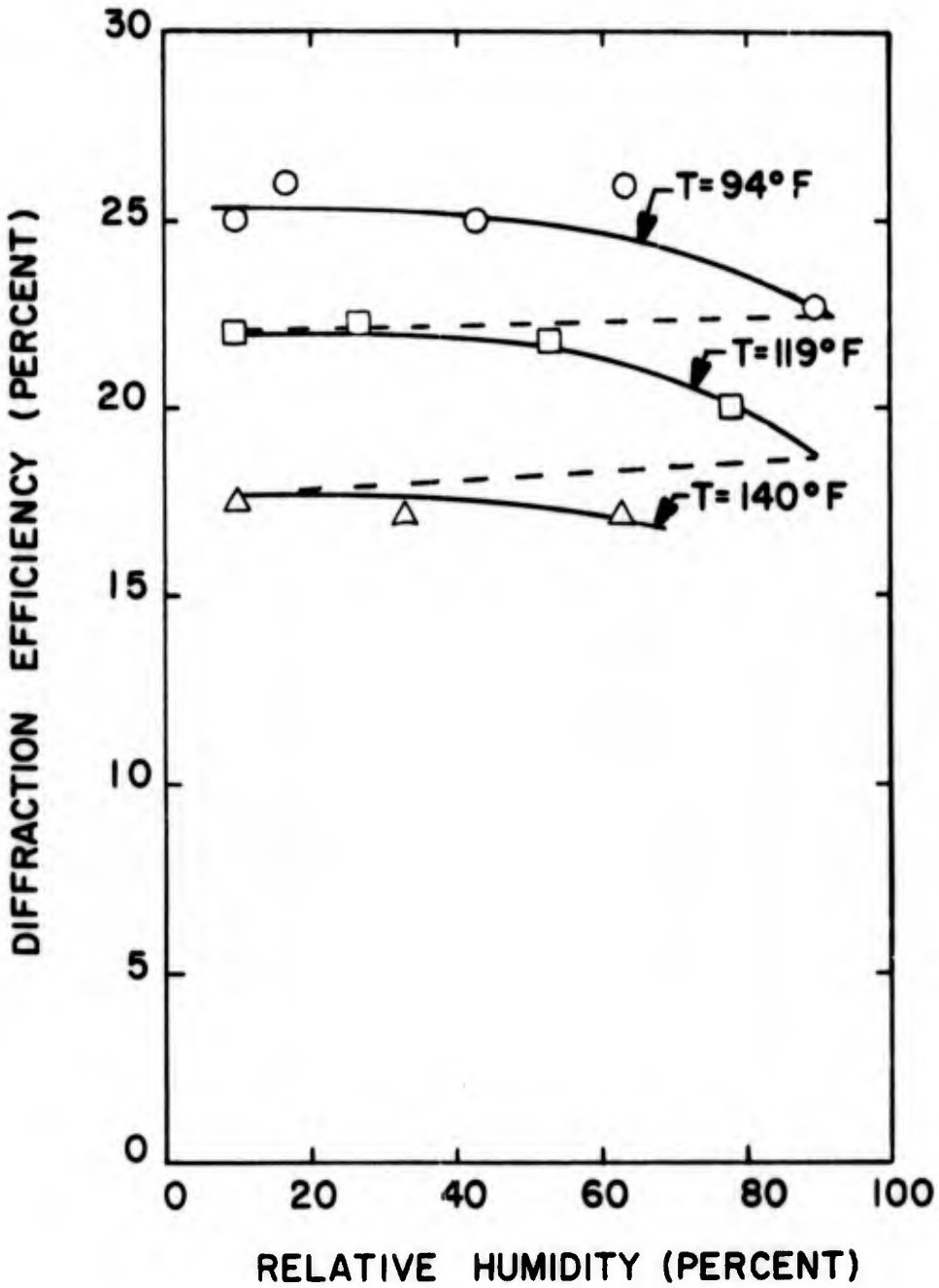

Figure 22

Diffraction efficiency as a function of relative humidity for gratings recorded in bleached 649F plates (35 μm thick).

The intensity limit for nondestructive laser readout of bleached holograms depends on the exposure, or more precisely, on the absorption of the hologram. Figure 23 is a curve showing the intensity necessary to cause destruction of the hologram as a function of the readout duration. Taking the laser readout intensity that causes burnout in 60 seconds as the minimum burnout intensity, we find the minimum is about 37 w/cm^2 for this hologram. Other holograms with less absorption have higher destructive intensity limits.

Finally, the holograms that were exposed to direct solar illumination in the out-of-doors environment were considerably degraded by the environmental conditions. The diffraction efficiency of these holograms decreased by 60 to 90%. The change in efficiency of a typical hologram is shown in Figure 24; this hologram was recorded in 649F (17 μm thick emulsion) at 633 nm. Much of the decrease in efficiency was due to darkening of the hologram caused by the solar illumination. The remainder of the decrease was probably due to humidity effects, including exposure to a few drops of rain.

3.2 Dichromated Gelatin

Dichromated gelatin is one of the most promising materials for holographic optical elements because of the high diffraction efficiencies and good signal-to-noise ratios that can be realized. The low absorption losses in dichromated gelatin holograms permits their use with high power laser beams. Dichromated gelatin is limited somewhat by its restricted spectral response and by its well-known sensitivity to high humidity.

3.2.1 Mechanism of Hologram Formation. — Holograms are believed to form in dichromated gelatin through a process of layer splitting or cracking.[13] This phenomenon is unique to dichromated gelatin and is

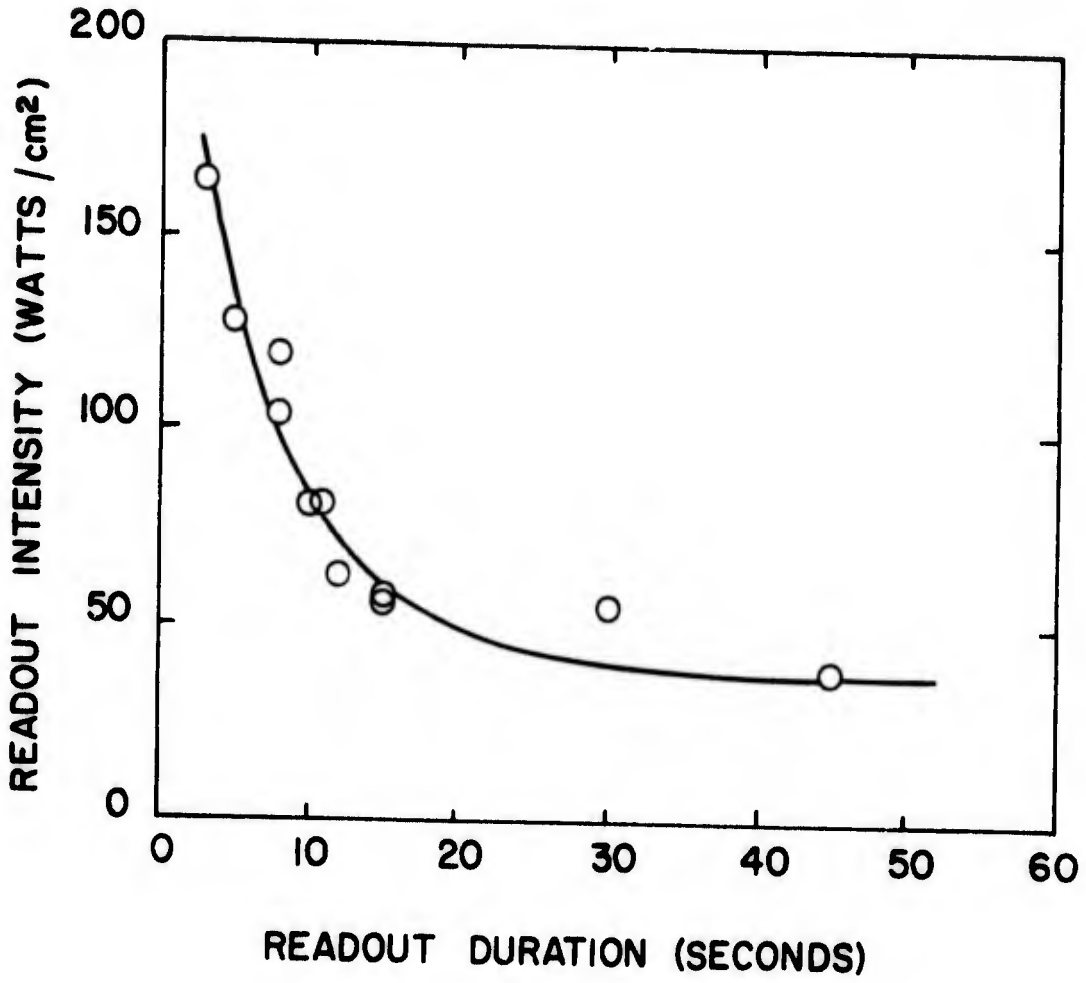

Figure 23

Destructive readout intensity as a function of readout duration for bleached 649F (17 μm thick).

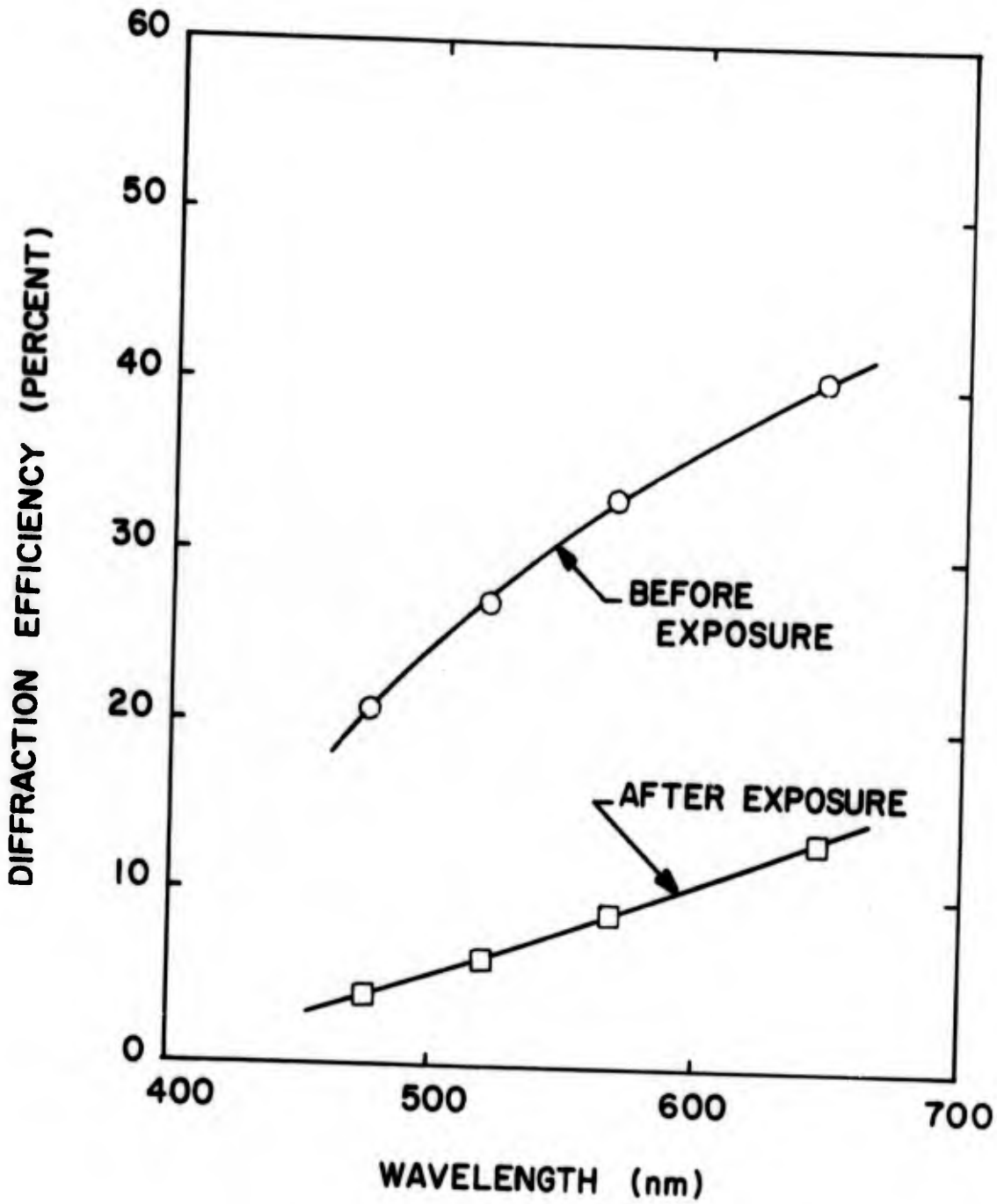

Figure 24

Diffraction efficiency as a function of wavelength for bleached 649F gratings (17 μm thick) before and after outdoor exposure.

responsible for the large values of Δn obtainable with this material. The reasons for this behavior are not entirely understood but it appears that the following explanation is consistent with experimental facts. First, exposure in the UV-blue region of the spectrum initiates cross-linking between various side groups of adjacent gelatin molecules. In this step the hexavalent chromium ion Cr^{6+} is photoreduced to trivalent Cr^{3+}, which is thought to form a complex with two or more gelatin molecules. Exposed regions appear dull yellow-brown in color in contrast to unexposed regions which are a bright yellow-orange. This is because exposed regions contain a mixture of dichromate (yellow orange), chromate (yellow), and chromic (green) ions. During the processing steps the various reaction products are removed, and the gelatin layer swells to a significant extent. In exposed regions, especially the fringe maxima, much less water is absorbed than in unexposed regions. This creates a condition of strain with a definite orientation within the gelatin layer. Finally, in the last step of processing, as the gelatin layer is rapidly dehydrated with isopropanol, there is both an increase in strain and a change in orientation. The combination of these effects causes the gelatin layer to split, or crack, in order to relieve the strain. The splitting is assumed to occur in regions of minimum exposure since crosslinked regions would have greater physical strength.

The merit of the proposed mechanism rests chiefly with the extensive experimental work of Curran and Shankoff[13] and the following observations. It is possible to obtain with consistency diffraction efficiencies approaching 100% for plane wave gratings formed in properly prepared gelatin layers derived from 649F plates. Since the gelatin layer is quite hard and very little material is removed during processing, surface relief is negligible. The layer thickness is on the order of 15 μm, implying that a Δn of about 10^{-2} is required for maximum efficiency.

However, direct measurements by Shankoff show that the maximum Δn obtainable by crosslinking alone is approximately 5×10^{-4}, or about 20 times too small. But the differential index between air and gelatin in the regions of splitting and cracking is near 5×10^{-1}; thus, a maximum Δn of 2.5×10^{-1} is possible. A more precise model that assumes the air-gelatin interfaces to be voids in a gelatin matrix, analyzed with Lorenz-Lorentz theory, implies a smaller effective maximum Δn that is still adequate to produce the high observed efficiencies.

3.2.2 Method of Use. — Dichromated gelatin is a hologram recording material of intermediate exposure sensitivity. Typical exposure requirements are 50-100 mJ/cm^2 for a 5% dichromate concentration. Spectral response extends from 350 nm to 520 nm. It appears possible to induce sensitivity in the red region of the spectrum by means of various triphenolmethane dyes.

Properly prepared dichromated gelatin plates are bright orange-yellow in color. The surface of the gelatin layer should be uniform in appearance and free from crystallized dichromate or other precipitious matter. Properly aged gelatin layers are dry to the touch after about 2 hours of free air drying following preparation. Imperfections present during hologram recording are generally not removed by processing.

At room temperature, dichromated gelatin rapidly undergoes a dark reaction. As a rule, the room temperature shelf life of gelatin layers sensitized with ammonium dichromate is about 48 hours. The most obvious sign of deterioration is the color change: overage dichromated gelatin plates are red-brown in color compared to fresh plates, which are orange-yellow in color. Under conditions of cold storage, the shelf life is on the order of 3 months or more.

Holograms are recorded in dichromated gelatin by simply exposing the plates to a predetermined average exposure level. Low efficiency holograms are produced immediately upon exposure due to crosslinking; processing greatly enhances the efficiency of these holograms. Optimum exposure levels can be precisely determined by monitoring the initial diffraction efficiency with a He-Ne laser beam. An alternative method of exposure control is provided by the variation of intensity transmission with exposure that occurs in dichromated gelatin.

Dichromated gelatin layers can be prepared by a number of methods. The highest quality holograms are obtained when the method of Chang[14] is employed to prepare the gelatin layer. The procedure begins with an unexposed Kodak 649F plate. After the silver halide is removed by fixation, the gelatin is conditioned and finally, dichromated. The steps are outlined in Table 4. An alternative method is to perform only steps 1, 8, and 11 through 13 in the table. The main advantages gained from the gelatin conditioning steps (2 through 10) appear to be better surface quality and more consistent experimental results.

It is possible, of course, to make gelatin layers, if required. They can be dichromated as described above or ammonium dichromate can be added directly to the gelatin solution before coating. A procedure for preparing gelatin layers is given in Table 5. Our experience indicates that results are comparable with dichromated gelatin prepared by either method.

Exposed dichromated gelatin can be processed by either of two methods. the first method is straightforward and consists of the following steps:

TABLE 4. Dichromated Gelatin Preparation

Preparation*

1. Fix in Part A of Kodak Rapid Fixer - 10 minutes.
2. Wash with running water at 90°F for 15 minutes.
   Start at 70°F and raise temperature at approximately 2.5°F/min. to 90°F.
3. Stand in air 1 minute.
4. Rinse in distilled water with 2 drops per liter of Photo-Flo 600 for 30 seconds.
5. Dry completely in room environment.
6. Soak in room temperature water for 2 minutes.
7. Harden in both Part A and Part B of Rapid Fixer for 10 minutes.
8. Wash for 15 minutes at 70°F in running water.
9. Rinse in Photo-Flo solution for 30 seconds.
10. Dry overnight at room temperature.
11. Soak plates for 5 minutes in 5% ammonium dichromate solution with 2 drops per liter of Photo-Flo 600.
12. Wipe ammonium dichromate off glass side of plates.
13. Dry at room temperature for at least 2 hours.

*Start with 649F plates.

TABLE 5. Preparation of Gelatin Layers

1. To 94 ml of distilled water at 70°F add 6 gm of gelatin and gently mix.
2. Warm the gelatin solution slowly to 80°F and stir thoroughly until all the gelatin has dissolved.
3. Dissolve into the gelatin solution .03 gm of ammonium dichromate.
4. Coat a 3-5 mil wet thickness of gelatin on a leveled glass substrate.
5. Cover the gelatin layer to protect it from dust and allow to dry for at least 24 hours.
6. Bake for 2 hours at 150°F and cool slowly to room temperature.
7. Proceed with dichromation as outlined in Table 4.

1. Rinse in running water for 5 minutes.
2. Dehydrate with 100% isopropanol for 5 minutes.
3. Free air dry for 1 hour.

While this procedure is quite simple it has the disadvantage of leaving a white precipitous material on the gelatin surface. The second method is more complicated than the first but provides excellent surface quality. It is outlined in the following steps:

1. Rinse in a 0.5% solution of ammonium dichromate for 5 minutes.
2. Bathe with agitation in Kodak Rapid Fixer for 5 minutes.
3. Rinse in water for 10 minutes.
4. Dehydrate in a 50/50 solution of water and isopropanol for 3 minutes.
5. Dehydrate in 100% isopropanol for 3 minutes.
6. Free air dry for 1 hour.

Dichromated gelatin holograms are easily abraded and reconstruction parameters are unfavorably affected by high levels of relative humidity. To overcome these problems the dried hologram should be baked for 2 hours at 180°F to remove residual moisture. Then a clean glass cover plate can be epoxied to the gelatin layer; a low-temperature, optical lens bonding cement is recommended for this purpose.

3.2.3 Experimental Results. — We prepared dichromated gelatin plates from standard 649F photographic plates (17 μm emulsion) with the method outlined in Table 4. Using this technique of processing the gelatin prior to sensitization, we obtained consistent and repeatable high quality holograms without the deleterious white precipitate that often forms in dichromated gelatin holograms. All holograms were recorded at a wavelength of 488 nm.

3.2.3.1 Holographic Parameters. — We measured the diffraction efficiency of plane wave gratings recorded in dichromated gelatin with K-ratios of 1, 10, and 50. These measurements are shown in Figure 25. Diffraction efficiencies range as high as 90% at an exposure level of approximately 30 mJ/cm^2 for K = 1. We found that over a wide range of exposure the incremental change in refractive index of the sensitized gelatin is linearly proportional to the exposure. At high exposures, however, some phenomenon within the gelatin tends to cause erratic behavior, as is evident in the figure.

Dichromated gelatin forms holograms with low noise. Figure 26 shows diffraction efficiency and SNR as a function of exposure for holograms of the diffuse signal recorded at K = 1. The peak SNR is 230 (24 dB) at 0.4% diffraction efficiency. At 10% diffraction efficiency, however, the SNR is less than 10.

We obtained better results at K = 10 as illustrated by Figure 27. In this case, the peak SNR reached is 550 (27 dB) at a diffraction efficiency of 1%. At 10% diffraction efficiency, the SNR is still high, at 210 (23 dB).

As with the 649F emulsions, the bandwidth of dichromated gelatin is well known to be quite high[15] so we did not measure it. Figure 28 shows the spectral variation in readout efficiency for plane wave gratings recorded in dichromated gelatin at K = 1 and K = 10. The curves follow approximately Kogelnik's expression (given in Section 3.1.3.1) relating diffraction efficiency and wavelength of volume phase gratings.

Figure 29 shows the spectral variation in both readout efficiency and transmittance of dichromated gelatin in the visible portion of the spectrum. As in the previous figure, the curve of efficiency is a monotonically decreasing function with wavelength. The transmittance of dichromated gelatin is very high, indicating little or no loss due to absorption or scattering. Most of the 10 to 15% loss is due to reflection of the laser beam at the surfaces of the plate.

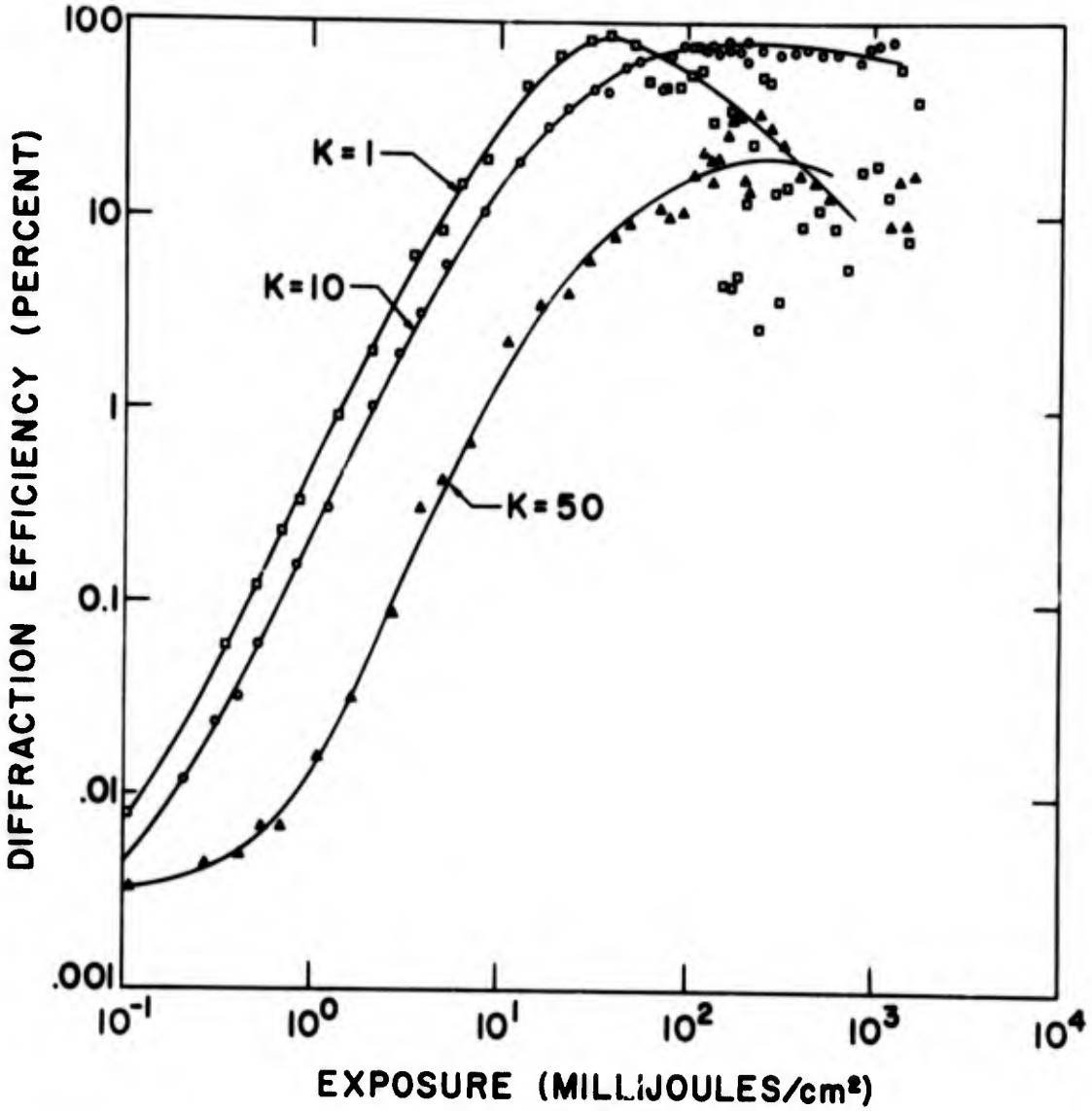

Figure 25

Diffraction efficiency as a function of exposure for plane wave gratings recorded in dichromated gelatin.

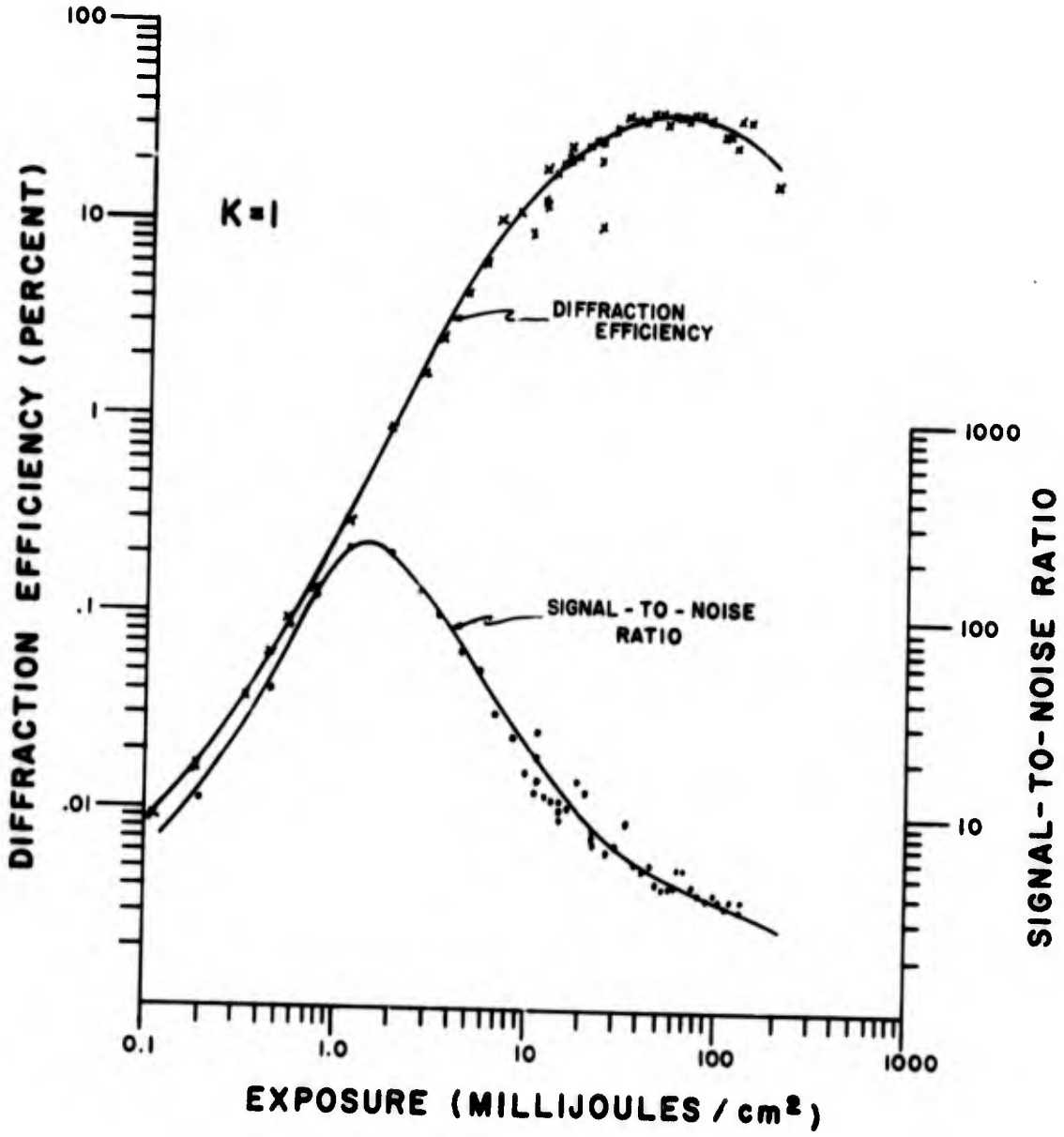

Figure 26

Diffraction efficiency and R as function of exposure for holograms recorded in dichromated gelatin

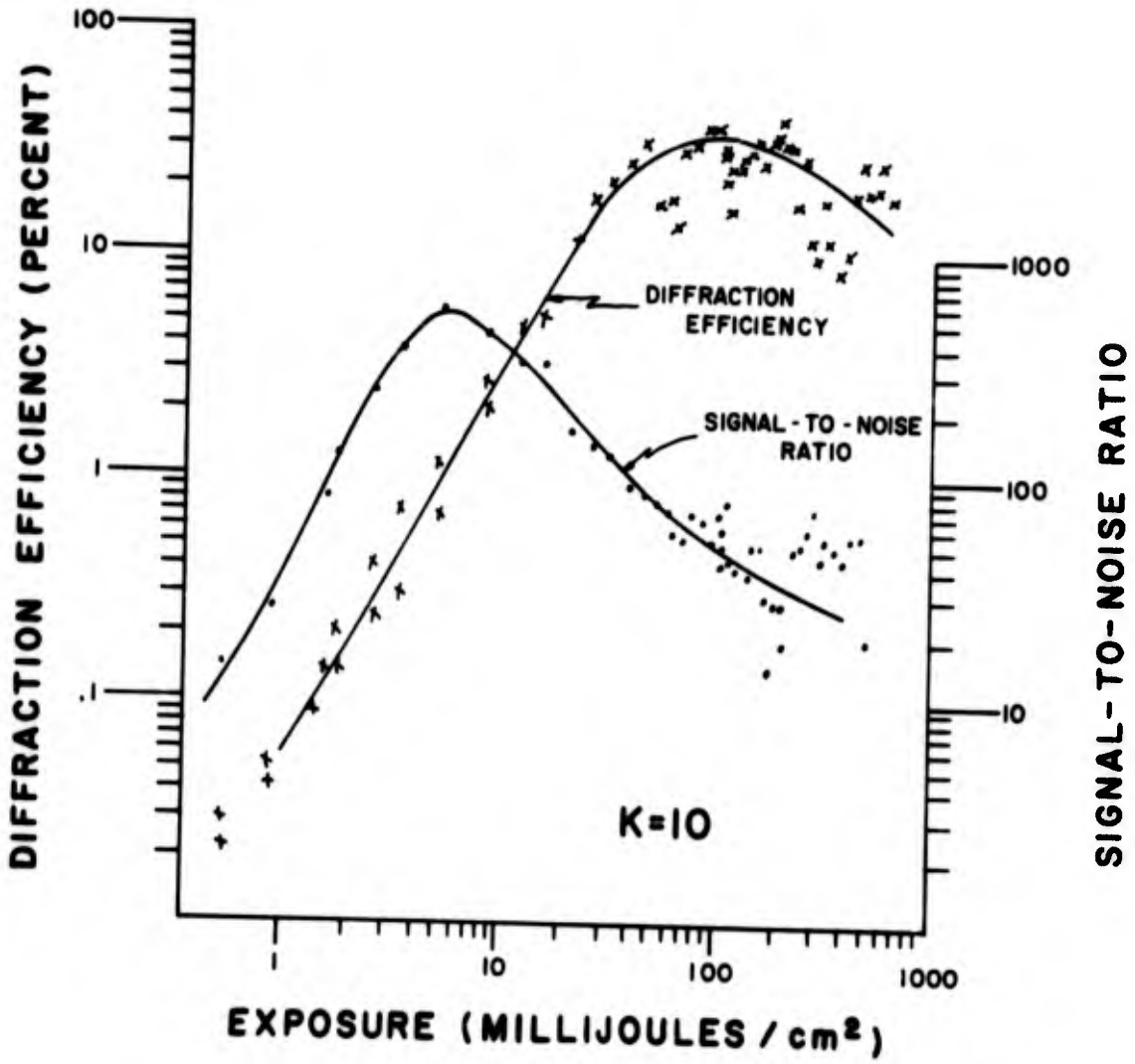

Figure 27

Diffraction efficiency and SNR of holograms recorded in dichromated gelatin with K=10.

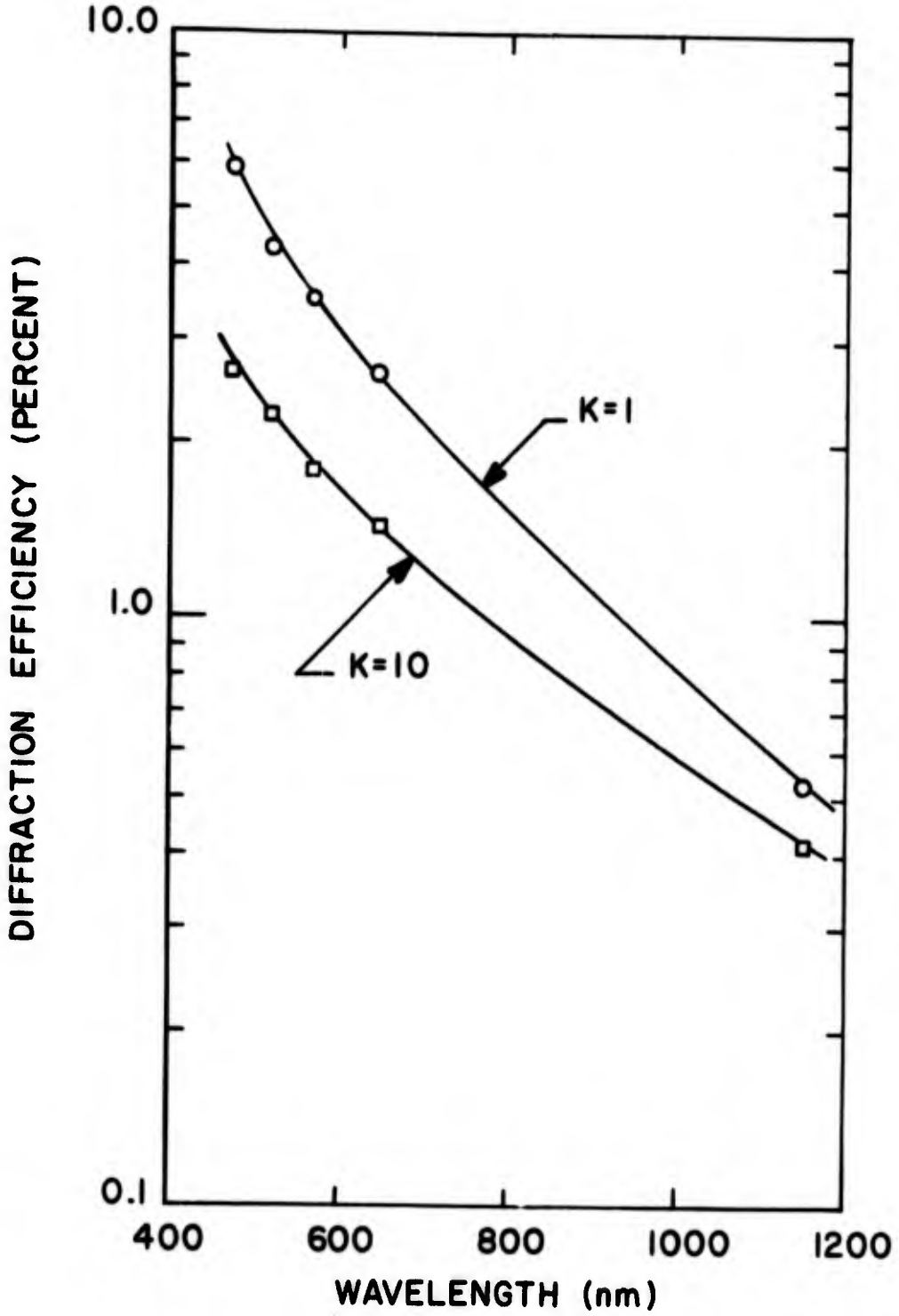

Figure 28

Spectral variation of readout efficiency for gratings recorded in dichromated gelatin

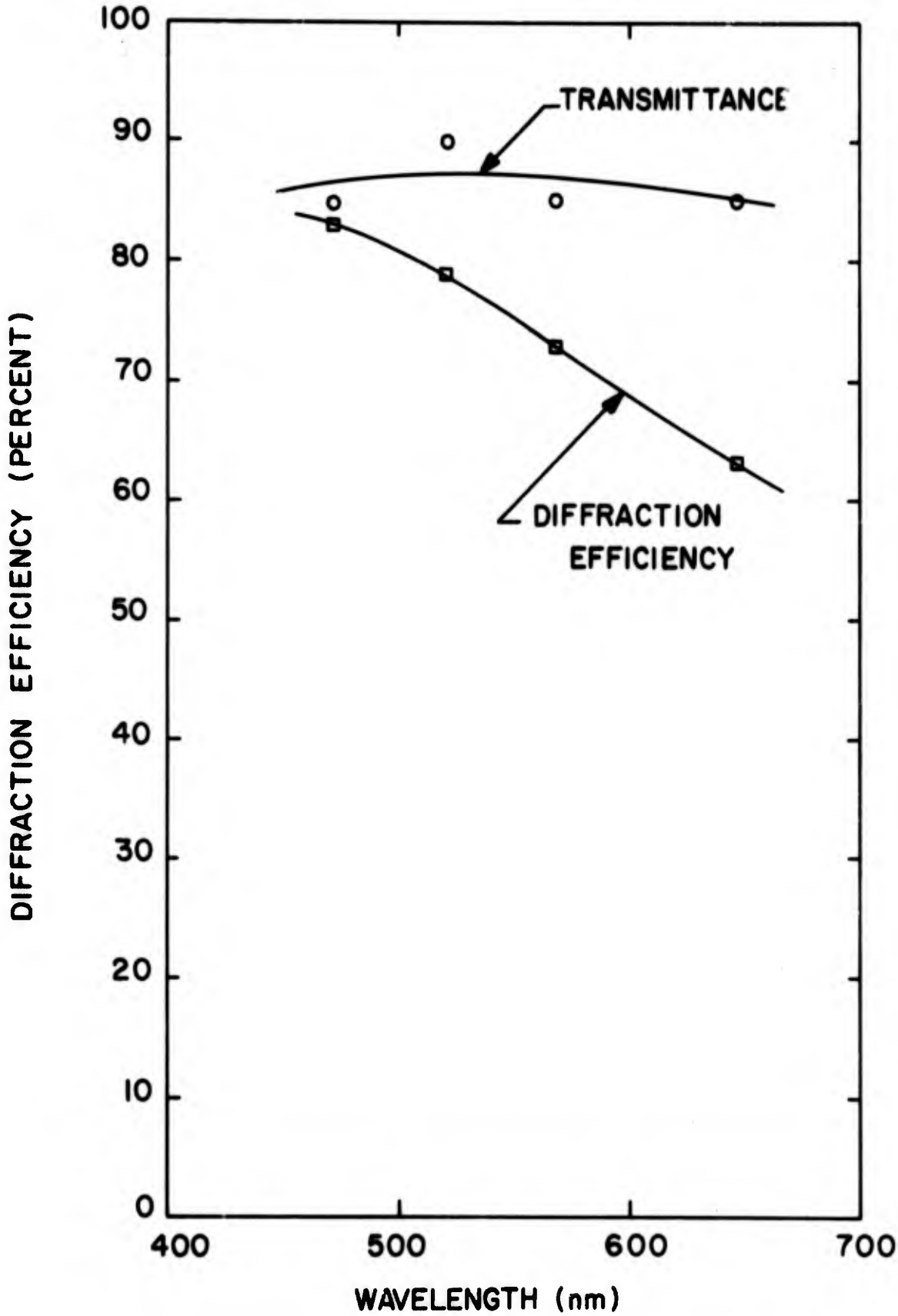

Figure 29

Spectral variation of transmittance and readout efficiency for a grating recorded in dichromated gelatin.

3.2.3.2. Environmental Testing. — Holograms recorded in dichromated gelatin are well known to be extremely sensitive to humidity; high humidity causes a drastic decrease in diffraction efficiency. This decrease in efficiency is apparently due to a swelling of the gelatin at high humidity healing the cracks that form the hologram. The degradation can be expected to be aggravated at elevated temperatures which tend to further soften the gelatin. Because of this extreme sensitivity to humidity, we restricted our investigations to dichromated gelatin holograms that were overcoated with various materials. It was hoped that these materials would form layers impervious to water vapor. These materials were first tested on layers of plain gelatin; those which formed good coatings over the gelatin were selected for testing on actual dichromated gelatin holograms. Materials that failed this initial test include allyl diglycol carbonate monomer, which failed to polymerize on gelatin; diethylene glycol diacrylate monomer, which did not adhere well following polymerization; and several resins, which formed poor surfaces.

We achieved good coatings with two materials, polyvinylcarbazole (PVK) and dichloroethylene (Saran). These materials were dissolved in appropriate solvents (tetrahydrofuran and methyl ethyl ketone, respectively) to concentrations of 4 to 8%, and the gelatin plates dip coated with the solutions. Although the coatings did not appear to affect the diffraction efficiency of dichromated gelatin holograms, they were not impervious to water vapor. Holograms coated with these materials degraded at relative humidity levels of 50 to 80%. Figure 30 shows the diffraction efficiency as a function of relative humidity at room temperature (72°F) for a dichromated gelatin hologram coated with Saran. In this case the diffraction efficiency decreased greatly when the relative humidity reached 80%.

We were able to eliminate the sensitivity of dichromated gelatin holograms to elevated temperature-humidity conditions by cementing

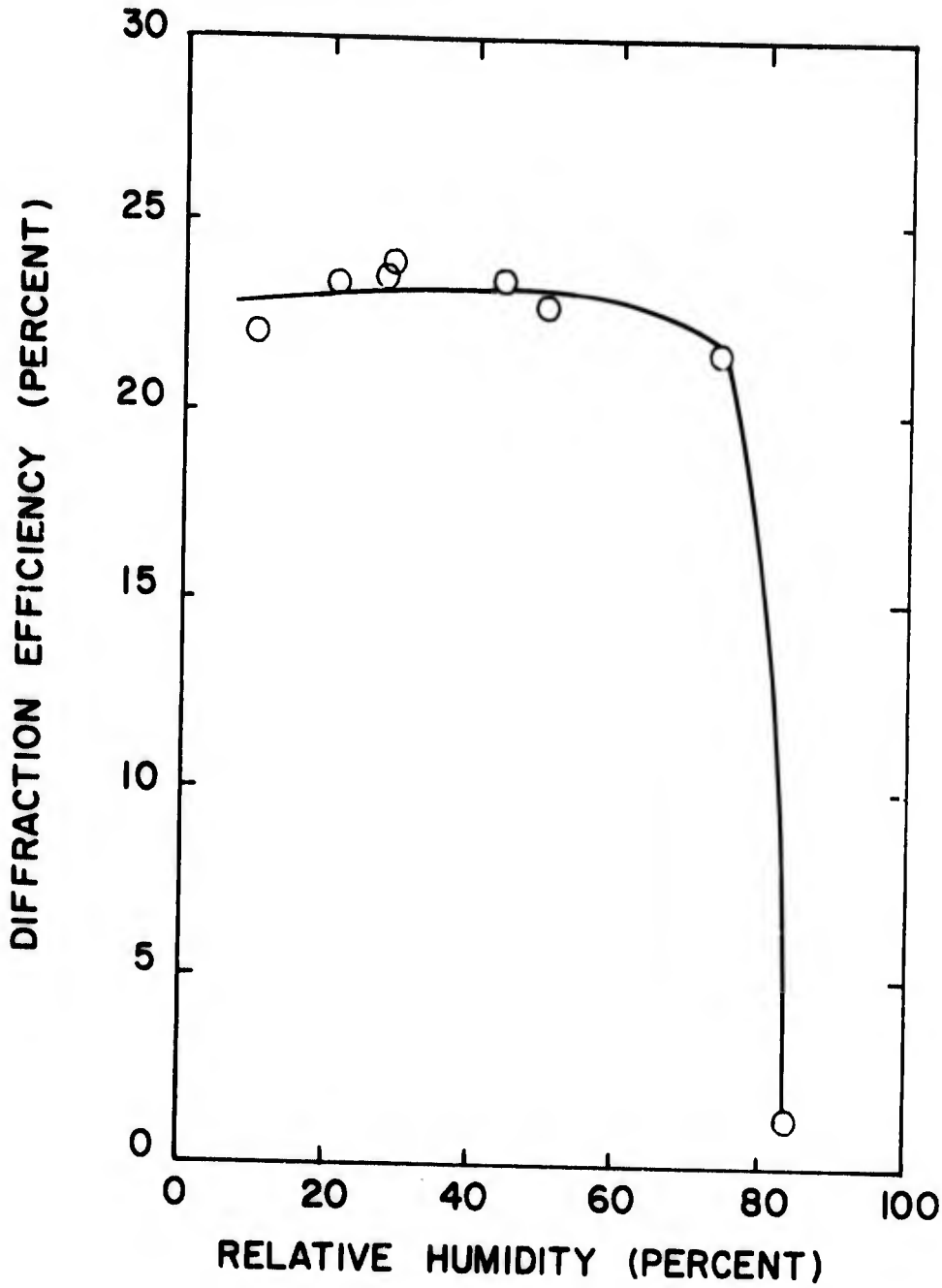

Figure 30

Diffraction efficiency as a function of relative humidity for a dichromated gelatin grating that was overcoated with Saran.

a glass cover plate to the gelatin surface. It is important first to dry the gelatin layer completely, since the combination of residual water and high (120 to 140°F) temperature apparently soften the gelatin sufficiently to cause irreversible degradation. By baking the gelatin layer at 180°F prior to cementing the cover plate, we were able to prevent degradation of holograms at elevated temperature and humidity.

Dichromated gelatin holograms were not affected by exposure to UV radiation. There was no change in diffraction efficiency of holograms that were given 80 hours of UV exposure.

The low absorption of dichromated gelatin holograms gives them a high limit of nondestructive illumination intensity. Figure 31 shows the destructive intensity as a function of the duration of readout. At a duration of 60 seconds, the minimum destructive intensity is about 3000 watts/cm^2. This is one of the highest intensity figures for the materials we tested.

Dichromated gelatin holograms did not withstand well the 50 hours exposure to direct solar illumination and out-of-doors environment. Since these holograms were not protected with a cover plate, the degradation was undoubtedly due to the humidity. Figure 32 shows the large change in diffraction efficiency that resulted. This illustrates again the need for protecting dichromated gelatin holograms from the effects of humidity.

3.3 Photopolymer

Photopolymer materials are capable of recording high quality volume phase holograms. In addition, they are self-developing, grain-free, and can be prepared in films of any reasonable thickness. Before exposure, these materials generally consist of several components, including a monomer, an initiator system, and a spectral sensitizer. Several photopolymer systems are known such as those reported by Close et al.[16] and

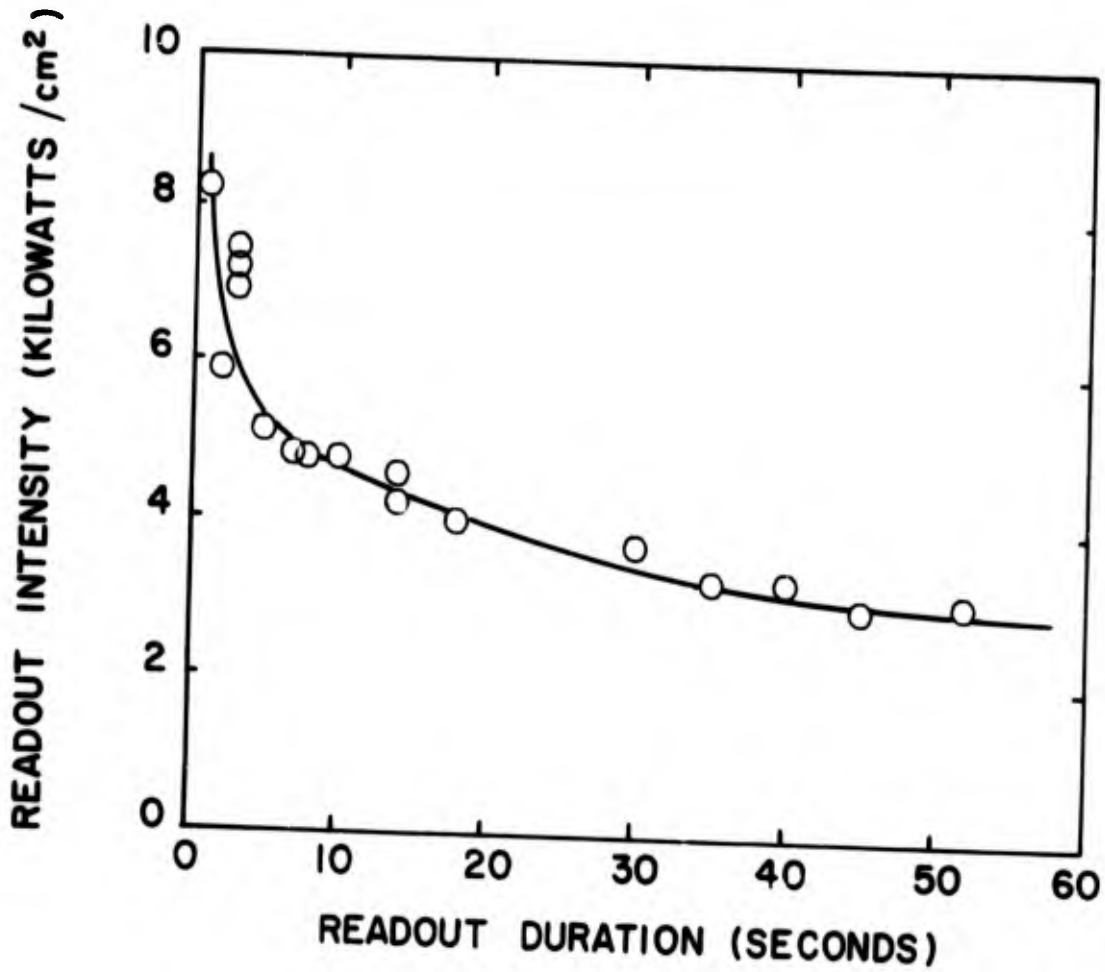

Figure 31

Destructive readout intensity as a function of readout duration for dichromated gelatin.

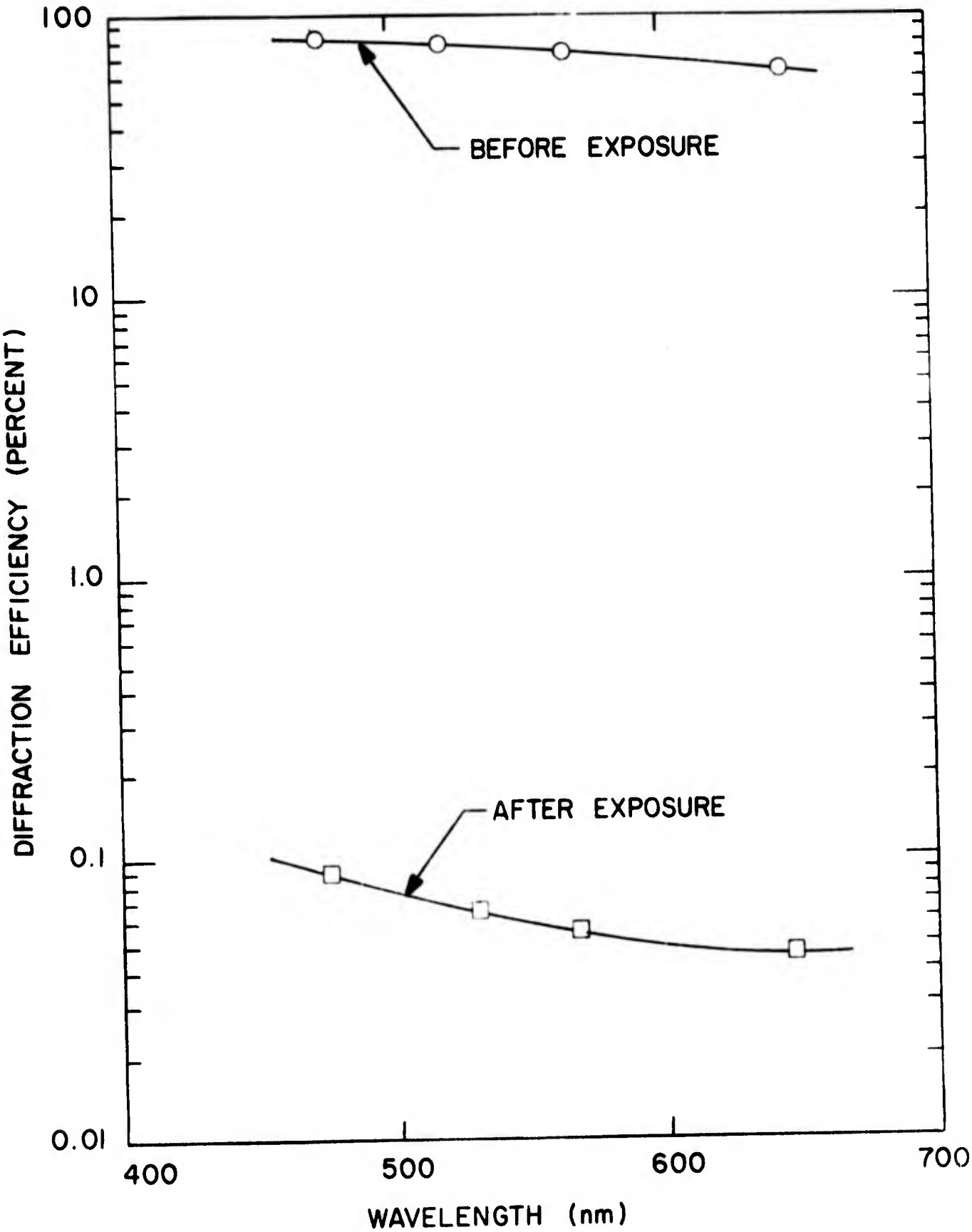

Figure 32

Diffraction efficiency as a function of wavelength for dichromated gelatin gratings, before and after outdoor exposure.

Jenney[17], which form holograms in part as surface modulation. We chose to concentrate our investigations on a photopolymer material developed by E. I. duPont de Nemours and Co.[18] Previous results[19] with this material suggest that it is among the most promising photopolymer systems for holography.

The DuPont photopolymer consists of four components: a liquid monomer, an initiator system, a binder, and a small amount of plasticizer. Upon exposure to active radiation, the initiator system forms free radicals that start polymerization of the monomer. The binder is a cellulosic polymer that forms a matrix to hold the other components. The mixture is generally coated on a substrate of glass or film.

3.3.1 Mechanism of Hologram Formation. — Holograms are formed in photopolymer through a complicated process of polymerization and monomer diffusion. Hologram formation can be considered as occurring in the three steps outlined in Figure 33. In the first step, exposure to the holographic interference pattern polymerizes some of the monomer in amounts proportional to the light intensity. Since most of the polymerization takes place in the high intensity fringes, spatial variations are left in the concentration of remaining monomer. In the second step, with the photopolymer in darkness, the relatively small monomer molecules diffuse (as shown by the arrows in the figure) to reduce the concentration gradients. When the diffusion process is complete, a final exposure to actinic radiation of uniform intensity polymerizes the remaining monomer leaving a stable and permanent hologram.

When it is polymerized in bulk form the material shrinks and its refractive index increases. The variation in exposure of the holographic interference pattern might be expected to cause a thickness variation that corresponds to the amount of polymerization. Furthermore, the mass transport due to the diffusion process might also be expected to cause a thickness variation in the material. At holographic spatial frequencies,

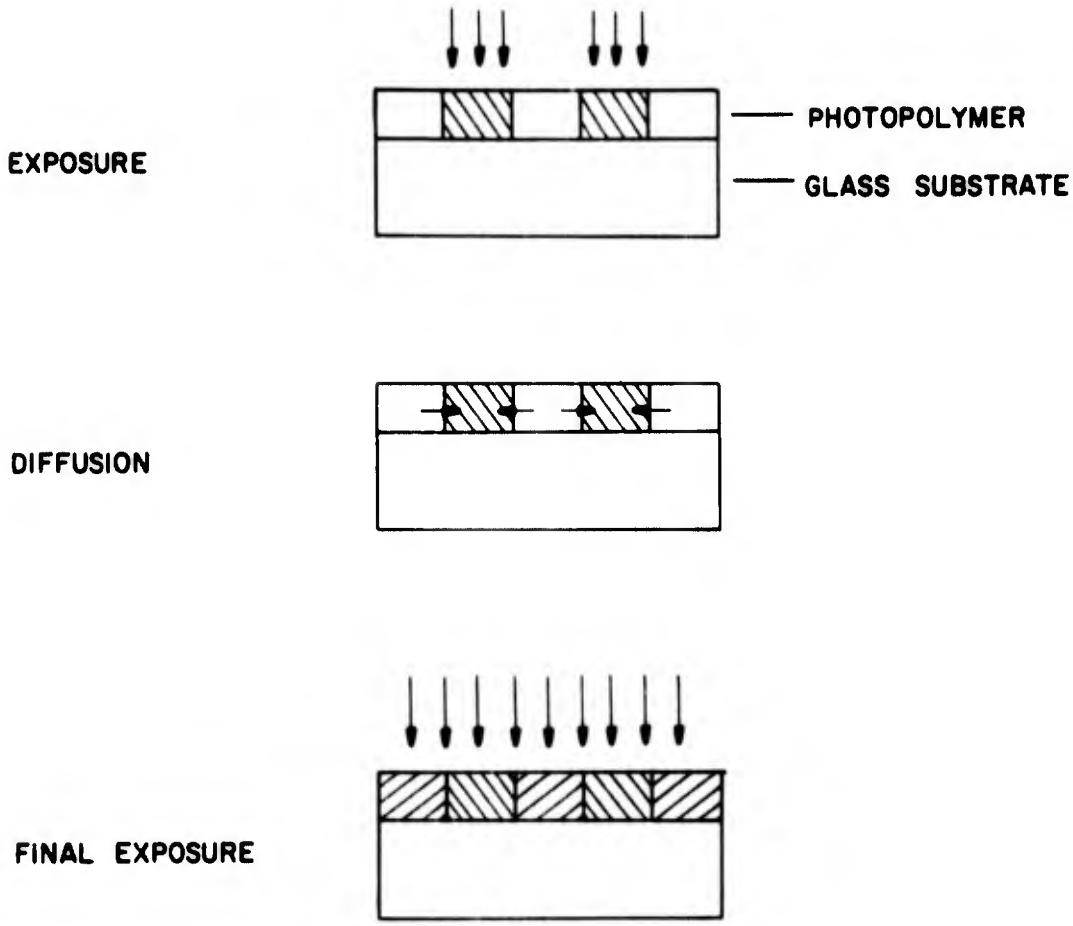

Figure 33

tems of hologram formation in photopolymer.

however, no such thickness variation is observed, indicating that instead, density variations are created in the material. These imply variations in refractive index that give rise to the diffraction of light by the hologram.

The three steps are illustrated by Figure 34, a curve of diffraction efficiency as a function of time that was recorded during the formation of a hologram. This curve was obtained by reading out the hologram with nonactinic light from a He-Ne laser. The upper curve is a recorder trace of the output of a detector that monitored the diffracted He-Ne light. The lower curve is the output of a detector that monitored the UV radiation that was used to record the hologram; it shows the initial exposure, diffusion period, and final exposure, which, for convenience, was made with the reference beam. The upper curve shows that the diffraction efficiency rises during and immediately following the initial exposure. While monomer is diffusing, the diffraction efficiency decreases to zero and rises slowly. Finally, the diffraction efficiency rises rapidly to its highest value during the final exposure.

This view of a three step process separating polymerization and diffusion is convenient, but not completely accurate; in practice, some diffusion occurs during the polymerization steps and probably some monomer polymerizes during the diffusion step. In the extreme case of low intensity exposures, the rate of diffusion may equal or exceed the rate of polymerization, and the hologram is recorded in one long continuous exposure.

3.3.2 Method of Use. — The DuPont photopolymer is basically UV sensitive. Exposure sensitivity at 364 nm (one UV line of the argon laser) is approximately 1 mJ/cm^2. An orange dye can be added to sensitize the material to the blue-green region of the visible spectrum; the sensitivity is then about 20 to 50 mJ/cm^2 for the blue or green light.

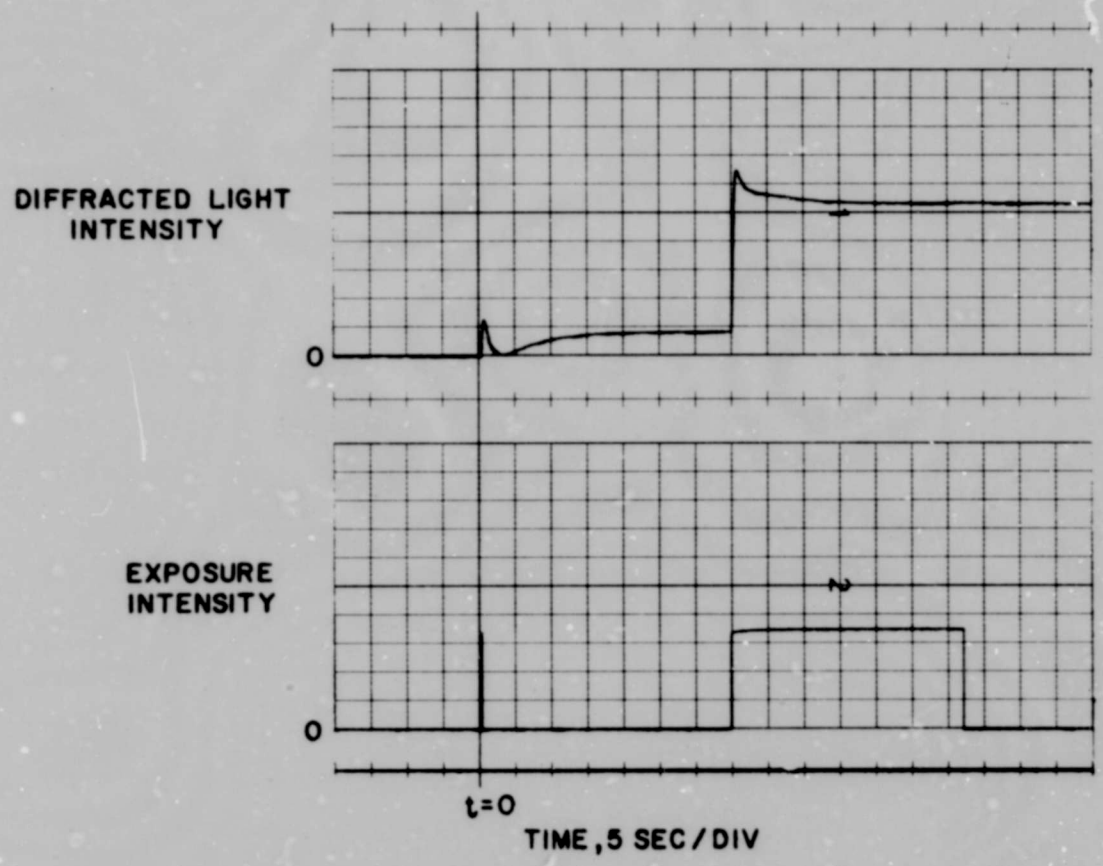

Figure 34

Diffracted intensity at 633 nm as a function of time (dia-
gram for ablation in photoresist).

Photopolymer films are prepared by first dissolving the mixture in an appropriate solvent such as methylene chloride or acetone. Films can be prepared from the solution by coating or casting; we generally made coatings 50 to 70 μm thick on glass plates with a Gardner variable thickness coating knife. After the solvent evaporates, a solid but soft and somewhat tacky layer of photopolymer remains. This can be covered with a sheet of clear film to protect it from dust and scratches as well as oxygen, which is an inhibitor to the polymerization.

Oxygen inhibits polymerization by terminating the polymer chains. One of three steps can be taken to eliminate this problem: oxygen can be kept from the photopolymer by a cover sheet, the photopolymer can be exposed in an oxygen-free atmosphere, or the photopolymer can be exposed with radiation of sufficient intensity that the rate of polymerization exceeds the rate of oxygen diffusion into the photopolymer layer. The last method requires exposure times of the order of one second or less.

3.3.3 Experimental Results. — The photopolymer materials we used in this investigation were supplied in solution form by the Photo Products Department of DuPont. We coated the solution onto glass plates to dry thicknesses of 50 to 70 μm. Oxygen was kept from the photopolymer surface with a polyester cover sheet approximately 4 mils thick. Our standard recording procedure was to expose the material to the holographic interference pattern for the desired time, allow at least two minutes for diffusion, and polymerize the remaining monomer with incoherent UV light from an intense source. The final polymerization could be conveniently carried out with the reference beam, but polymerization was faster with the UV light.

The blue-green sensitizing dye appears to cause the formation of scattering centers in the photopolymer. Since the material is otherwise very free of light scattering, we chose to investigate only materials

without the blue-green sensitizer, at the cost of considerable sensitivity at the blue wavelengths we employed.

3.3.3.1 Holographic Parameters. Figure 35 shows diffraction efficiency as a function of exposure for plane wave gratings recorded in DuPont photopolymer that was about 70 μm thick. These gratings were recorded at a wavelength of 458 nm with K-ratios of 1, 8, and 62. A peak diffraction efficiency slightly over 80% was reached with K = 1 at an exposure of $2J/cm^2$. The sensitivity was very low because, as mentioned previously, the material was not sensitized to the blue light. Unlike our investigations with most of the materials, we oriented the photopolymer so that the angle of incidence was the same for both beams; we found that the holographic performance was more consistent with the interference fringes perpendicular to photopolymer surface.

Figure 36 shows the variation of SNR and diffraction efficiency with exposure for holograms recorded in photopolymer that was about 50 μm thick. These holograms were recorded at a wavelength of 488 nm with K = 4. The sensitivity is somewhat lower at the longer wavelength. The SNR reaches a peak of 200 (23 dB) with a diffraction efficiency of 3%. At 10% diffraction efficiency, the SNR is 160 (22 dB). Earlier results with 70 μm thick material at 458 nm were better although less complete. These are given in Table 6. The high SNR's at several precent diffraction efficiency are comparable to the results obtained with dichromated gelatin.

Photopolymer has a bandpass response to spatial frequencies. This is illustrated by Figure 37 a curve of diffraction efficiency as a function of spatial frequency for plane wave gratings recorded at various offset angles. The response is low at low spatial frequencies because of the limited distance over which the monomer can readily diffuse. The poor response at low spatial frequencies can be an advantage since low frequency intermodulation noise is reduced. It is not clear why the high

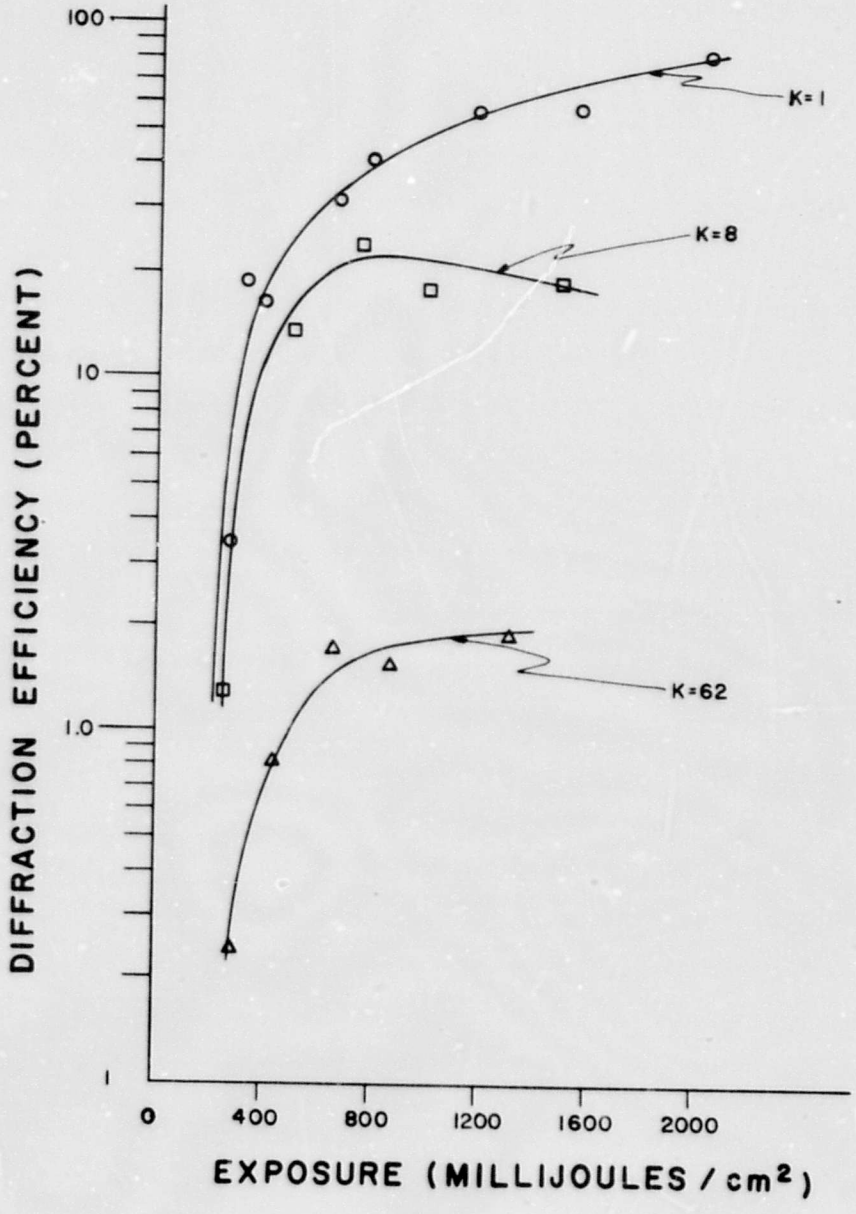

Figure 35

Diffraction efficiency as a function of exposure for plane wave gratings recorded in 70um thick photopolymer at 458nm.

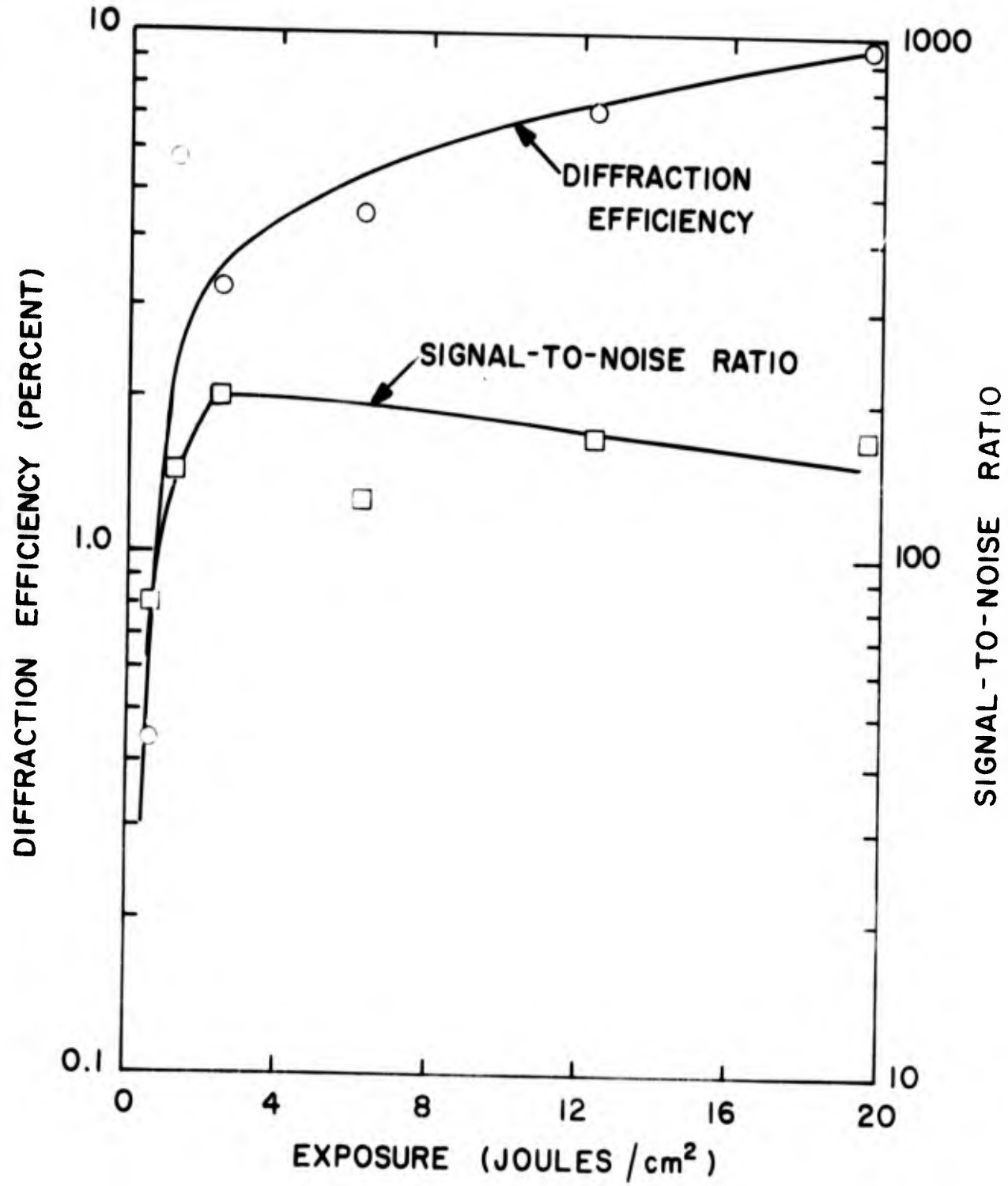

Figure 36

Diffraction efficiency and SNR as functions of exposure for holograms recorded in 50 μ thick photopolymer at 488 nm.

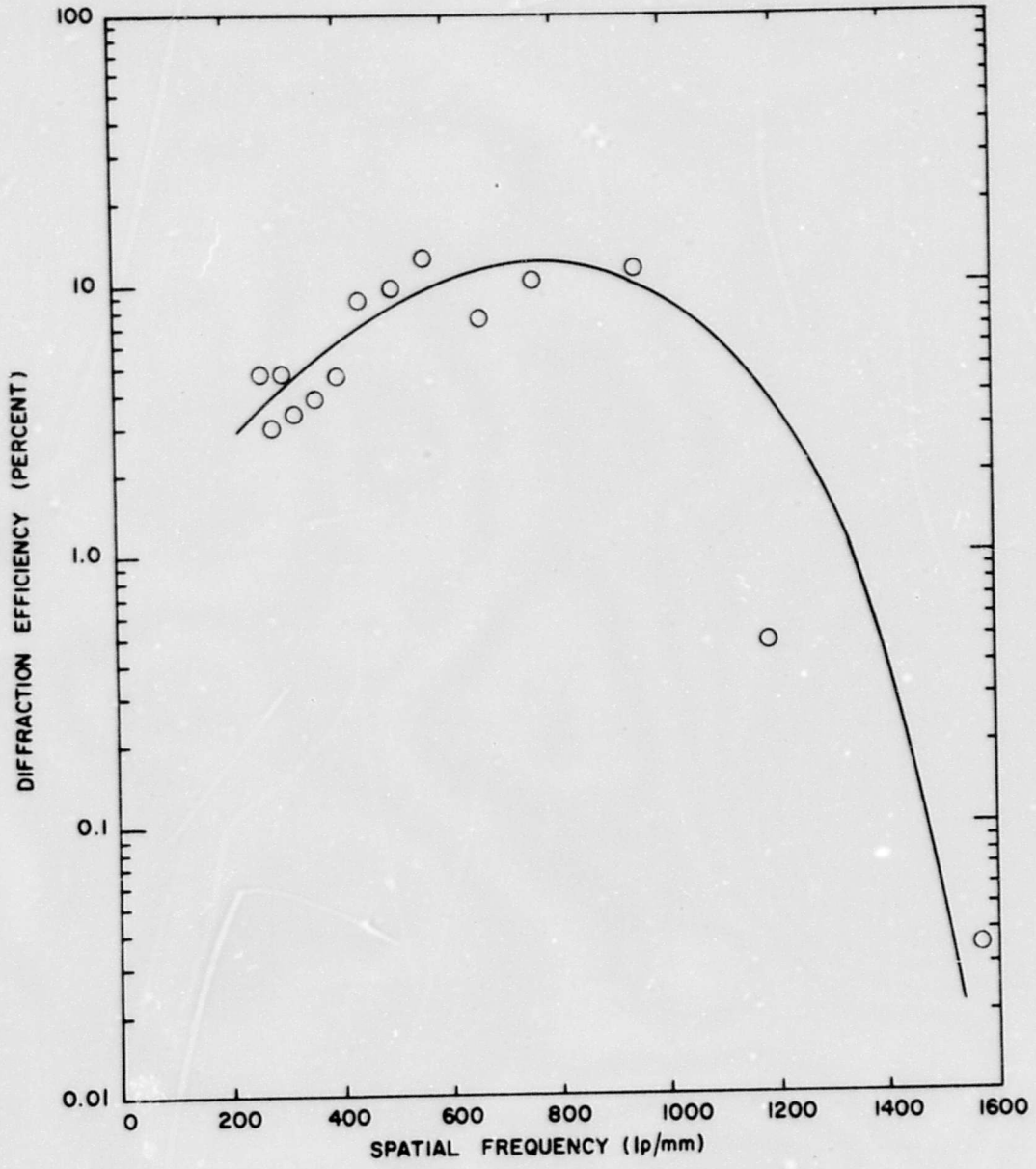

Figure 37

Spatial frequency response of photopolymer

frequency response is limited to about 1000 lines/mm; this may be a function of the length of the polymer chains that are formed.

K-ratio	Exposure	Diffraction Efficiency	SNR
12.5	1060 mJ/cm^2	10.0%	24 dB
55	738 mJ/cm^2	1.4%	28 dB

TABLE 6

SNR and Diffraction Efficiency Data for Photopolymer

Figure 38 shows the spectral variation in readout efficiency and transmittance for a photopolymer hologram of high efficiency. The curves are similar to those of dichromated gelatin. The diffraction efficiency decreases with increasing wavelength faster than Kogelnik's expression predicts for the change in wavelength alone. Evidently, the refractive index modulation decreases at longer wavelengths. Absorption of light by the photopolymer is very low throughout the visible spectrum. (Significant absorption occurs in the blue-green region of the spectrum when the extra dye is added to sensitize the material to light of that wavelength region).

3.3.3.2 Environmental Testing. As mentioned previously we kept oxygen from the photopolymer during the recording process with a polyester cover sheet. Once polymerization is complete, the cover sheet may be either left on the photopolymer to protect its surface, or removed as desired. We found that the presence of the cover sheet affected the ability of the photopolymer to withstand adverse environmental conditions.

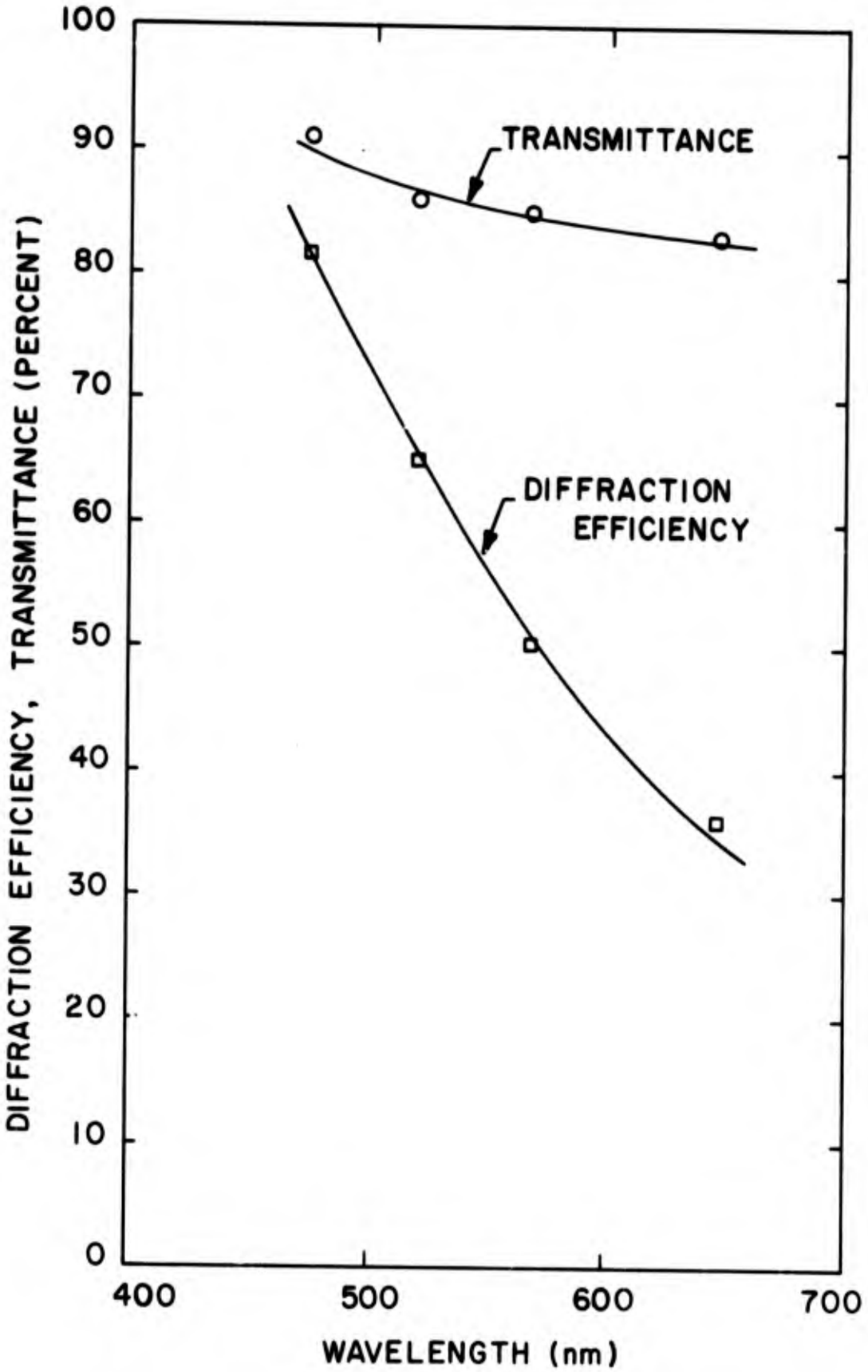

Figure 38

Spectral variation of transmittance and readout efficiency for a grating recorded in photopolymer.

With the cover sheet, photopolymer holograms began to degrade at 100°F with low humidity. This is illustrated by Figure 39 which shows constant temperature curves of diffraction efficiency as a function of relative humidity. High humidity causes some change in efficiency but less than occurs due to the increasing temperature. (The large change that occured in the increase from 85°F to 112°F is due to an inadvertant but brief temperature overshoot to 150°F.) A possible explanation for this behavior is that residual monomer diffuses at the elevated temperatures to decrease the density variations that form the hologram. This is not consistent, however, with our observation that, at low humidity, temperatures as high as 140°F do not significantly affect holograms without the cover sheet. In this case high temperature (140°F) and high humidity (80%) reduced the diffraction efficiency permanently by 50%. Although humidity would not be expected to affect this photopolymer once it is completely polymerized, it may be possible that the combination of high temperature and humidity tend to anneal the material, reducing the density variations that form the hologram. Photopolymer holograms were not affected by low temperatures (to -40°F).

Exposure to UV radiation did not affect photopolymer holograms for up to 25 hours. Longer exposure caused gradual deterioration of the holograms, with a 25% decrease in efficiency occurring after 40 hours exposure. This deterioration was unexpected, since once the material is polymerized, it is considered to be very stable.

Figure 40 shows the readout intensity required to destroy the hologram as a function of the readout duration. The curve extrapolates to slightly more than 2000 watts/cm^2 at 60 seconds. This high figure, third highest of the materials we tested, is due to the low absorption of the readout beam by the photopolymer. Photopolymer that is sensitized to the blue-green region of the spectrum has a yellow to orange color.

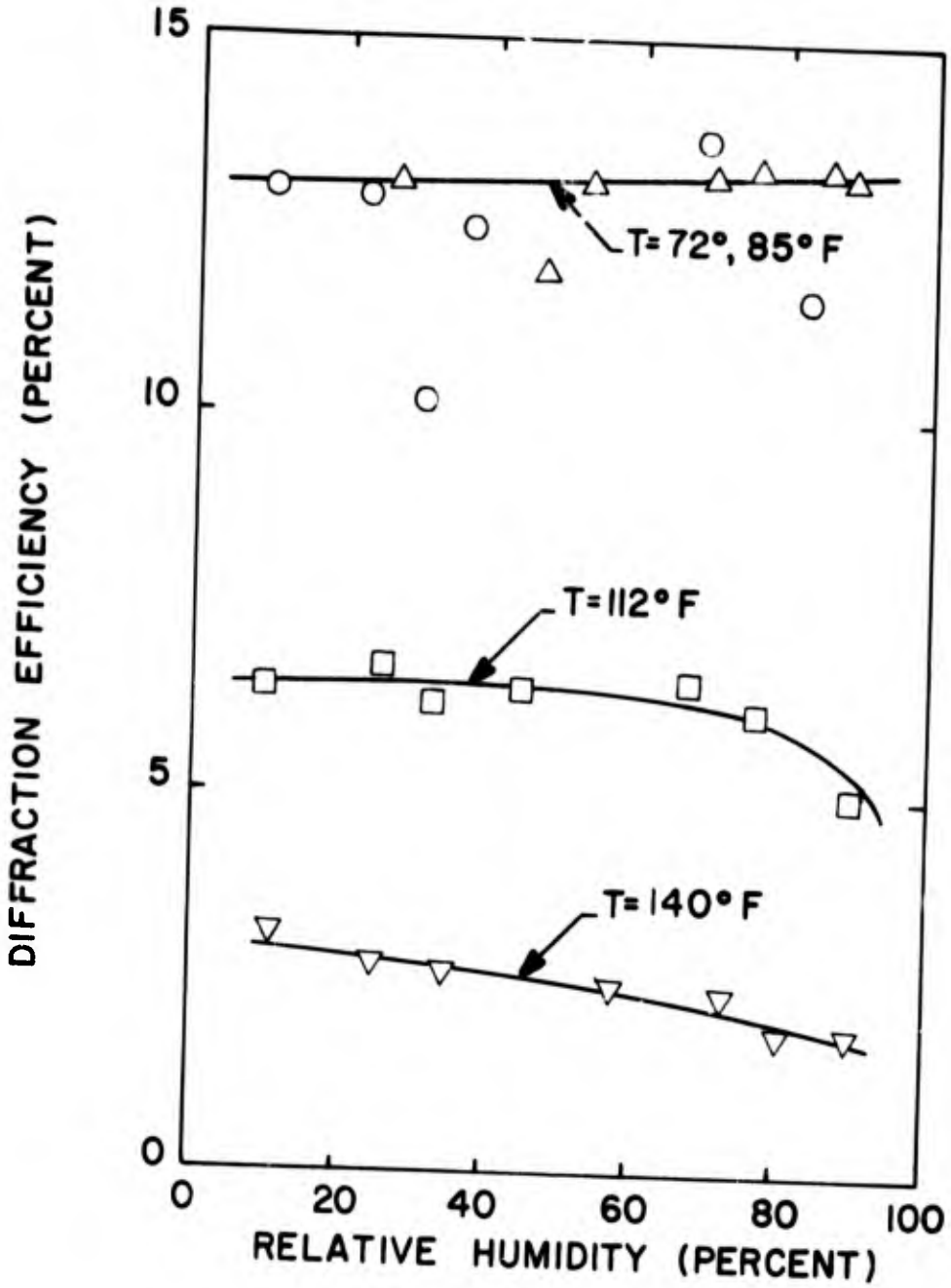

Figure 39

Diffraction efficiency as a function of relative humidity for a photopolymer grating.

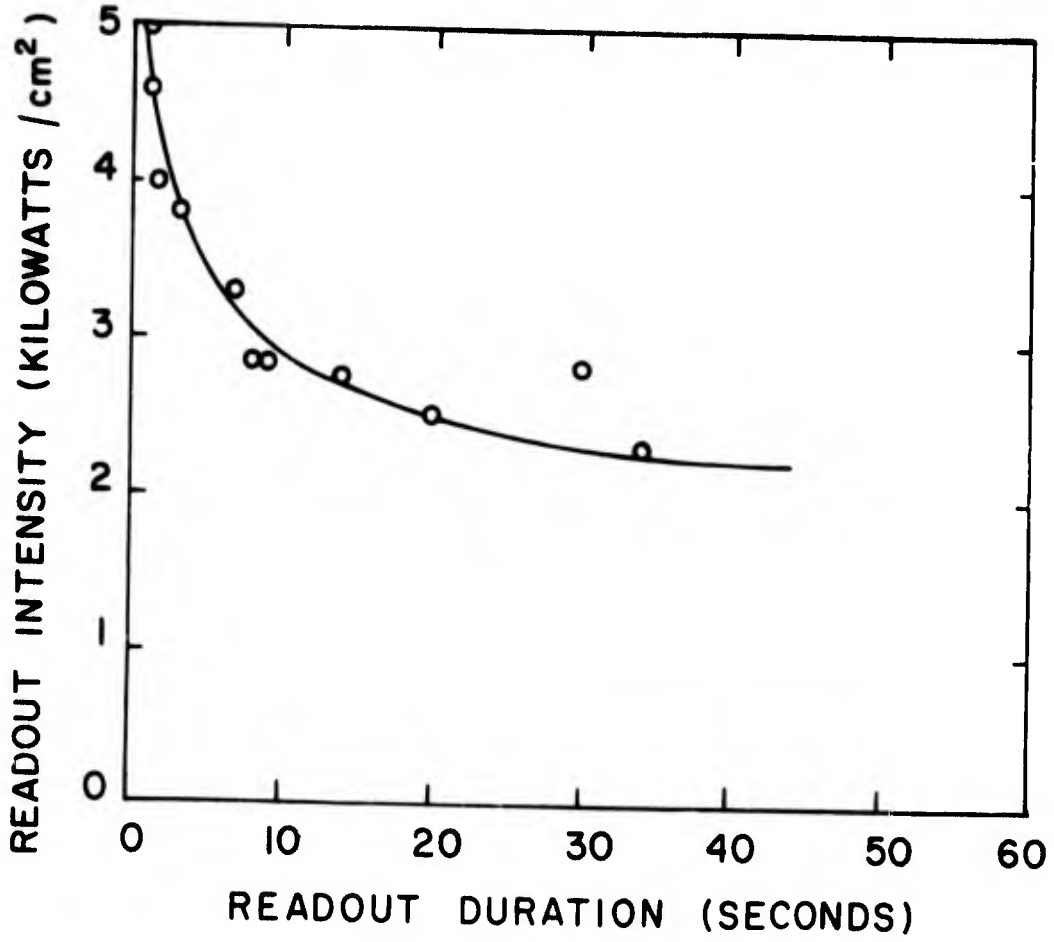

Figure 40

Destructive readout intensity as a function of readout duration for holograms recorded in photopolymer.

Although much of this color can be bleached away by exposure to UV light following formation of the hologram, enough remains to increase significantly the absorption of blue light. In this case the nondestructive illumination intensity limit would be considerably lower.

Figure 41 shows the change in diffraction efficiency of one of the photopolymer holograms (without a cover sheet) exposed to direct solar radiation and the out-of-doors environment. The efficiency in the blue to yellow region of the spectrum decreased by about 50%; it appeared to remain constant at the red end of the spectrum. Since photopolymer holograms are affected somewhat by elevated temperature and humidity and by UV radiation, it is reasonable to assume that the degradation is due to a combination of these causes.

3.4 Thick Thermoplastics

A number of thermoplastic materials are useful for recording thick phase holograms.[20] Two specific examples are polymethylmethacrylate (PMM) and cellulose acetate butyrate (CAB), which are doped with p-benzoquinone to provide spectral sensitivity in the blue-green region of the visible spectrum. PMM and CAB are tough, hard plastics with optical properties similar to fused silica. These materials can be formed from solution, by casting, or by injection molding; they can be cut, shaped, and polished. Thick thermoplastics are attractive for holographic optical element applications because we are able to record efficient holograms in thick castings of the materials.

Optical degradation of PMM has been studied extensively over the past twenty years.[21,22] Most of the early experimental work was carried out at the 253.7 nm line of Hg; other investigations were performed using x-rays, γ-rays, and electron beams. With PMM that was polymerized using azobisisobutyronitrile (AIBN) as an initiator, gratings were

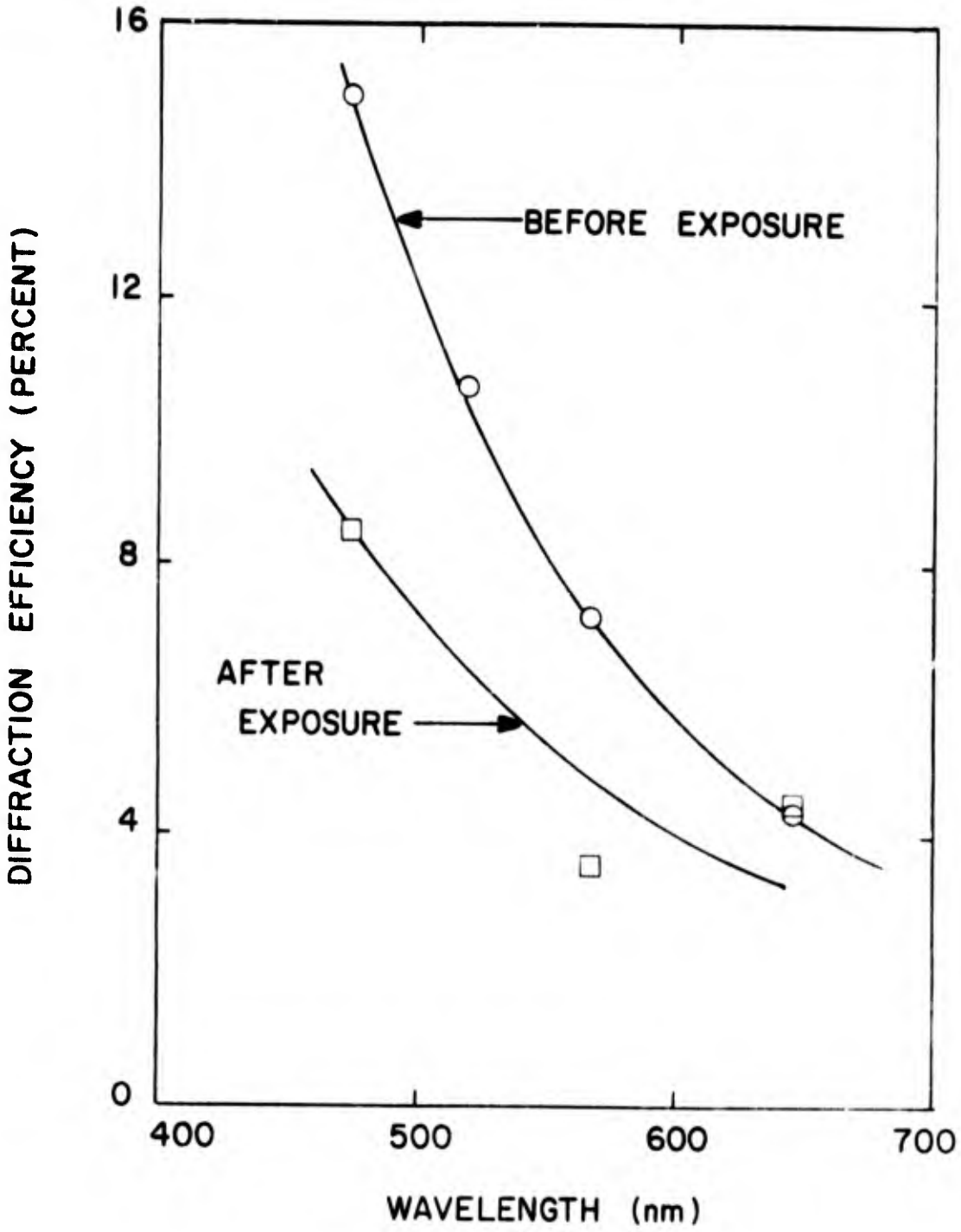

Figure 41

Readout efficiency as a function of wavelength for a photopolymer grating, before and after outdoor exposure.

recorded at 325 nm with diffraction efficiencies on the order of 70% and angular bandwidths of about 2 mrad in a one millimeter thick sample.[22] These experimental results imply a maximum differential index change $(\Delta n)_{max}$ of about 5×10^{-4}. Polymer degradation in a PMM (p-benzoquinone) system has also been studied. The p-benzoquinone extends the sensitivity of the plastic well into the visible part of the spectrum; in fact, maximum sensitivity occurs near 488 nm permitting a high power CW argon laser to be used for exposure. Furthermore, the p-benzoquinone is itself photosensitive and forms highly unreactive quinhydrone when irradiated with UV light and thus provides a means of fixing the stored information.[20]

3.4.1 Mechanism of Hologram Formation. — Holograms are formed in thick thermoplastics by photodegradation, which occurs principally through chain scission or crosslinking. In many instances chain scission is the perferred mode of photodegradation; usually crosslinking is more readily initiated, however, and if there are photon energy limitations, it is the most probable process. These observations bear particular relevance for wavelengths greater than 300 nm, since most thermoplastics do not exhibit significant absorption in the visible spectrum. The presence of peroxides or other dopants also tends to enhance the probability of crosslinking. The behavior of the poly(methylmethacrylate) (PMM)/p-benzoquinone (PBQ) system at 488 nm provides strong evidence for these facts and will be used as an example to discuss the photochemistry of crosslinking. Other plastics such as cellulose acetate butyrate (CAB) and poly(vinylacetate), (PVA) could serve as well.

The chemistry of PMM-PBQ crosslinking is relatively simple. The reaction begins with the absorption of a photon by a molecule of the sensitizer PBQ. At 488 nm, the energy involved is equivalent to about 50 Kcal/mole; this is roughly the lower limit for the (n,π^*) triplet state excitation of PBQ. (At 514 nm, however, the PMM-PBQ does have

about 20% of the sensitivity at 488 nm.) The excited PBQ molecule attacks a quiescent PMM molecule and abstracts a hydrogen atom, undergoes a structural change, and forms a polymer free radical R·. Further propagation steps result in the crosslinking of a number of PMM molecules at various locations by means of quinone-derived molecular bridges. Tables 7 and 8 outline the details of the chemical reaction.

3.4.2 Method of Use. — As sensitized thick plastics are not commercially available, light-sensitive layers must be prepared in the laboratory. Fortunately, all required chemicals can be purchased directly from suppliers such as Eastman Organic Chemicals. They are as follows: thick plastics, PMM and CAB; solvent, chloroform or acetone; sensitizer, p-benzoquinone. Whenever possible the use of reagent grade chemicals is highly recommended.

The following steps should be followed to prepare a light-sensitive solution:

1. Dry the plastic with flowing hot air at 150-180°F for at least 2 hours.

2. Dissolve 100-150 gm of plastic in 1,000 ml of solvent.

3. Filter the CAB solution; this not required for PMM in general.

4. Prepare about 10 gm of resublimed PBQ. Use only the low temperature phase; do not heat the PBQ above 115°C.

5. Just before casting, add 5 to 10 gm of PBQ to the plastic solution and mix.

6. Store excess solution at room temperature and at low relative humidity (less than 50%).

Initiation:

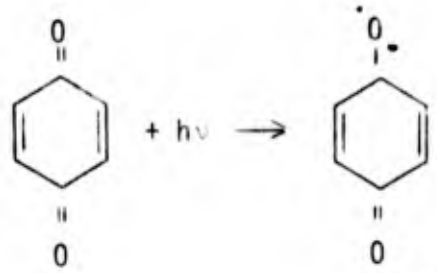

Propagation:

(a)

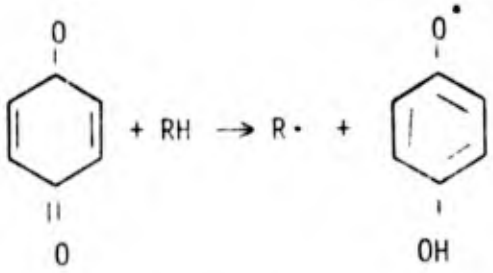

(b) R· +

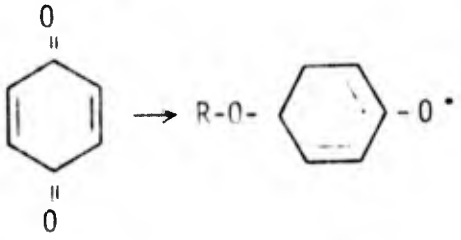

(c)

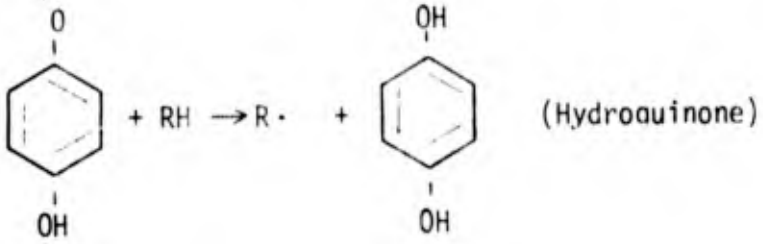

(Hydroquinone)

Termination:

R-O-

-O· + R· → R-O-

-O-R (Crosslinked Polymer)

TABLE 7. The Chemistry of Quinone-Doped Thermoplastics
Principle Reaction

Initiation:

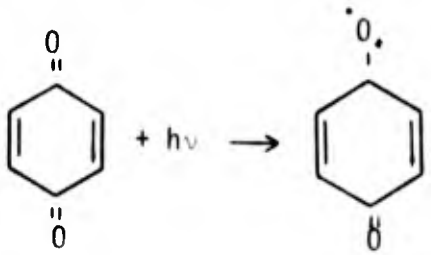

Propagation:

(a)

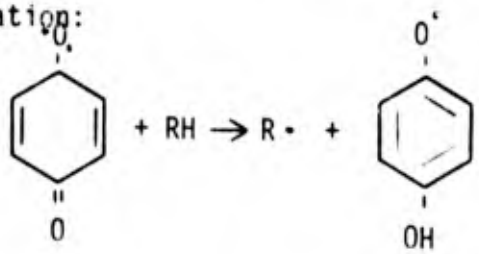

(b)

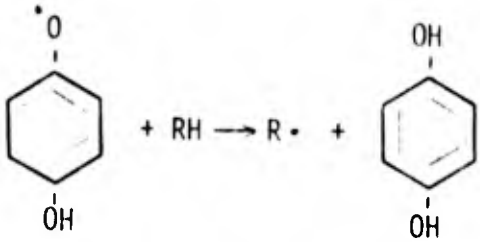

Termination: R• + R• → R - R

TABLE 8. The Chemistry of Quinone-Doped Thermoplastics
Secondary Reaction

The preparation of thick plastic layers of good optical quality is not a trivial problem. Through trial and error experimentation we have found that the following procedure produces good results in a consistent manner.

1. Thoroughly clean a glass substrate.
2. Level the glass substrate.
3. Pour a measured amount of the light-sensitive solution on the substrate. Outline the perimeter of the substrate near the edges first. Then pour the remainder in the center. The rule of thumb is 0.2 ml of solution/cm^2 of substrate area, assuming a solution viscosity of 2,000 cp.
4. Cover the cast layer with an inverted glass dish or equivalent. The cast layer must dry slowly in an atmosphere of its own solvent to avoid blushing.
5. Dry slowly for 24-48 hours.
6. Bake for two hours at 70°C. Start at room temperature and slowly raise the temperature to 70°C. Cool slowly. This procedure removes residual solvent and anneals the plastic layer.

Depending on the plastic concentration, pour casting yields layers ranging in thickness from 50-300 μm for PMM and CAB (17% butyrate). CAB (55% butyrate) is extremely soluble and layers 750 μm thick are easily prepared. Layers of PMM up to 2 mm thick can be cast using masking tape dams on the substrate to prevent overflow. CAB is too brittle to form layers this thick. Exploratory work indicates that injection molding may provide an alternative method for constructing thick layers.

Hologram recording in quinone-doped thick plastics simply requires exposure to a hologram interference pattern. The material is self-developing and essentially real time. The exposure sensitivity of both PMM and CAB is quite low: about 2.5 J/cm^2 at 488 nm is required for maximum

diffraction efficiency. The known spectral sensitivity of PBQ sensitized plastics lies in the spectral range 450-520 nm. The combination of these effects permits hologram recording under conditions of high ambient illumination.

Index matching is desirable, but unfortunately most organic index matching liquids attack either the plastic or the PBQ. To minimize the effects of multiple reflections, we recommend that the plastic layer be exposed through the substrate.

Because of the low sensitivity of thick plastics to radiation of wavelengths greater than about 550 nm, the progress of exposure can be conveniently monitored with a low power He-Ne laser. A direct beam is suitable for this purpose with allowance, of course, in beam angle of incidence to account for Bragg mismatch. Through the use of a photodetector to detect diffracted power and a chart recorder, the dynamic behavior of thick plastics can be studied.

Thick plastics are self developing. The chemical reaction that produces the hologram formation mechanism occurs very rapidly. Except for a short induction period, hologram formation begins with the initiation of exposure, and at the termination of exposure the hologram is ready for reconstruction.

There is, however, generally an excess of PBQ. Since unused sensitizer cannot be removed, it must be deactivated to fix the hologram exposure at its termination level. This is accomplished by flooding the thick plastic hologram with long wave UV light. A 100 w high pressure Hg lamp used with a long wave filter provides enough energy at a distance of 25 cm to achieve fixation with a 4 hour exposure for a 250 μm thick plastic layer. Fixation is believed to occur by the conversion of PBQ to unreactive quinhydrone.

3.4.3 Experimental Results. — We recorded holograms on samples of CAB and PMM up to 250 μm thick. In the results we report, the holograms were recorded at 488 nm, although the exposure sensitivity is increased by up to an order of magnitude at 458 nm. After they were recorded, the holograms were fixed by exposure to uniform UV radiation. Except where noted, the holograms were read out at 488 nm.

3.4.3.1 Holographic Parameters. — Figure 42 shows curves of diffraction efficiency as a function of exposure for plane wave gratings recorded in CAB with 55% butyrate. These gratings were recorded at 1000 lines/mm with K-ratios of 1.7, 9.2, and 109. At K = 1.7, a peak diffraction efficiency of 25% is reached at an exposure of 23 J/cm^2. The shape of the curves indicate that greater exposure would have led to higher peak efficiencies. Figure 43 is a curve of diffraction efficiency as a function of exposure for plane wave gratings recorded in PMM that was sensitized with 0.025 parts (by weight) of p-benzoquinone to one part of PMM. The gratings were recorded with K = 1. The curve reaches a peak of 56% efficiency at an exposure of 12 J/cm^2.

Figure 44 shows curves of SNR and diffraction efficiency as a function of exposure for holograms recorded in CAB with 17% butyrate. The holograms were recorded with a K-ratio of 9.5. The SNR peaks at 70 (18.5 dB) with a diffraction efficiency of about 7%. At a diffraction efficiency of 10%, the SNR is 50 (17 dB). The highest signal-to-noise ratios occur at relatively light exposures, on the order of 1 J/cm^2. At greater exposures holograms were recorded with very high efficiencies although the SNR was poor. When the K-ratio was increased to 25, the results were essentially unchanged, as shown in Figure 45.

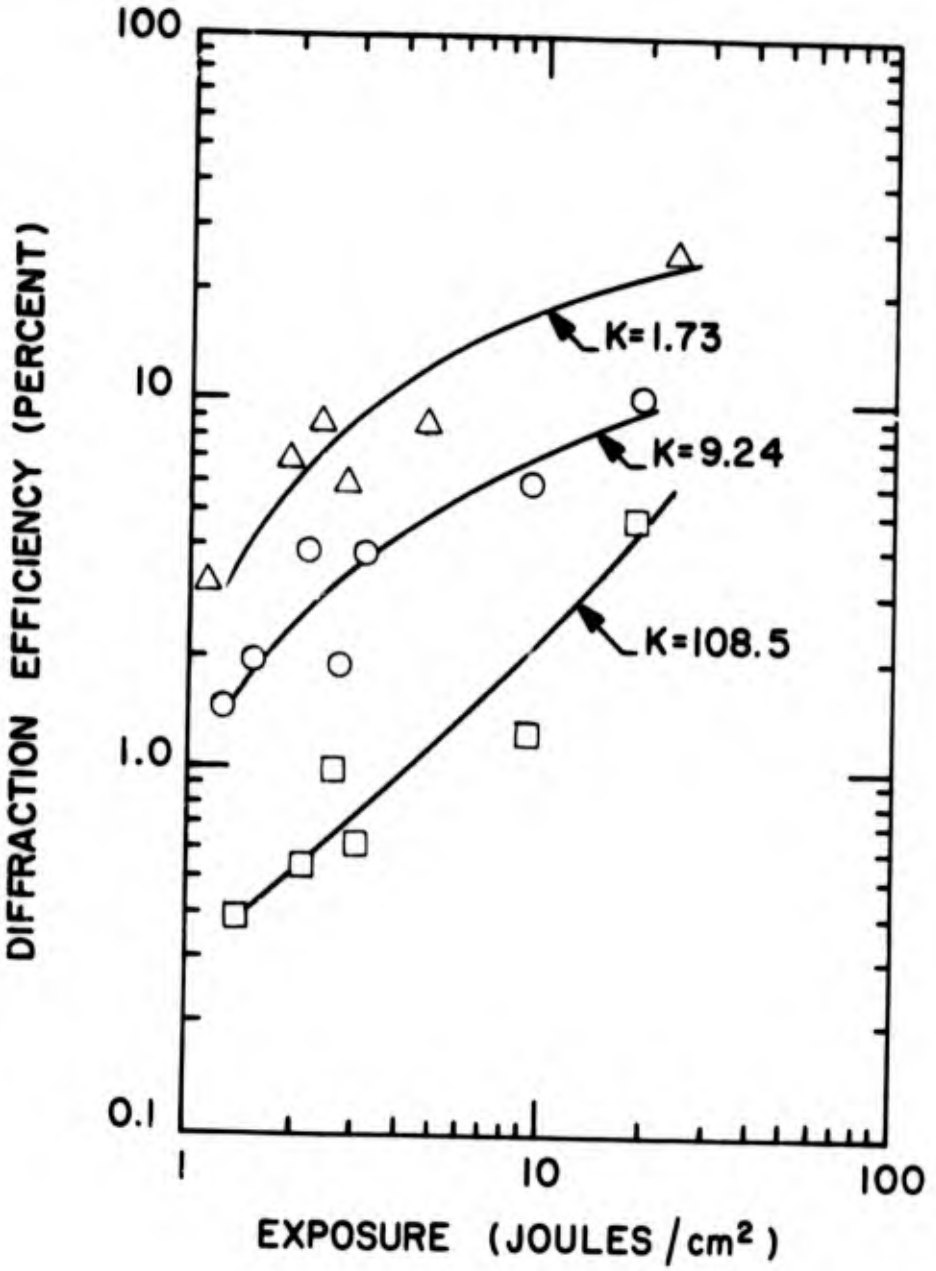

Figure 42

Diffraction efficiency as a function of exposure for plane wave gratings recorded in CAB, 55% butyrate.

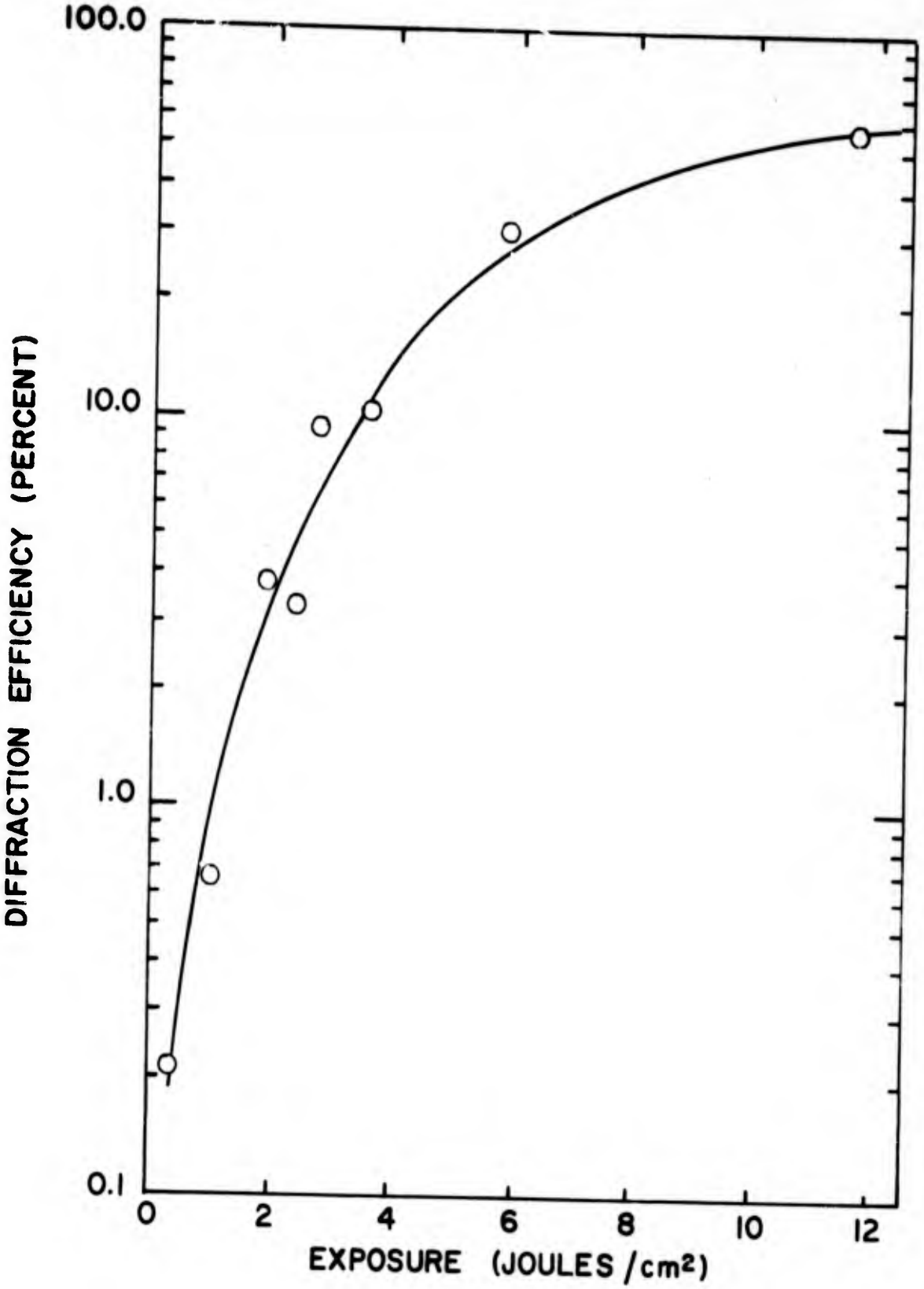

Figure 43

Diffraction efficiency as a function of exposure for plane wave gratings recorded in PMM.

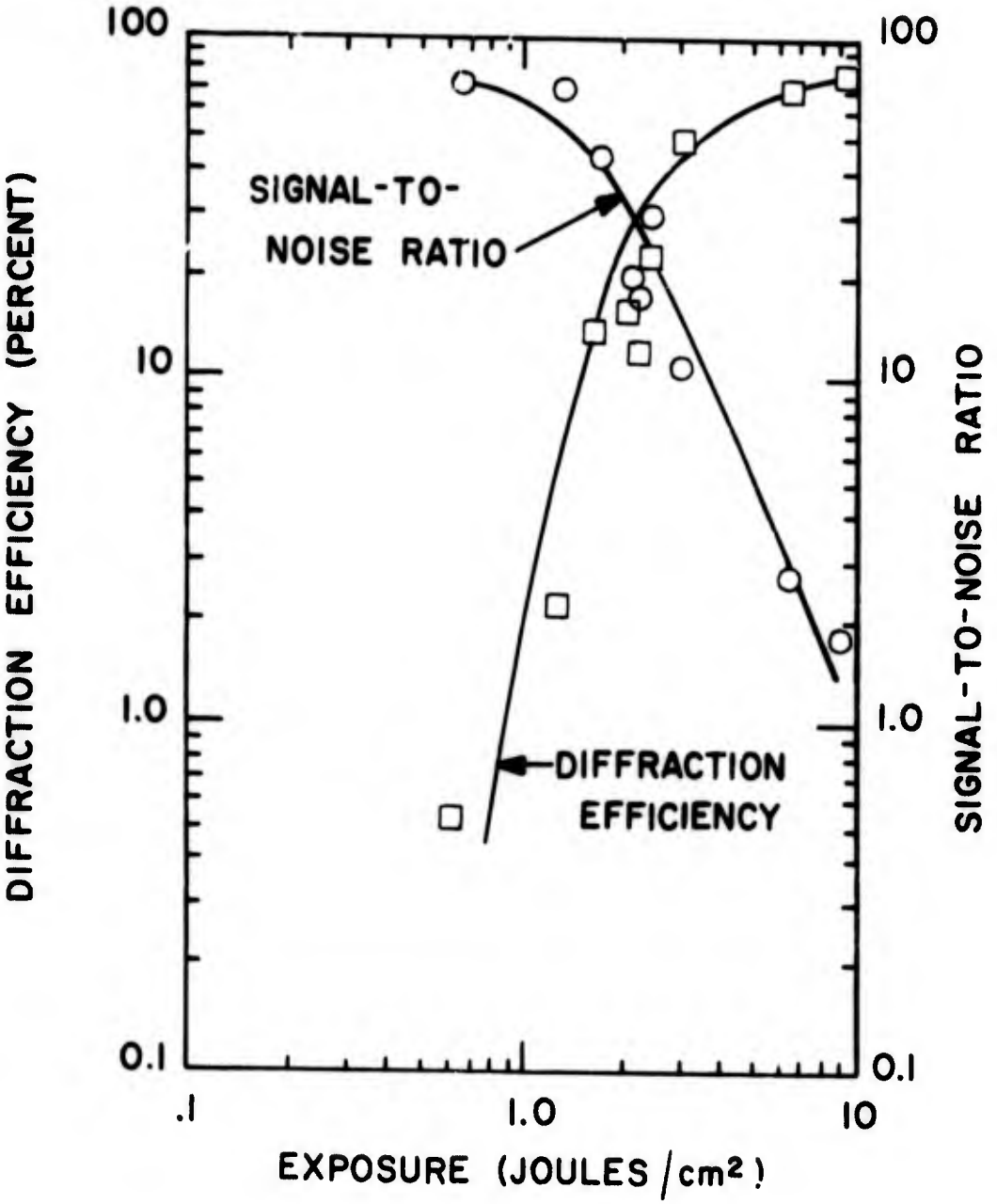

Figure 44

Diffraction efficiency and SNR as functions of exposure for holograms recorded in CAB at K = 9.5.

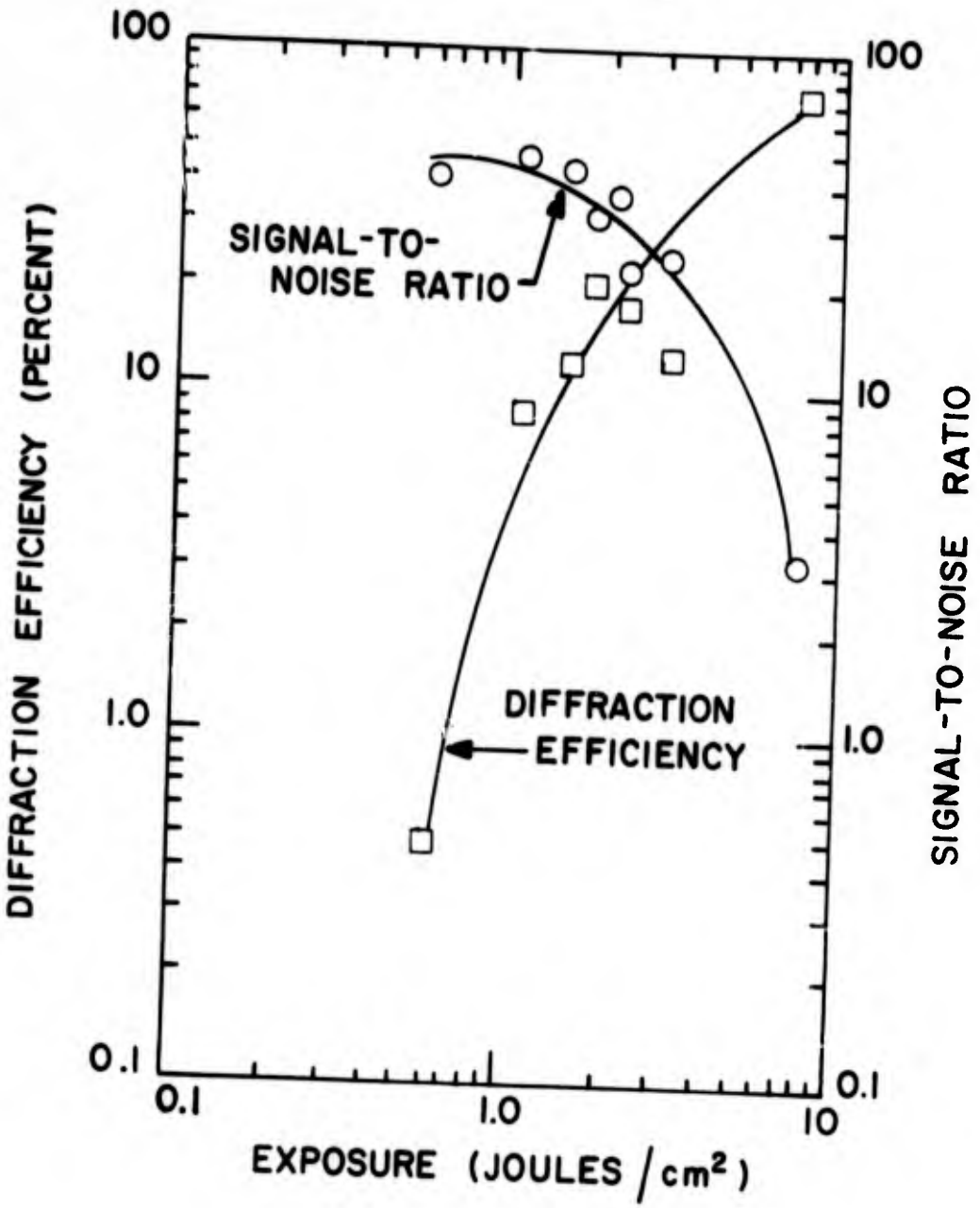

Figure 45

Diffraction efficiency and SNR as functions of exposure for holograms recorded in CAB at K = 25.

The frequency response of the thermoplastics appears to be flat to 2000 lines/mm. There is no indication of a bandpass response such as we observed with photopolymer. Reflection holograms were made at spatial frequencies as high as 6000 lines/mm; the response at this frequency was reduced, however, and the maximum efficiency was 2%.

Figure 46 shows the spectral variation of readout efficiency and intensity transmittance for CAB in the visible spectrum. The diffraction efficiency increases with increasing wavelength because of the high absorption of short wavelengths caused by the sensitizer. The extent of this absorption is indicated by the transmittance curve. The gratings used for the measurements shown in Figure 42 were also read out at 1150 nm. Figure 47 shows the diffraction efficiency curves for the gratings recorded with K-ratios of 1.7 and 9.2. The efficiency decreased by a factor of about six in changing the wavelength from 488 nm to 1150 nm. Although Figure 47 is representative of most of the thermoplastic holograms, in some cases there was a smaller decrease in diffraction efficiency due to the wavelength shift. In these cases efficiencies as high as 50% were measured, (in a sample of CAB with 17% butyrate); these were the highest efficiencies that we measured at 1150 nm.

3.4.3.2 Environmental Testing. — We tested several samples of cast PMM in the environmental chamber. We found generally inconsistent behavior of the material at elevated temperature and humidity. Figure 48 shows the effect of temperature and humidity on the diffraction efficiency of a typical hologram recorded in unsensitized PMM. At 95°F and below, the efficiency increased; at 120°F, the efficiency decreased; and at 140°F (not shown in the figure), the efficiency increased again. Some of this anomalous behavior may be due to imperfect readout alignment, which is critical for such thick holograms. Other samples of PMM were affected physically by elevated temperature and humidity. In

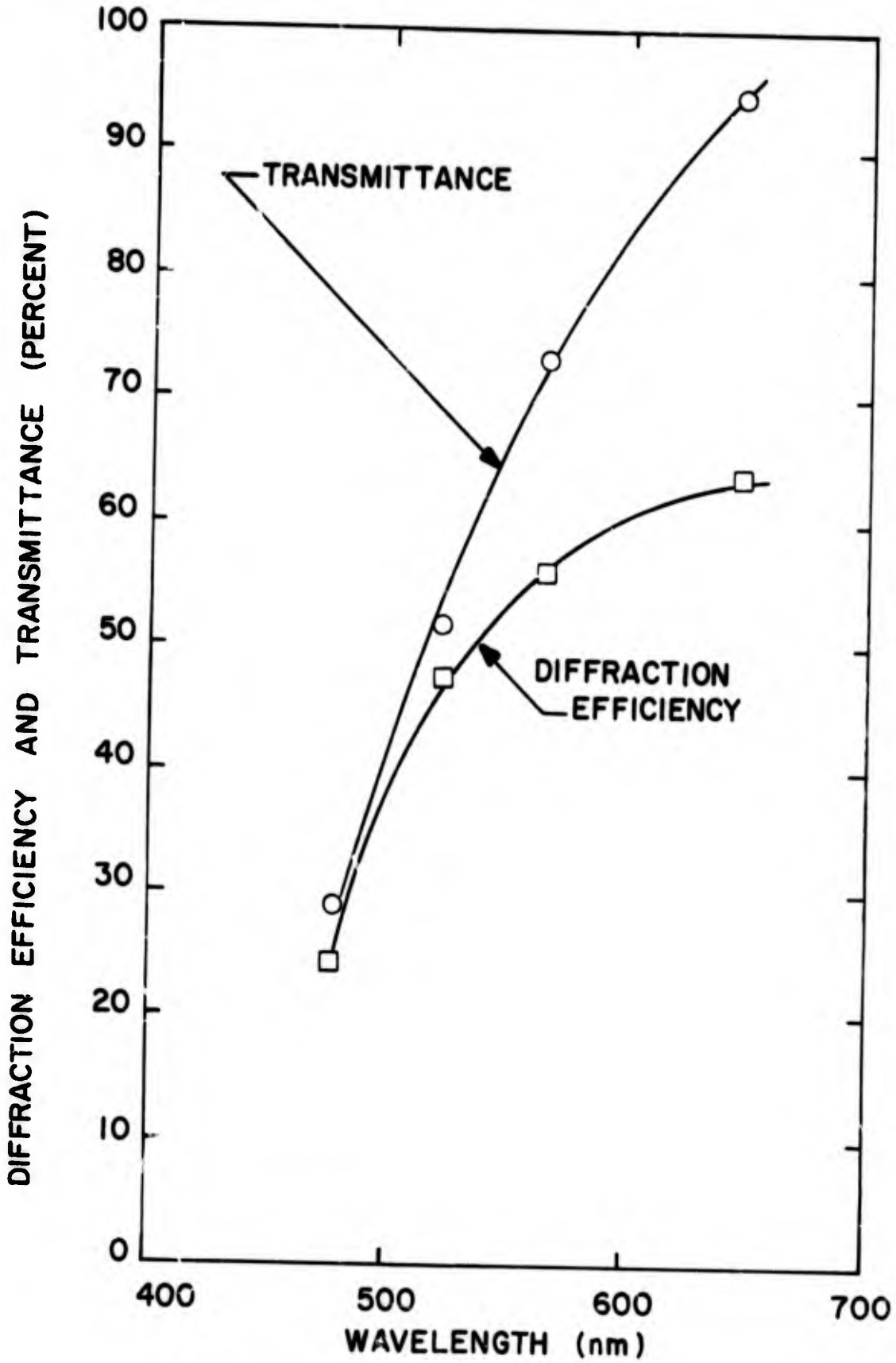

FIGURE 46

Spectral variation of transmittance and readout efficiency for a grating recorded in CAB.

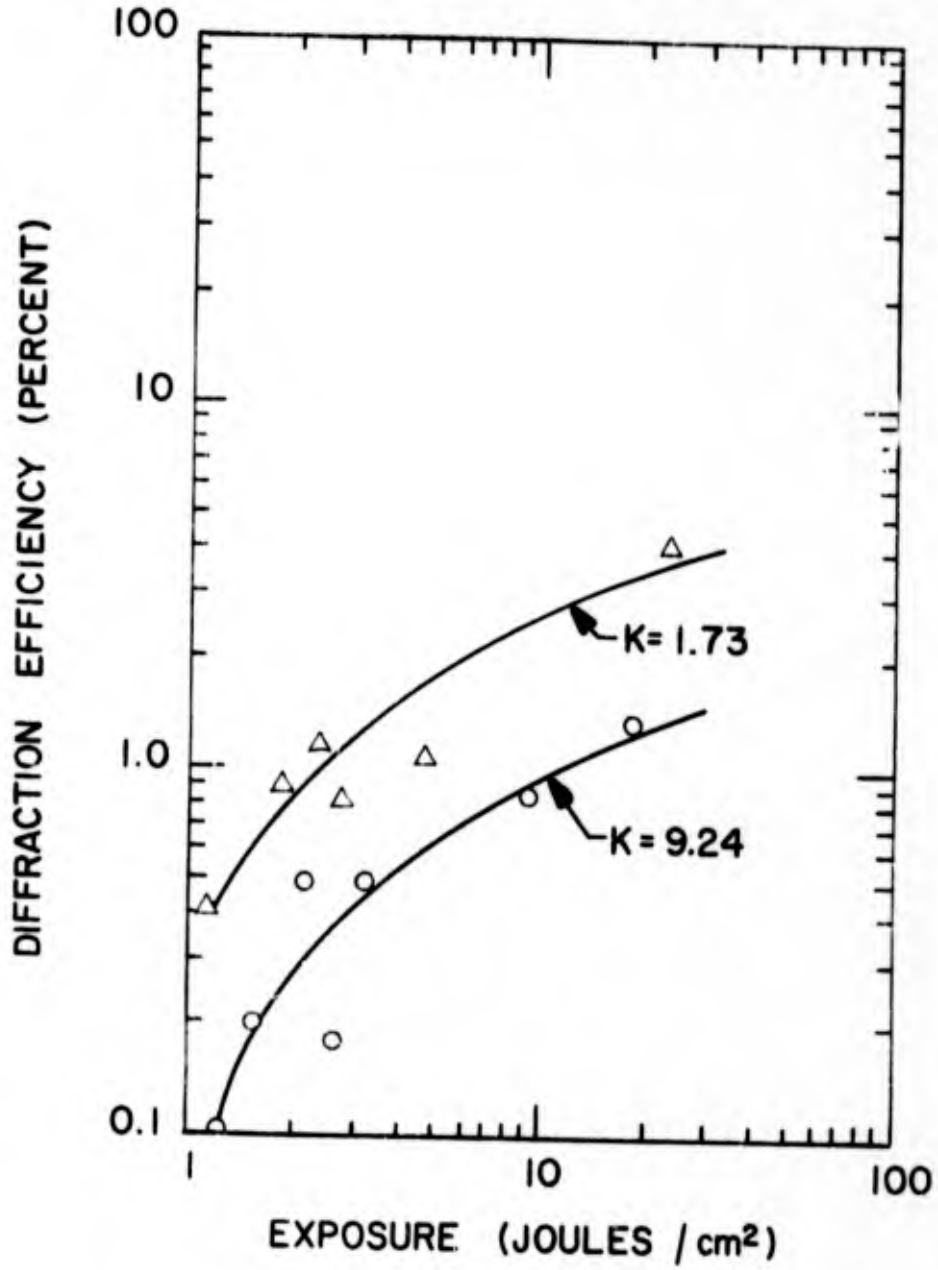

FIGURE 47

Diffraction efficiency at 1150 nm as a function of exposure for CAB gratings recorded at 488 nm.

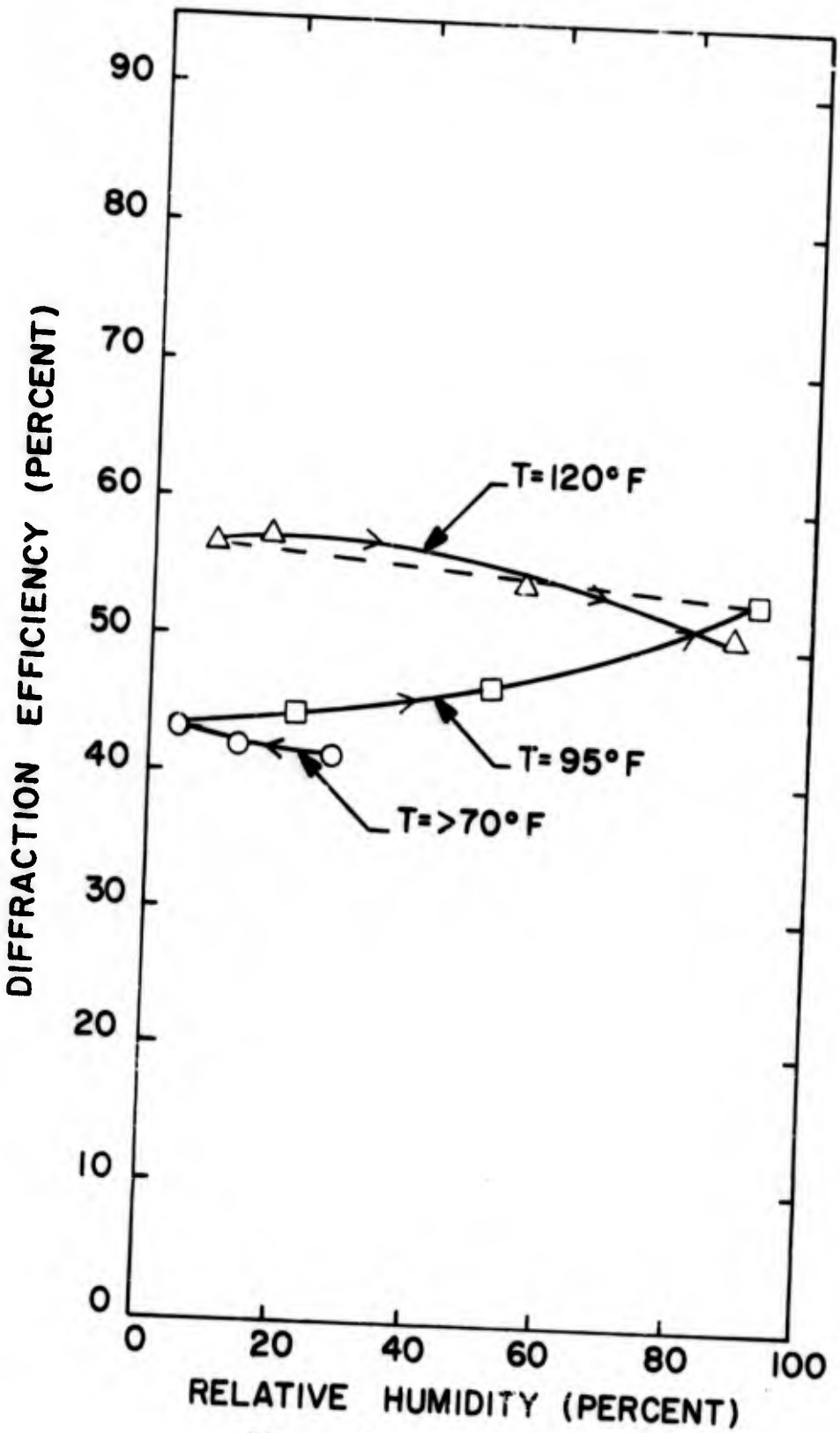

Figure 48

Diffraction efficiency as a function of relative humidity for a grating recorded in PMM.

some cases the thermoplastic lifted off the glass substrate. Cast PMM sensitized with crystal violet dye adhered to the glass substrate, but at 140°F and 90% humidity it pulled in from the edges of the glass until it had shrunk in size by 10%. In addition it became hazy due to the absorption of water; we later eliminated the haze by heating the material to 190°F in a low humidity atmosphere. We found that the diffraction efficiency of thermoplastic holograms was unchanged by cycling to temperatures of -40°F.

Figure 49 is a curve of destructive readout intensity as a function of the readout duration. Extrapolation of the curve to 60 seconds gives a limit of about 3 watts/cm^2 as the minimum destructive readout intensity. This very low intensity results from the high absorption of the 488 nm readout light by the thick thermoplastic. The hologram is destroyed by localized melting of the plastic.

Figure 50 shows the effect of exposure to direct solar illumination and out-of-doors environment on the diffraction efficiency of holograms recorded in CAB with 17% butyrate. The efficiency decreased at all wavelengths, with the greatest decrease at long wavelengths. This degradation may be due to a combination of UV radiation and high humidity effects.

3.5 Photoresist

Photoresist forms holograms as surface modulation. Holograms are recorded in what is essentially a two step process: exposure followed by development. The developer removes material in the exposed regions for positive working photoresist and in the unexposed regions for negative working photoresist. In principle photoresist holograms can be overcoated with a reflective film to form efficient reflective elements.[23] Furthermore, the surface relief offers the possibility of large scale replication through pressing techniques.[24]

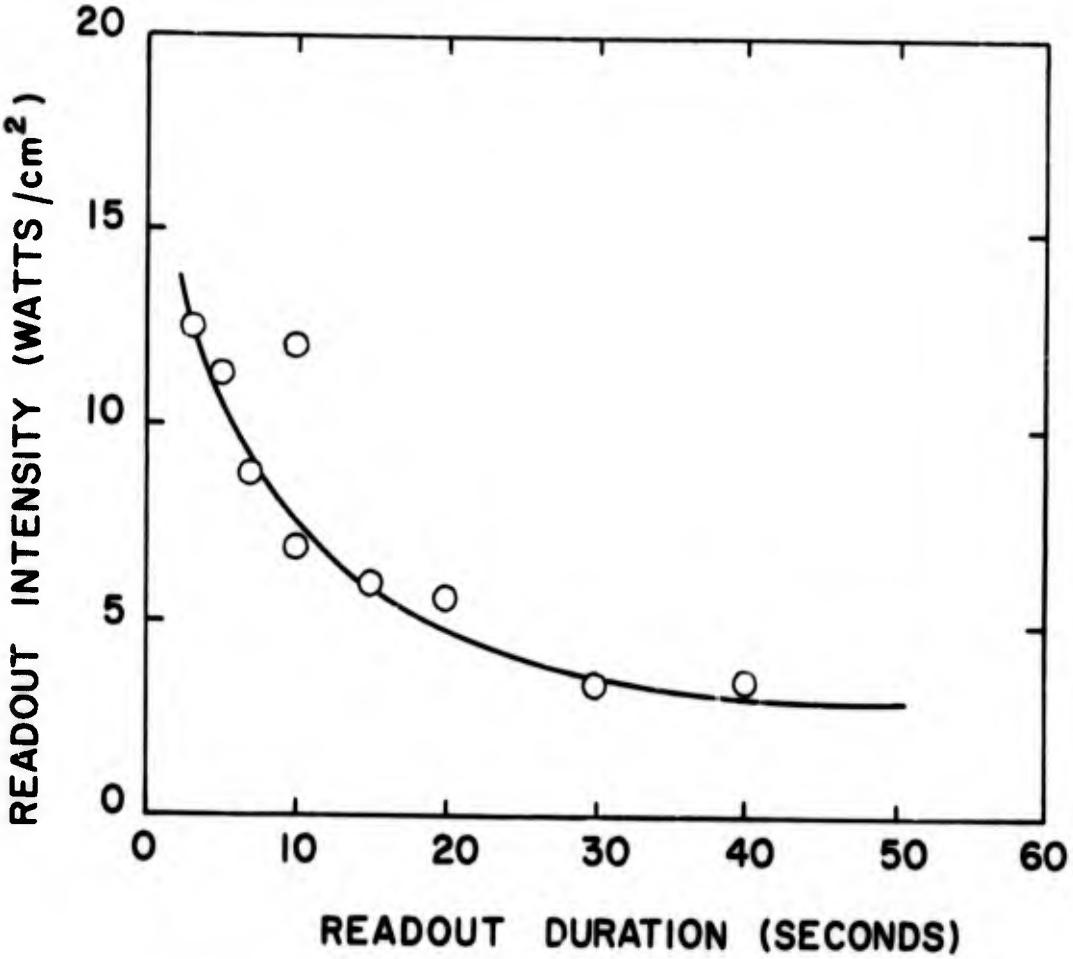

Figure 49

Destructive readout intensity as a function of readout duration for thick thermoplastic holograms.

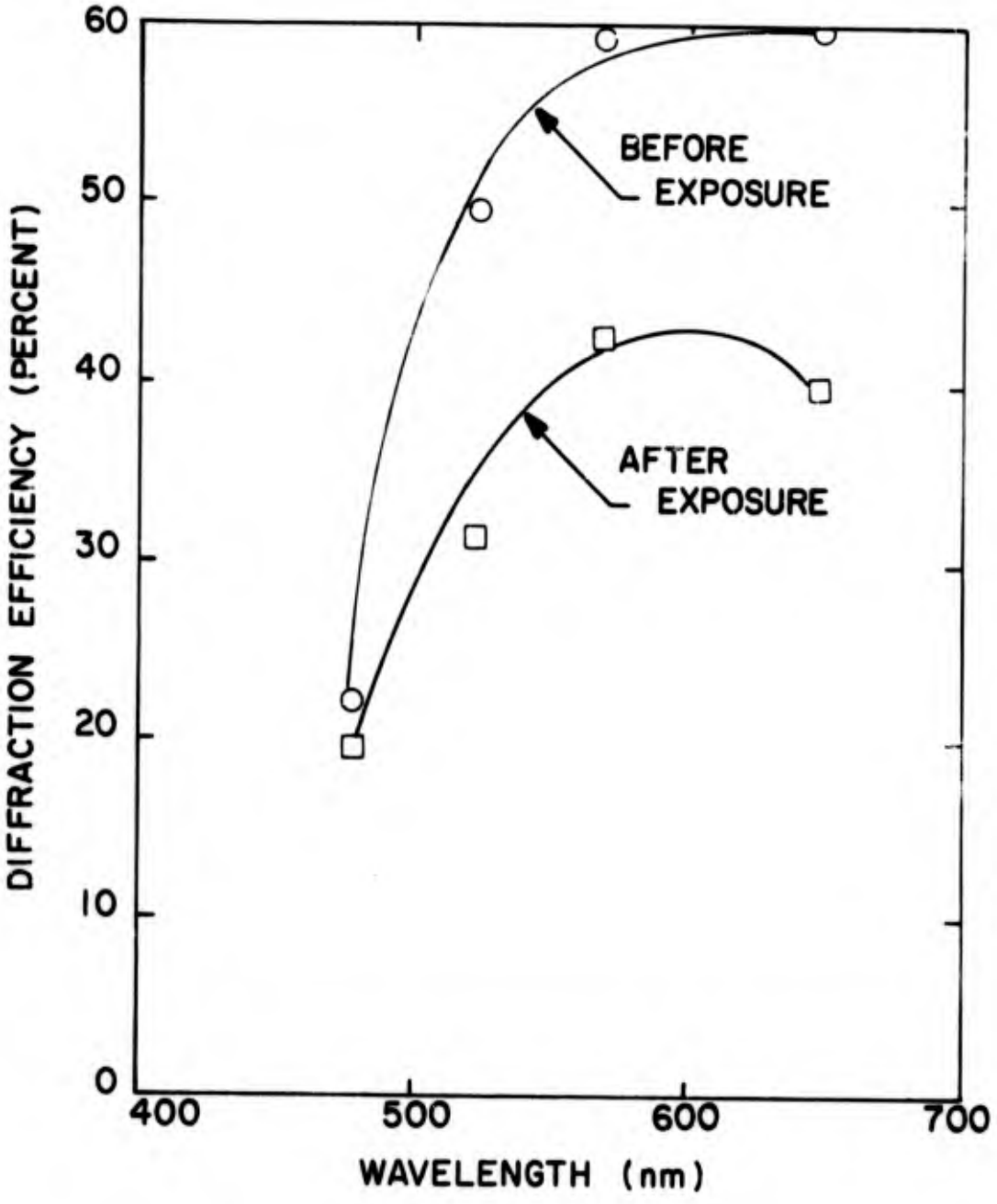

Figure 50

Readout efficiency as a function of wavelength for a grating recorded in CAB, before and after outdoor exposure.

3.5.1 Mechanism of Hologram Formation. — Holograms are formed in photoresist in a relatively straightforward manner. Exposure to actinic radiation causes crosslinking of the photoresist molecules; the crosslinking itself can form a weak volume hologram in the material. In a negative working resist, the crosslinked regions are insoluble in the developer, which dissolves the unexposed material. In a positive working resist, the crosslinked material is more soluble in the developer than the unexposed material. Exposure to the holographic interference pattern causes a spatial distribution of crosslinking that corresponds to the interference pattern. Development removes material so that a surface relief remains in proportion to the intensity distribution of the exposure. Since the photoresist is transparent, the surface relief forms a thin phase hologram. The maximum theoretical diffraction efficiency for sinusoidal modulation of the surface is 33.9%.[11]

3.5.2 Method of Use. — Photoresist is manufactured by several companies such as Eastman Kodak and Shipley. Probably the most widely used photoresists in holography are Shipley AZ 1350 and Shipley AZ1350H positive working photoresists. These can be developed with the standard Shipley AZ developer or with Shipley AZ 303 developer. It has been reported[25] that the latter, based on a sodium hydroxide solution, gives holograms that are linear over a wider range of exposure.

Photoresist films can be prepared by dip or spin coating the material onto substrates of glass or film. Spin coating is the perferred method since it produces coatings of very uniform thickness and quality. Careful attention must be given to the substrate to see that it is free of dirt and absorbed water vapor prior to the coating operation. Shortly before exposure, the films are heated to drive off any residual solvent: the heating can be carried out at 100°C for 15 minutes. The shelf life of the coated material is limited to several days, after which the exposure sensitivity decreases.

Although it can be exposed with blue light, photoresist is basically a UV sensitive material. The blue line of the He-Cd laser or the 458, 476, or 488 nm lines of the argon laser are possible wavelengths for recording holograms in photoresist. Because of its extremely low sensitivity to longer wavelengths, photoresist can be conveniently and safely handled under yellow room lights.

After the hologram has been recorded, the photoresist must be developed. A typical development procedure is 30 seconds in an appropriate developer, undiluted, with constant agitation. This is followed by rinsing with distilled water and forced air drying. Common alternatives to this process call for various dilutions of the developer with distilled water and various development times. With the Shipley AZ1350 and AZ1350H photoresist, we found that development times exceeding 30 seconds in undiluted AZ Developer began to remove photoresist at the glass-photoresist interface for holograms recorded with moderate to heavy exposures; this caused the holograms to lift off the substrate. It has been shown[26] that the efficiency of the hologram can be monitored during development with light from a He-Ne laser so that development can be terminated at a predetermined amount of surface modulation. After development, the photoresist hologram can be baked to harden the resist somewhat.

3.5.3 Experimental Results. — We tested photoresist films that were prepared from Shipley AZ1350H photoresist. These materials were spin coated onto 2-1/2 inch glass plates to a thickness of 1.4 μm. Immediately prior to use, the coatings were baked for 15 minutes at 100°C in a laboratory atmosphere. All holograms were exposed with the 458 nm line of the argon laser. The holograms were developed for 30 seconds in undiluted Shipley AZ Developer, rinsed with distilled water, and dried with forced air. As this is a positive resist, the developer removed material from the exposed regions.

3.5.3.1 Holographic Parameters. — We obtained some unexpected results with the photoresist when we recorded gratings at a spatial frequency of 1000 lines/mm. Several of the gratings diffracted nearly all of the incident light at 633 nm into one order, much more than the 33.9% theoretical maximum for a thin phase grating with sinusoidal modulation. Since the efficiency of those gratings was sensitive to angular orientation, it appears that the photoresist formed a transmissive blazed grating. In such a grating, the photoresist surface between grating lines would form an angle with the incident light that would tend to refract the incident light in the direction of the first order, in a manner similar to a prism.

The blazed effect is illustrated by Figure 51 a curve of diffraction efficiency as a function of exposure for plane wave gratings recorded in photoresist. The gratings were recorded at a spatial frequency of 1600 lines/mm, with K = 1. Although they were recorded at a wavelength of 458 nm, they were read out at 633 nm where absorption by the photoresist is a minimum. The diffraction efficiency reaches a peak of 79% at an exposure of 200 mJ/cm^2. The blazed effect is dependent on geometry; if the direction of the readout beam is reversed, the high efficiency of the blazed effect is not observed. If the readout beam is incident parallel but opposite in direction to the original strong diffracted order, the efficiency is again very high, with the strong diffraction anti-parallel to the original reference beam.

The blazed effect requires a relatively simple interference pattern. As shown by Figure 52, it does not occur for complex signals. This figure shows curves of diffraction efficiency and SNR as a function of exposure for holograms recorded with the diffuse signal. These holograms

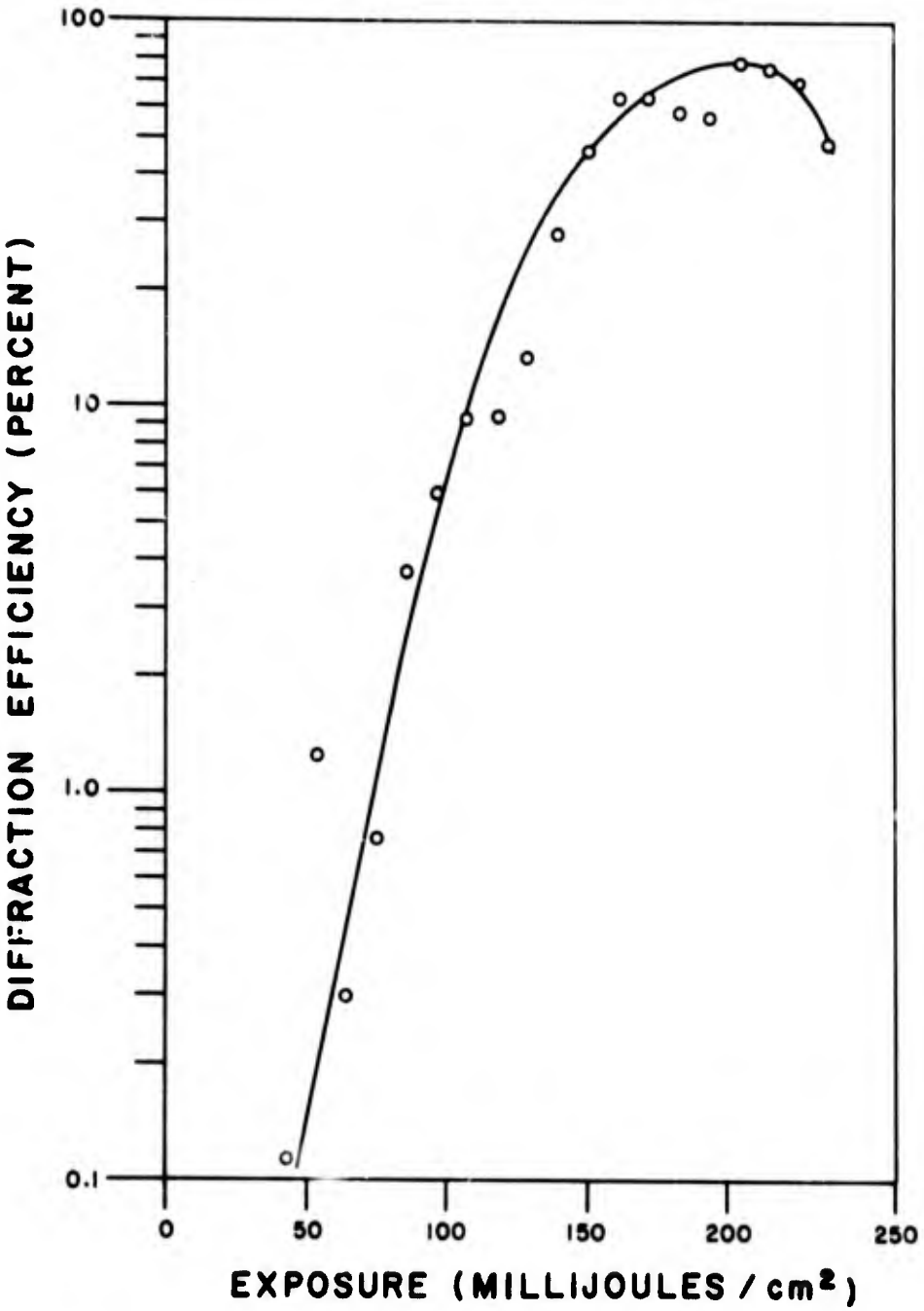

Figure 51

Diffraction efficiency at 633 nm as a function of exposure for lane wave gratings recorded in photoresist at 458 nm, K=1.

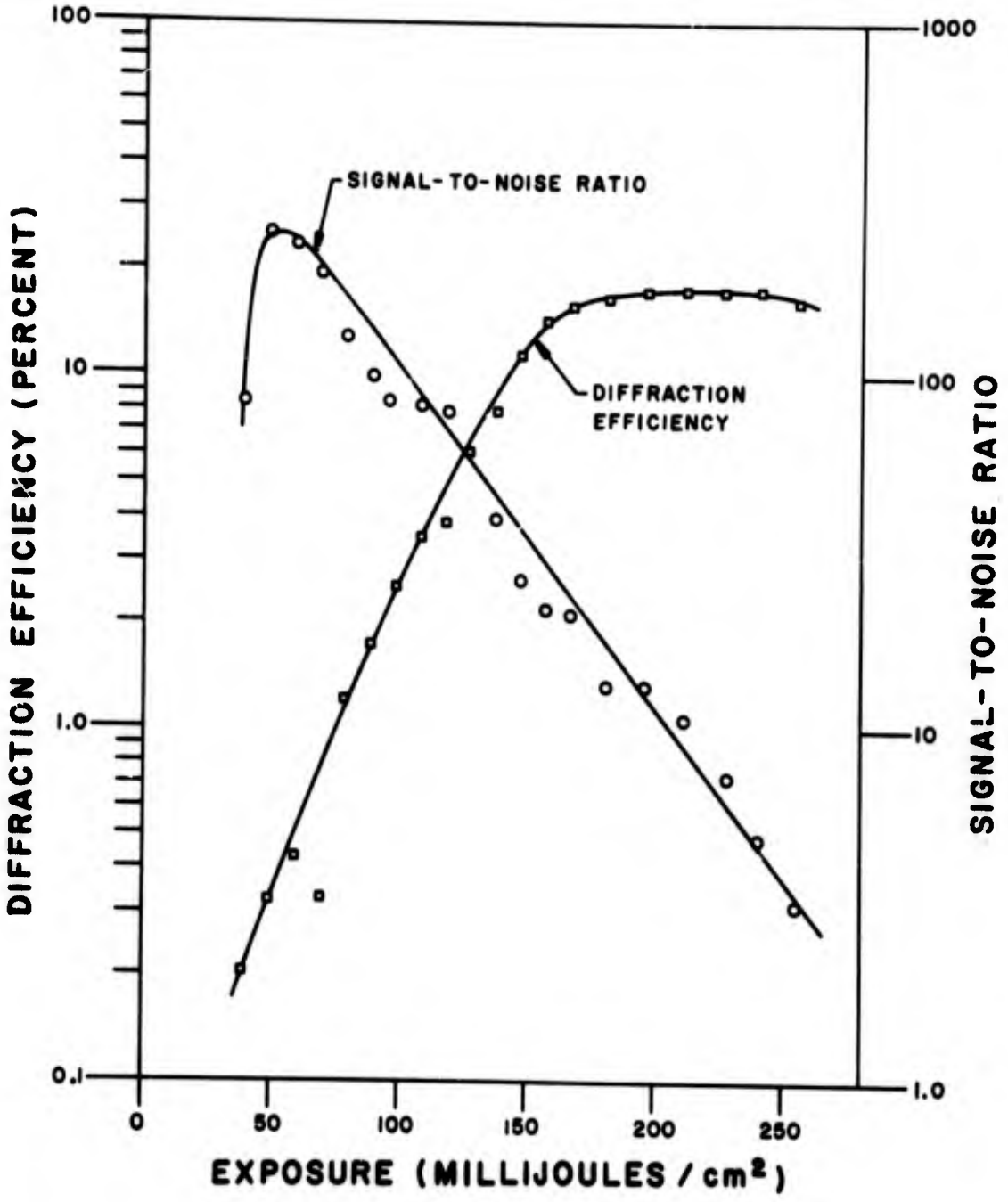

Figure 52

Diffraction efficiency and SNR as functions of exposure for holograms recorded in photoresist at 458 nm, K=27.

were recorded at 1040 lines/mm with K = 27; they were read out at 488 nm, close to the 458 nm recording wavelength. Since it is a grainless material, photoresist has the potential of recording holograms that are free of scattering noise. This is demonstrated by the high SNR at low exposures shown by the curve; the peak SNR is 255 (24 dB), occuring at a diffraction efficiency of only 0.3% and an exposure of 50 mJ/cm^2. At 10% diffraction efficiency, the SNR is slightly less than 40 (16 dB). The very pronounced tradeoff between diffraction efficiency and SNR suggests that the photoresist may be rather nonlinear. Although we were not able to test other developers, the response may be less nonlinear if Shipley AZ 303 Developer is used.[25]

We did not generate data for a curve showing the frequency response of the photoresist. From our experiments at frequencies of 500, 1000, and 1600 lines/mm, the response appears to be reasonably flat to 1600 lines/mm. This is confirmed by data reported by Bartolini.[27] We found the blazed effect strongest at 1000 and 1600 lines/mm.

Figure 53 shows the spectral variation of readout efficiency and transmittance of the blazed gratings recorded in photoresist. The photoresist has a yellow coloration that causes strong absorption of light at short wavelengths. This absorption reduces the diffraction efficiency of the gratings as well.

3.5.3.2 Environmental Testing. — Photoresist holograms were relatively insensitive to temperature variations but were affected by humidity (including frost that formed at very low temperatures). Figure 54 shows that diffraction efficiency alone is not appreciably affected by either temperature or humidity. The curve represents the variation in diffraction efficiency with relative humidity for plane wave gratings at 105 and 140°F; as is evident from the figure, there is little change in diffraction

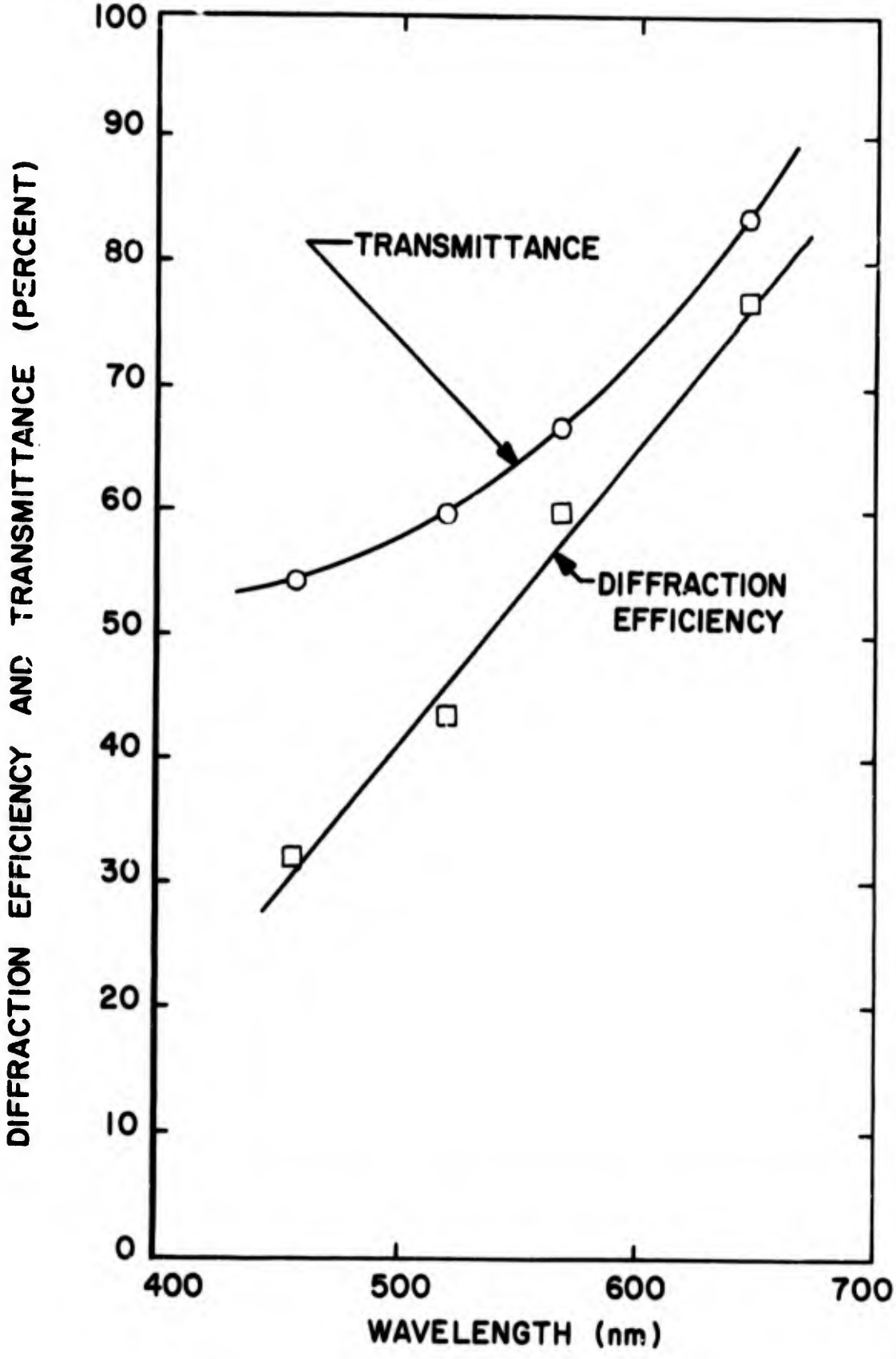

Figure 53

Spectral variation of transmittance and readout efficiency for a photoresist grating.

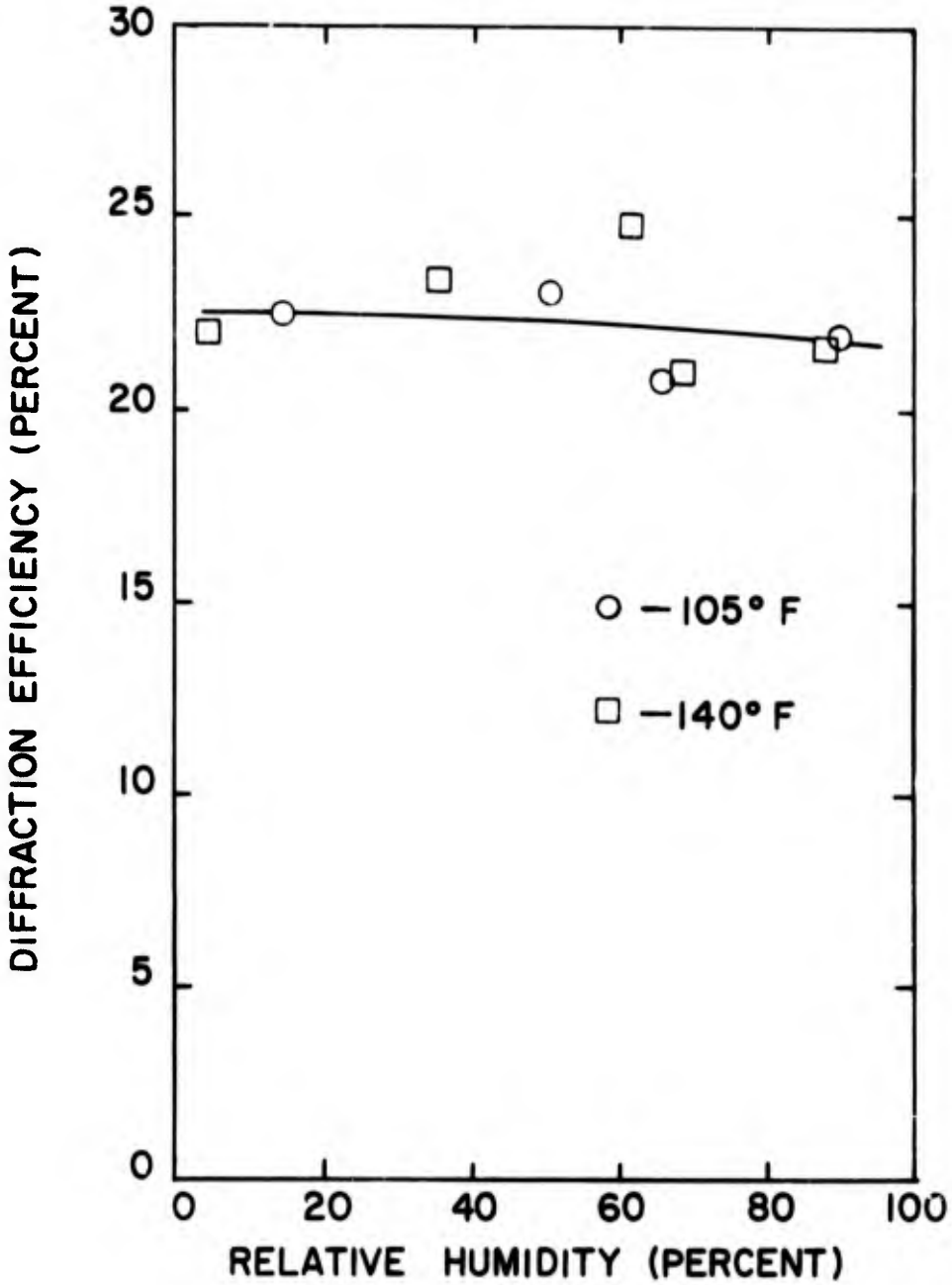

Figure 54

Diffraction efficiency as a function of relative humidity for a photoresist grating.

efficiency over the test conditions. High humidity lowers the SNR, however, by causing permanent fine cracks to form in the photoresist. This damage occurs at a relative humidity of about 70% and is aggravated by simultaneous high temperatures. At subzero temperatures photoresist holograms are damaged if frost is allowed to form on the material. Without frost, holograms were not damaged by temperatures to -40°F.

Photoresist holograms were degraded by UV radiation. Exposure to 25 hours radiation caused reductions of from 20 to 60% in diffraction efficiency of plane wave gratings. This degradation may be caused by the UV radiation rendering the photoresist soluble to traces of residual water or ambient water vapor. If photoresist is overcoated with a reflective metallic coating, UV radiation might be reflected sufficiently to prevent degradation.

Figure 55 shows the destructive readout intensity as a function of the readout duration. Very high intensities are required to damage photoresist holograms, higher than for any other material we tested. For readout durations approaching 60 seconds, the minimum destructive intensity is about 3500 watts/cm^2.

Figure 56 shows the degradation caused by the 50 hours exposure to direct solar illumination and the out-of-doors environment. Much of the decrease in efficiency is due to a darkening of the photoresist, probably caused by the solar radiation. High humidity, perhaps in combination with the solar illumination, caused the fine cracks to form in these holograms as well. Again, we would expect holograms coated with a metallic layer to be more resistant to degradation from solar radiation.

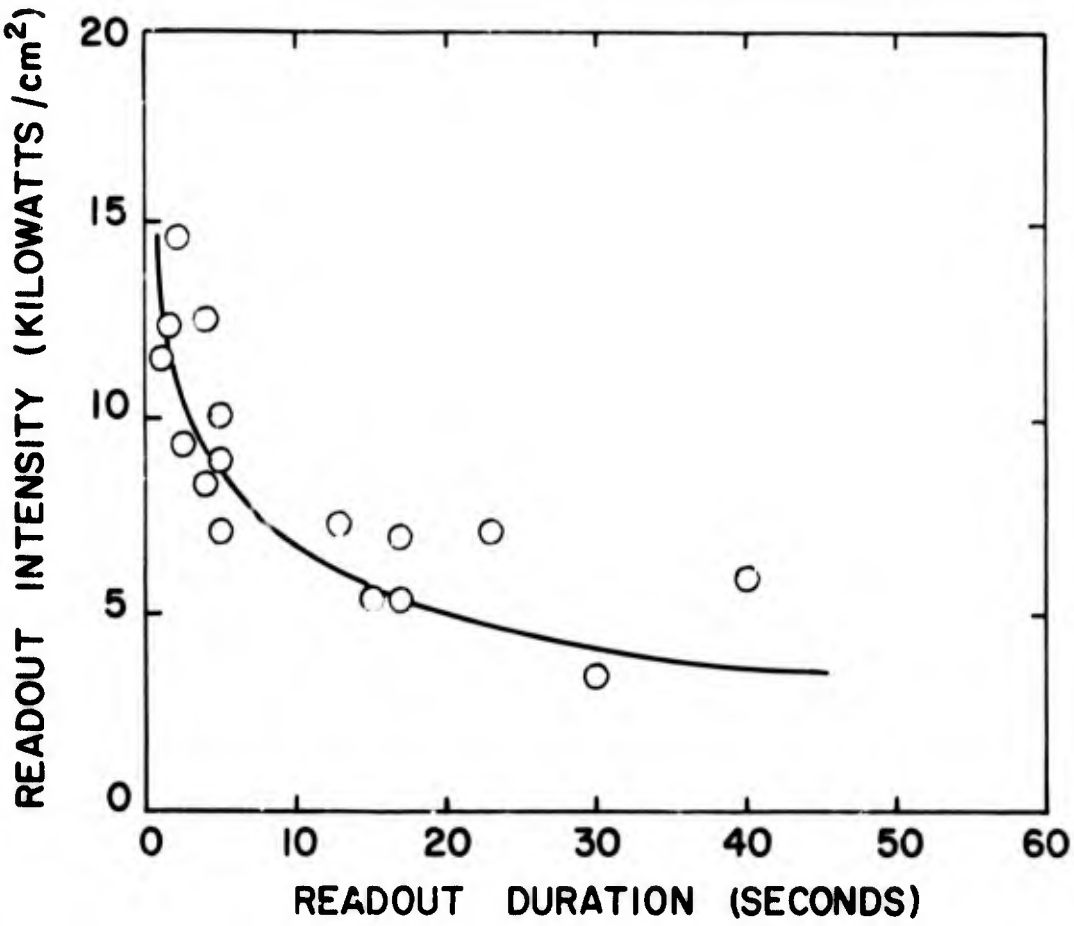

Figure 55

Destructive readout intensity as a function of readout duration for holograms recorded in photoresist.

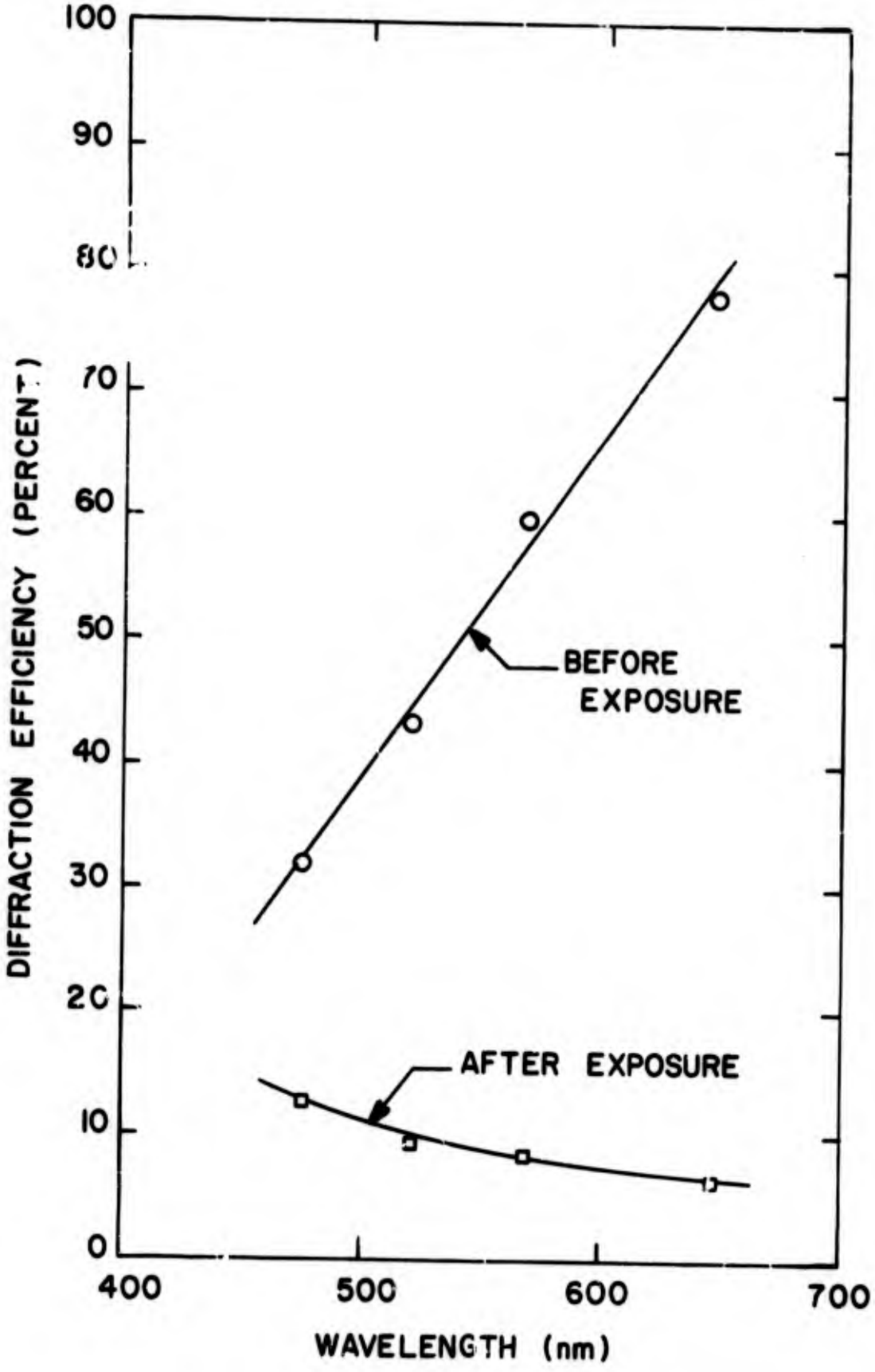

Figure 56

Readout efficiency as a function of wavelength for a grating recorded in photoresist, before and after outdoor exposure.

3.6 Iron Oxide

Iron oxide forms thin phase holograms as surface modulation. Since the iron oxide itself is not photosensitive, holograms are first recorded in an overcoating of photoresist. After the photoresist is developed, the holograms are transferred to the iron oxide film by means of a chemical etch process. Although they are thin holograms, iron oxide holograms are attractive because they are known to be impervious to adverse environmental conditions.[28]

3.6.1 Mechanism of Hologram Formation. — Holograms are recorded in thin films of iron oxide as outlined in Figure 57. The hologram is first recorded in the photoresist layer with UV or blue light. A relatively heavy exposure is made so that the developer removes enough photoresist to expose the iron oxide. The hologram is then formed in the iron oxide by chemically etching away the exposed areas of the film. After the iron oxide has been etched, the remairing photoresist is removed with an organic solvent.

Both the photoresist exposure and the iron oxide etch are critical steps that must be carefully controlled. If the photoresist is underexposed, the developer will remove insufficient material to expose the iron oxide to the etchant. After overexposure, on the other hand, the developer may remove all of the photoresist. Similar control is required during the etch process. Too little etching produces only a weak hologram; too much etching may undercut the photoresist and remove nearly all of the iron oxide.

3.6.2 Method of Use. — Iron oxide films are prepared by thermal decomposition of iron pentacarbonyl vapor in an oxidizing atmosphere. Iron pentacarbonyl compound, $Fe(CO)_5$, is selected as the source of iron since its propoerties combine high vapor pressure, which facilitates

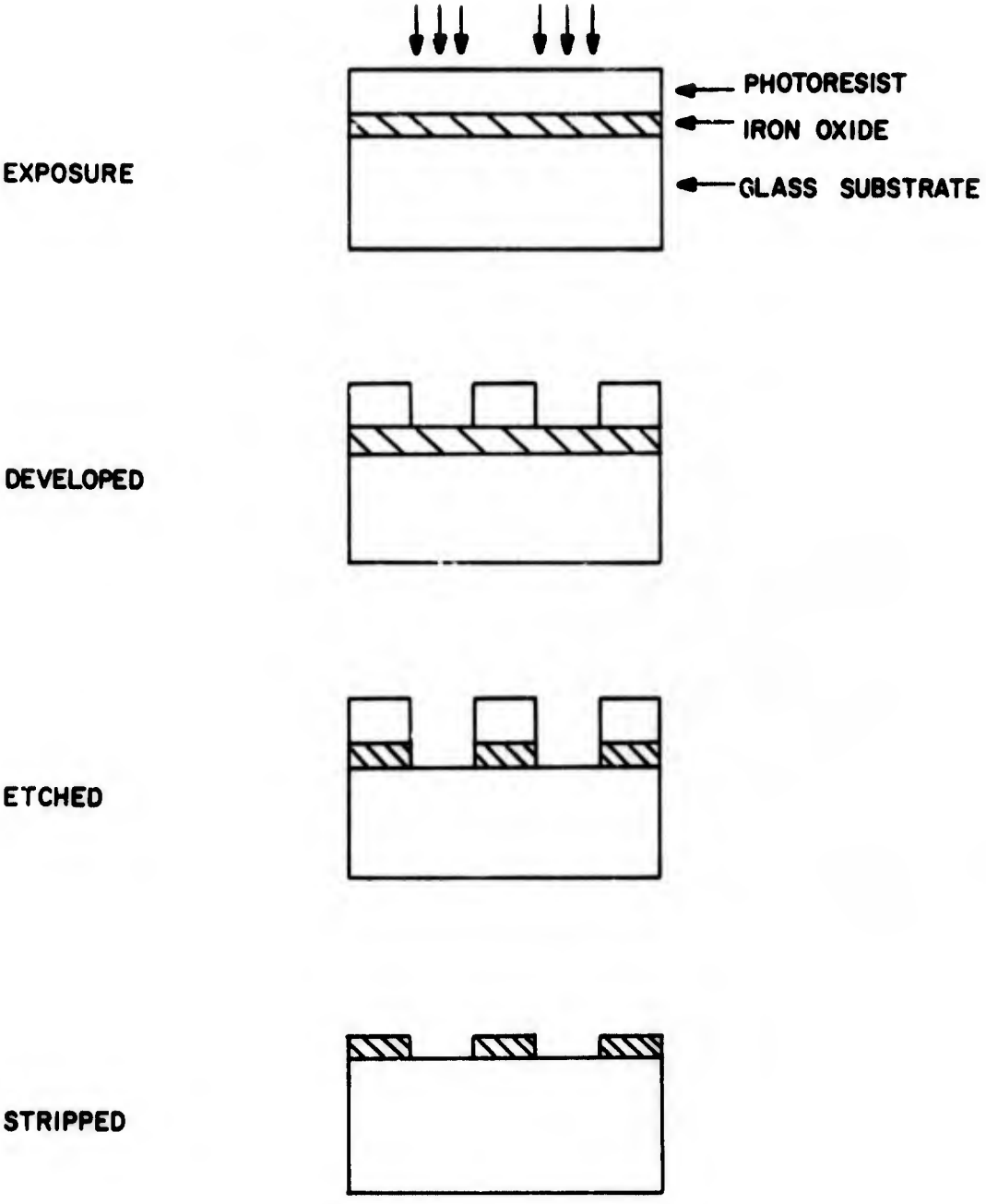

Figure 57

Steps of hologram formation in iron oxide.

transport in the vapor phase, and low decomposition temperature. The films are prepared in a deposition chamber resting on a hot plate. Iron pentacarbonyl vapor, generated by bubbling argon through a liquid solution contained inside a test tube, is transported to a "T" junction where it is mixed with oxygen or other gases prior to entering the deposition chamber. Film deposition occurs by thermal decomposition of the carbonyl vapor onto a heated substrate, which in our experiments was glass; excellent coatings can be achieved for film thickness of 90 nm to 400 nm.

After the iron oxide films are prepared, they are coated with a layer of photoresist. Spin coating techniques are used to produce uniform photoresist films. Immediately before recording the holograms, the photoresist should be baked to drive off residual solvent and water vapor. After the holograms are exposed and processed as described in Section 3.5 on photoresist, they are baked again to harden the photoresist for the etching step. In our experiments we baked the holograms in air for 30 minutes at 100°C. The time can be reduced if the holograms are baked in a vacuum oven.

The etchant we used was a slightly diluted solution of concentrated hydrochloric acid. The concentration of the solution is adjusted to give etching times of approximately 10 to 20 seconds. Fast etch rates are desirable because undercutting is minimized and cleaner edges are produced. For a given etchant, the rate of etching depends on the hardness of the iron oxide film (which can be controlled somewhat by proper heat treating). The time required to etch through the iron oxide layer also depends on the thickness of the layer. Therefore the acid concentration of the etchant must be adjusted according to the thickness and hardness of the iron oxide film. A typical etchant concentration is 10.0 M HCl.

Etching is terminated by rinsing the holograms with distilled water. The remaining photoresist can then be stripped by rinsing with an organic solvent such as acetone. Finally air drying leaves an iron oxide hologram on the glass substrate.

3.6.3 Experimental Results. — We evaluated holograms recorded in 170 and 400 nm thick layers of iron oxide. The holograms were initially formed in a 0.9 μm thick photoresist layer that was a 1:1 mixture of Shipley AZ1350 and AZ1350H photoresists. We developed the photoresist for 60 seconds in undiluted Shipley AZ Developer. In most of our experiments we read out the photoresist holograms before etching the iron oxide. Following the initial measurements, the holograms were baked for 30 minutes at 100°C to harden the resist. We etched the holograms in the acid solution for 10 seconds. After a complete rinse with distilled water, the photoresist was stripped with acetone, and the holograms dried with warm air.

Because of the increased sensitivity of the photoresist to short wavelengths, we recorded the holograms at 458 nm. We read out most of the holograms at 633 nm, however, since the absorption of the iron oxide was minimized at long wavelengths. This also allowed us to read out the photoresist holograms before etching the iron oxide without further affecting the photoresist.

3.6.3.1 Holographic Parameters. — Figure 58 shows diffraction efficiency as a function of exposure for plane wave gratings recorded in a 170 nm thick layer of iron oxide. These holograms were recorded with K = 1 at a spatial frequency of 570 lines/mm. The figure shows the diffraction efficiency of both the iron oxide and the photoresist; the photoresist measurements were made before the iron oxide was etched. The maximum efficiency of the iron oxide holograms is just over 10% at an exposure of 240 mJ/cm^2. The peaked nature of the iron oxide curve is typical of the results we obtained. This implies that only a narrow range of exposures exists in which sufficient photoresist is removed to expose the iron oxide to the etchant, without exposing so much of the iron oxide that it is completely etched away.

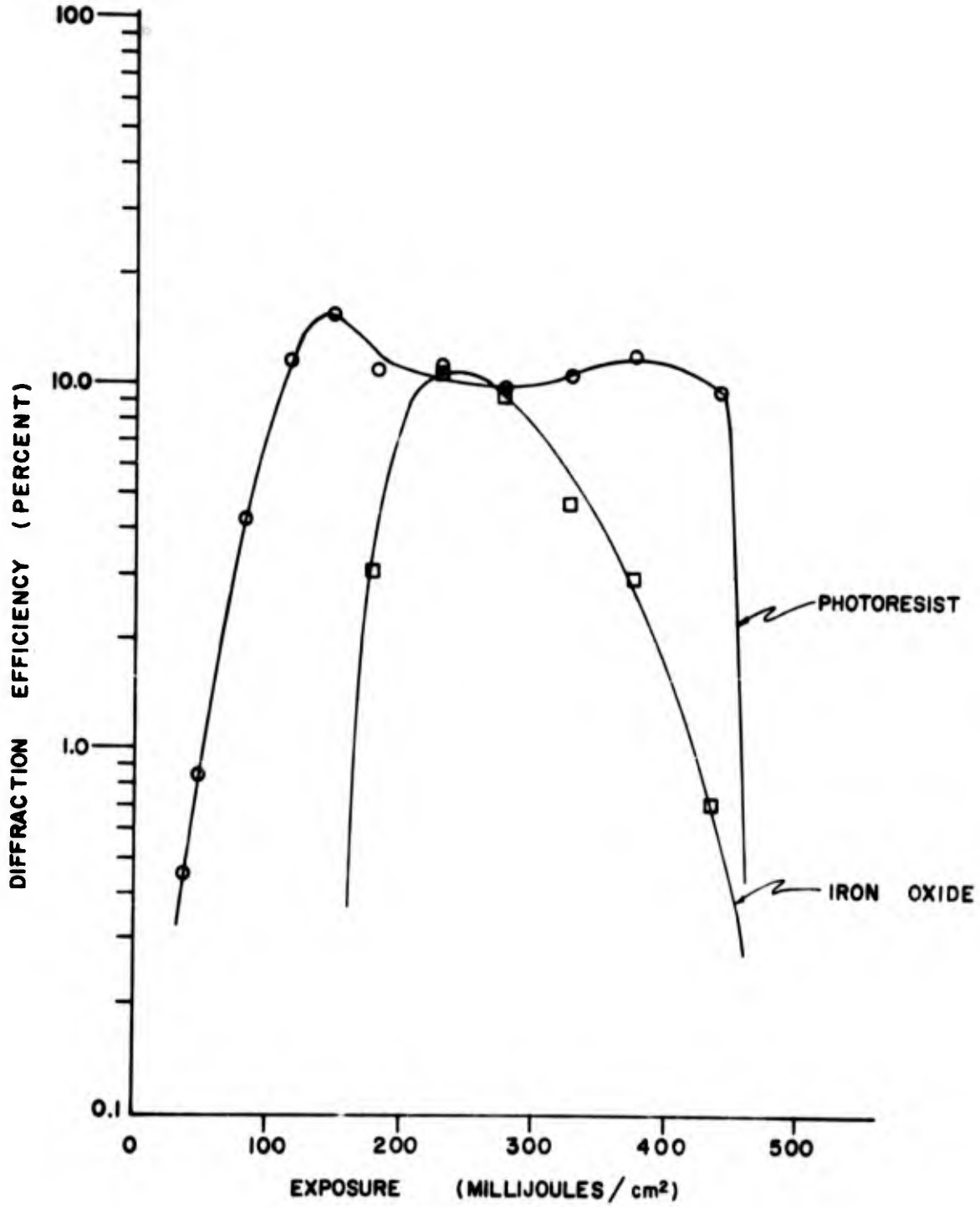

Figure 58

Diffraction efficiency at 633 nm of [illegible] ave gratings recorded in iron oxide (and photoresist) at 458 nm, [illegible] 1, and 570 [illegible]/mm.

Figure 59 shows diffraction efficiency as a function of exposure for plane wave gratings recorded at a spatial frequency of 1600 lines/mm. As with the previous figure, these holograms were recorded at 458 nm with K = 1 and read out at 633 nm. The diffraction efficiency of the iron oxide holograms reaches a peak of 20% at an exposure of 150 mJ/cm^2. The increased sensitivity compared with the previous figure is due to a fresher photoresist coating. The curve of iron oxide efficiency is extremely peaked here; we believe that this sharp peak occurs because the high spatial frequency limits still further the acceptable exposure range of the photoresist in which the iron oxide is etched neither too much nor too little. The second peak of the photoresist efficiency is due to the blazed effect. The photoresist diffraction efficiency reaches 48% and if we account for the approximately 40% absorption loss in the iron oxide, the peak is about 80%. This is comparable to our results with photoresist alone.

Figure 60 shows the diffraction efficiency of plane wave gratings recorded at 1600 lines/mm with K = 10. Again the efficiency curve of the iron oxide holograms is very peaked, reaching a maximum of only 7%. It is evident from this and the previous figure that at high spatial frequencies, the iron oxide is exposed to the etchant only at relatively high photoresist exposures.

We obtained a slightly broader peak in the efficiency curve of iron oxide holograms when we modified the geometry so that the reference and signal beams had equal angles of incidence. This is illustrated in Figure 61 where again the spatial frequency was 1600 lines/mm and K = 1.

Figure 62 shows curves of diffraction efficiency and SNR as a function of exposure for holograms recorded in iron oxide with the diffuse signal. These holograms were recorded at a spatial frequency

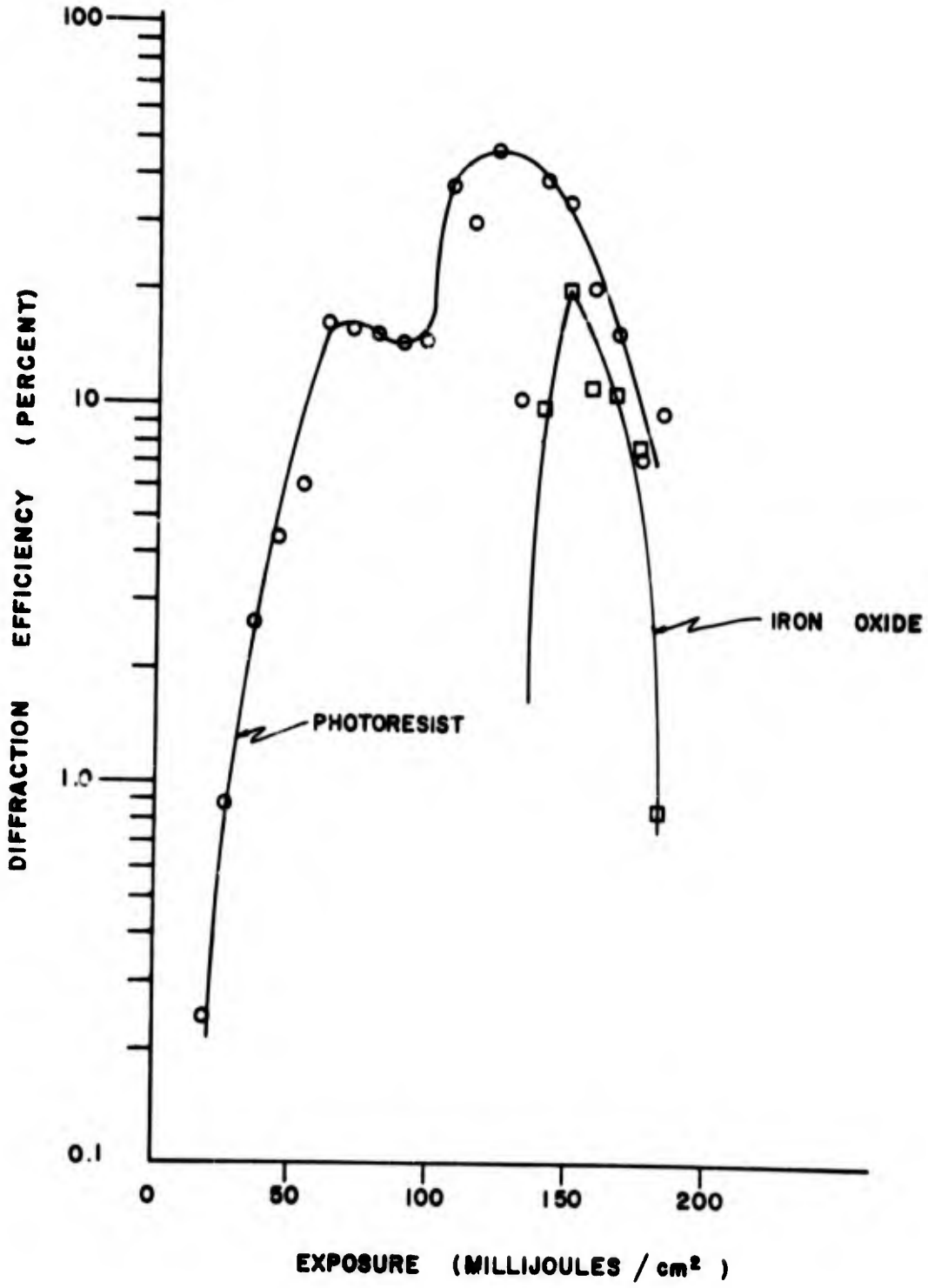

Figure 59

Diffraction efficiency at 633 nm as a function of exposure for plane wave gratings recorded in iron oxide (and photoresist) at 458 nm, K=1, and 1600 lines/mm.

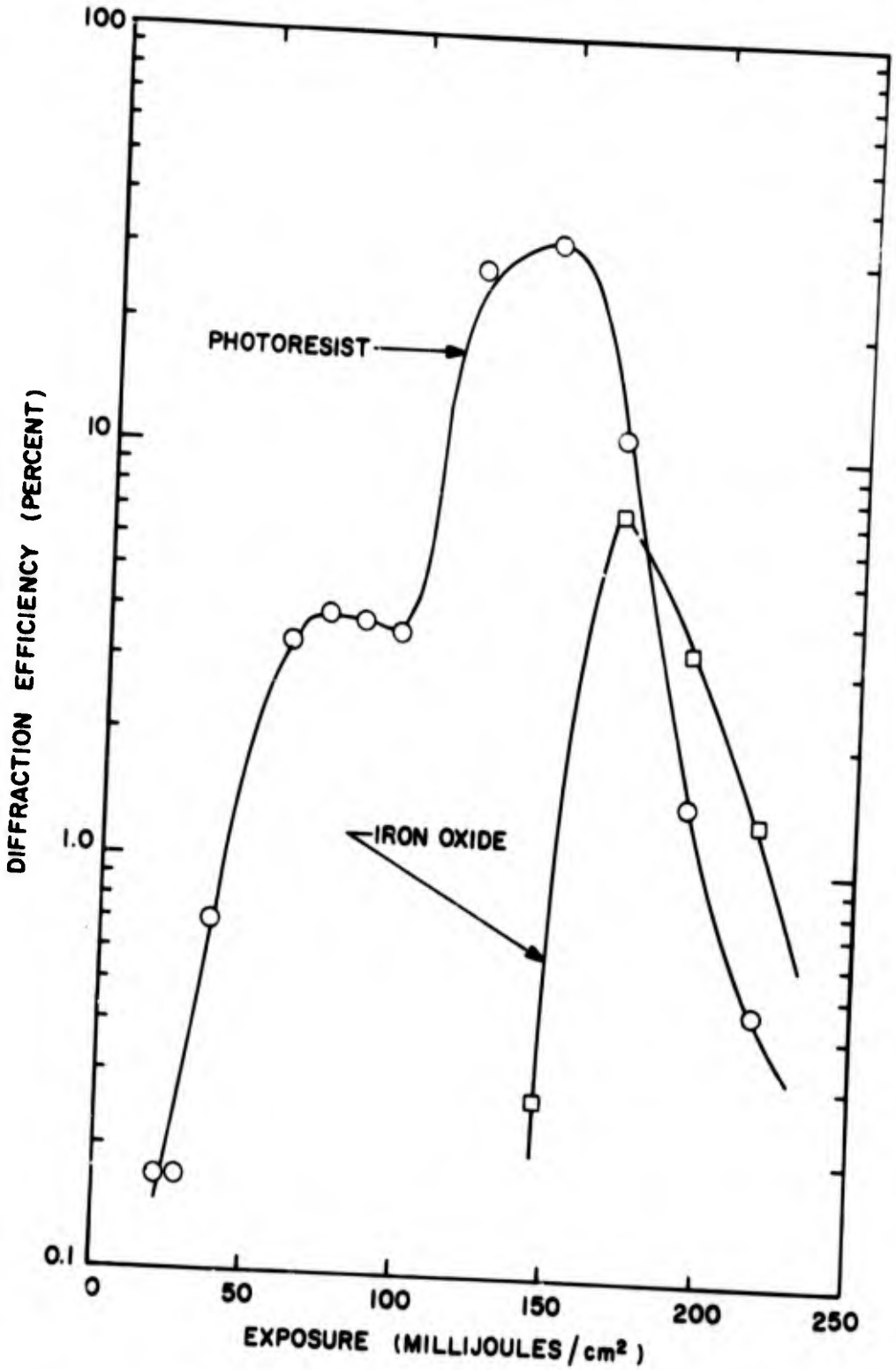

Figure 60

Diffraction efficiency at 633 nm as a function of exposure for plane wave gratings recorded in iron oxide (and photoresist) at 458 nm, 1010, and 1600 lines/mm.

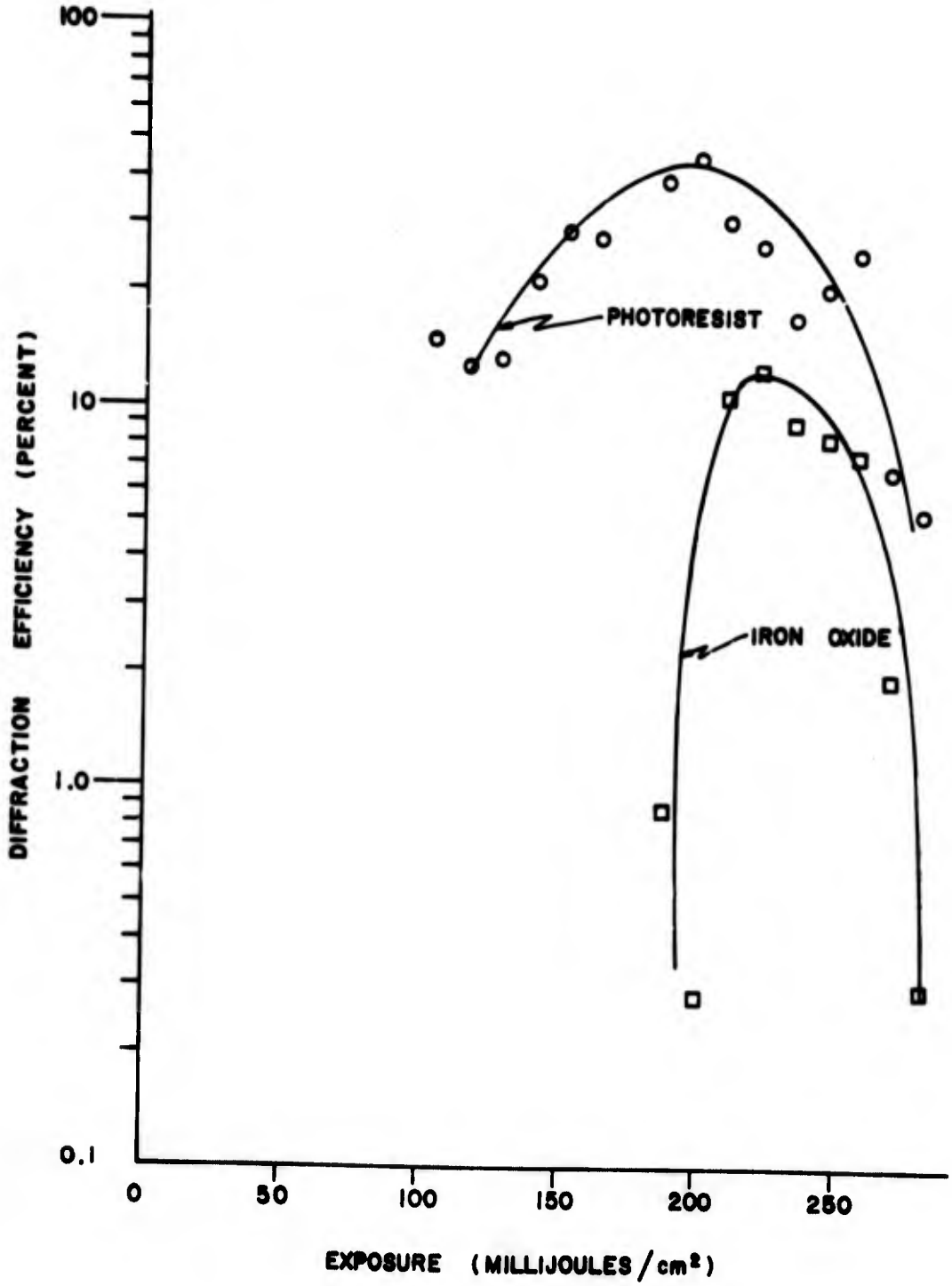

Figure 61

Diffraction efficiency at 633 nm as a function of exposure for plane wave gratings recorded in iron oxide (and photoresist) at 458 nm, K=1, and 1600 lines/mm.

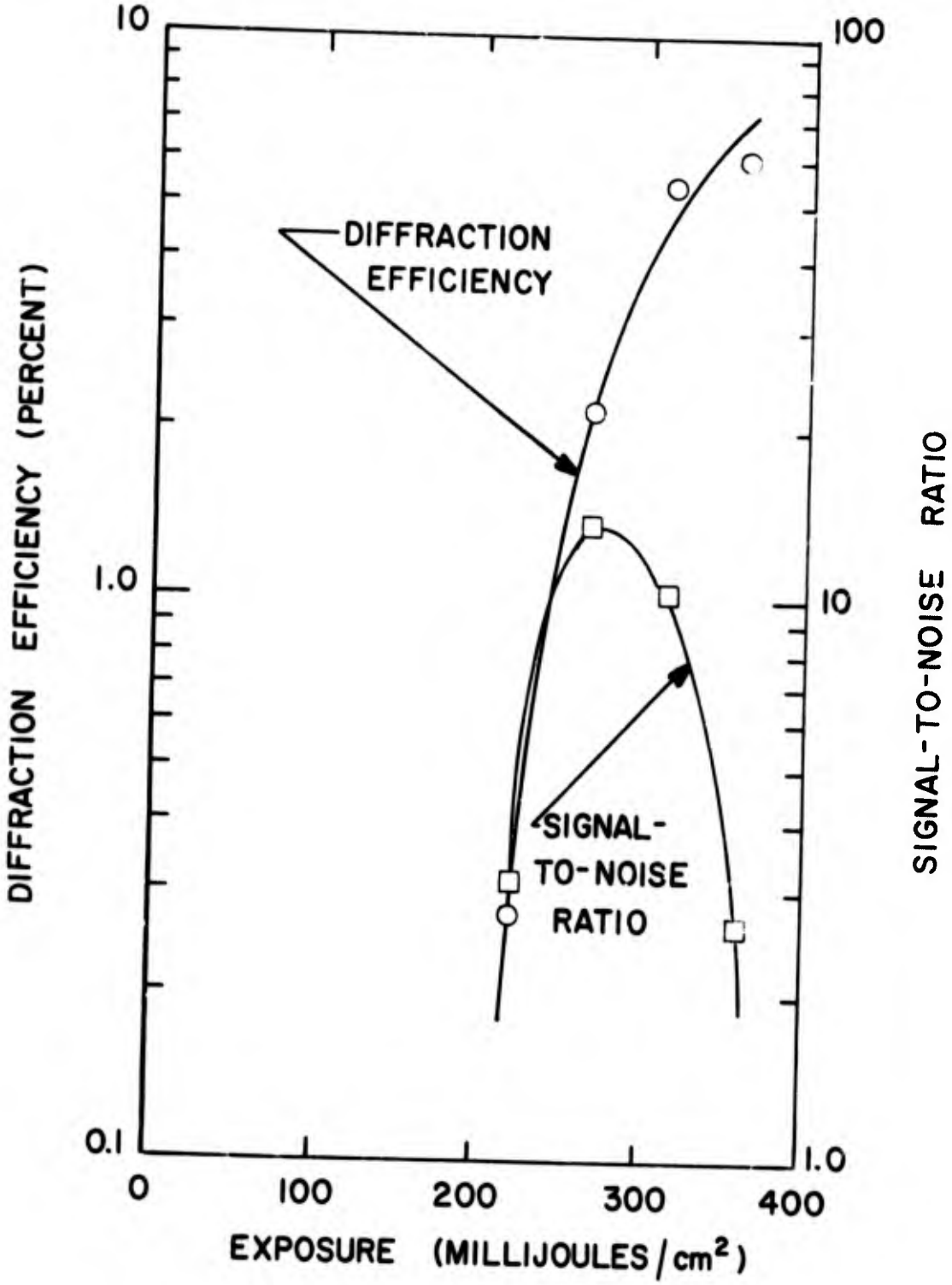

Figure 62

Diffraction efficiency and SNR at 633 nm as functions of exposure for holograms recorded in iron oxide at 458nm with K = 10.

of 570 lines/mm with K = 10. The maximum SNR was 14 (11.5 dB) which occurred at a diffraction efficiency slightly above 2%. Although the SNR was rather low, it should be pointed out that the iron oxide holograms required relatively heavy exposures of the photoresist, where as we showed in Section 3.5, the SNR of the photoresist itself was not particularly good. The maximum SNR of these holograms in the photoresist before etching the iron oxide was only 11.5 dB, whereas at light exposures that did not transfer to the iron oxide, the photoresist SNR reached 19 dB. Thus the SNR of the iron oxide holograms may have been limited by the photoresist. This limitation might be overcome with thinner photoresist layers so that the iron oxide is exposed to the etchant by lighter photoresist exposures.

Although we did not actually measure the frequency response of the iron oxide holograms, the figures show that iron oxide has a reasonably flat response to 1600 lines/mm.

In Figure 63, we show the spectral variation in readout efficiency and intensity transmittance as a function of wavelength for a typical plane wave grating recorded in iron oxide. Kogelnik[11] showed that the efficiency of thin phase holograms could be expressed as

$$\text{Diffraction Efficiency} = \exp\left[-\frac{\alpha(\lambda)t}{\cos\theta}\right] J_1^2\left[\frac{2\pi(n-1)}{\lambda}\, h\right]$$

where $\alpha(\lambda)$ = absorption coefficient of the material

λ = wavelength

θ = angle of incidence of the readout beam

J_1 = first order Bessel function

n = refractive index of the material

h = excursion of the surface deformation

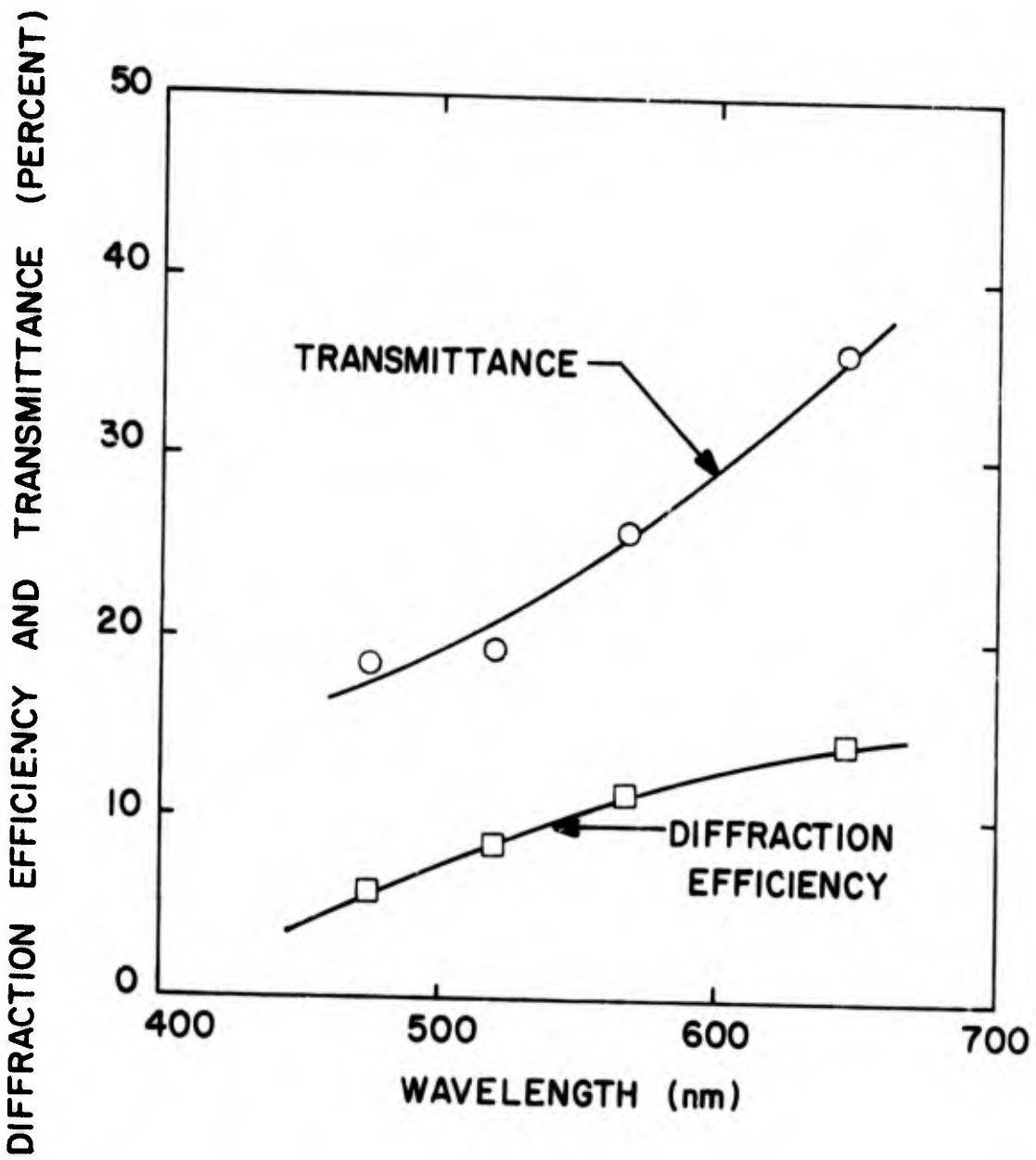

Figure 63

Spectral variation of transmittance and readout efficiency for a grating recorded in iron oxide.

We see from the curve of intensity transmittance that $\alpha(\lambda)$ varies inversely with λ. This increased absorption at short wavelengths causes a similar variation in diffraction efficiency. The diffraction efficiency at 1150 nm is less than at 633 nm, apparently due to the λ^{-1} term in the Bessel function. This is illustrated by Figure 64 which shows diffraction efficiency as a function of exposure for plane wave gratings read out at each of the two wavelengths. The peak efficiency decreased by a factor of four.

3.6.3.2 Environmental Testing. — As we anticipated, the iron oxide holograms were not affected by the environmental tests. Figure 65 shows the diffraction efficiency of a typical plane wave grating as a function of temperature and relative humidity. The diffraction efficiency remained constant over the entire range of elevated temperature and humidity. No change in efficiency was observed, either, for temperatures as low as -40°F.

A 36 hour exposure to UV radiation also failed to affect the efficiency of iron oxide holograms.

Figure 66 shows the destructive readout intensity for typical iron oxide holograms. Since the absorption of the readout beam was a function of the average exposure and amount of etching of the hologram, the destructive intensity varied somewhat among holograms. The minimum destructive readout intensity of the holograms we tested was approximately 800 watts/cm^2. This figure would be considerably higher at the red end of the visible spectrum where absorption by the iron oxide is about half.

In Figure 67 we show the results of the 50 hours exposure to direct solar illumination in the out-of-doors environment. Although there appears to be some change at the red end of the spectrum, we believe that the discrepancy is due primarily to experimental error.

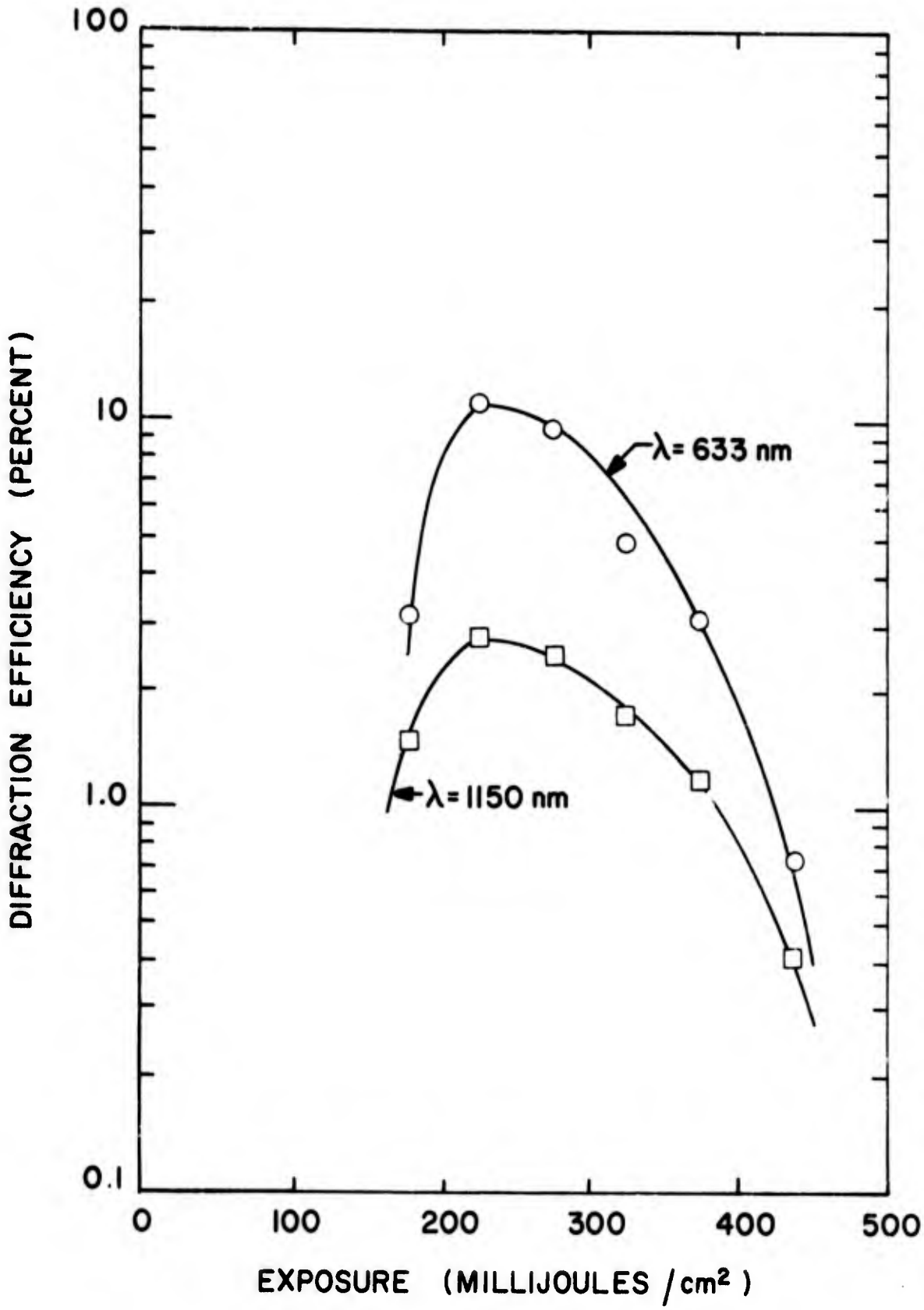

Figure 64

Diffraction efficiency at both 633 nm and 1150 nm for gratings recorded in iron oxide at 458 nm.

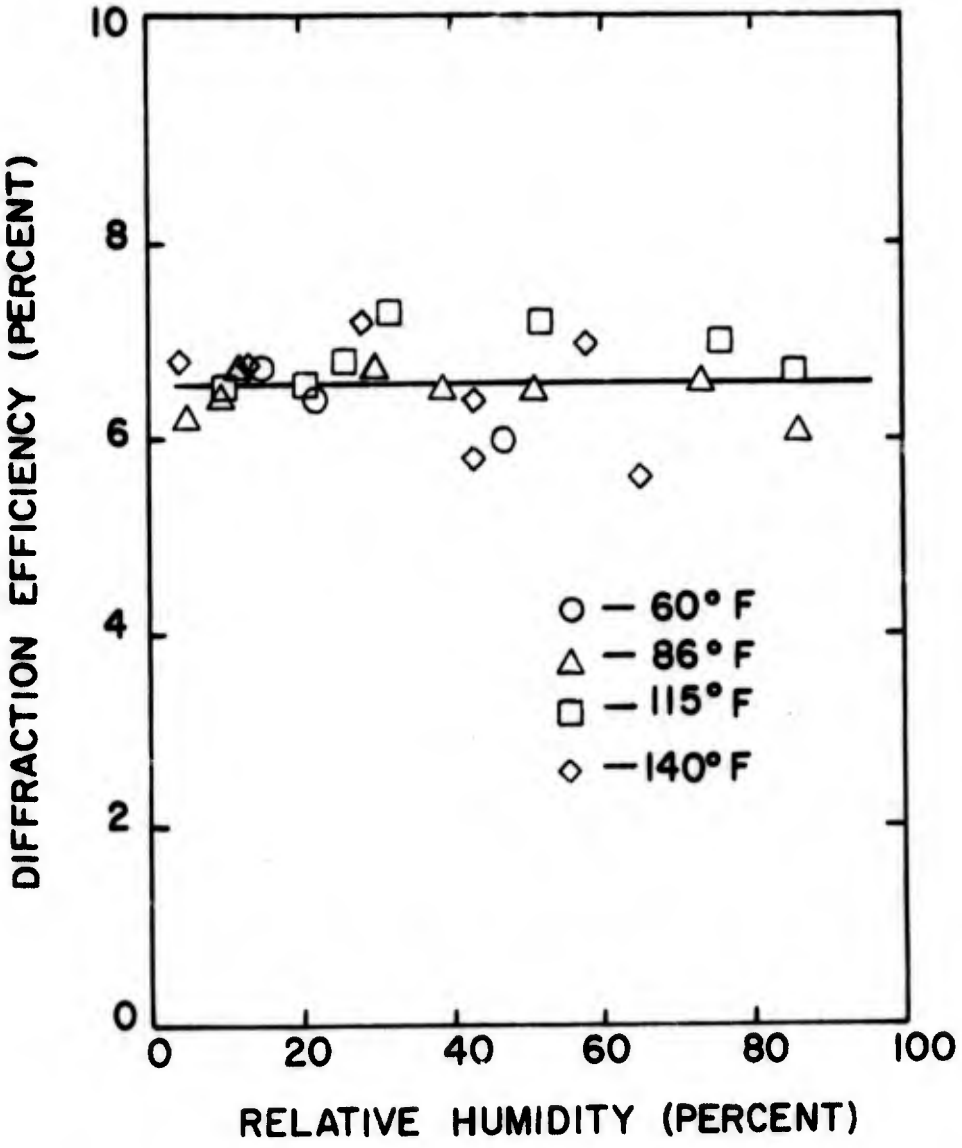

Figure 65

Diffraction efficiency as a function of relative humidity for iron oxide holograms.

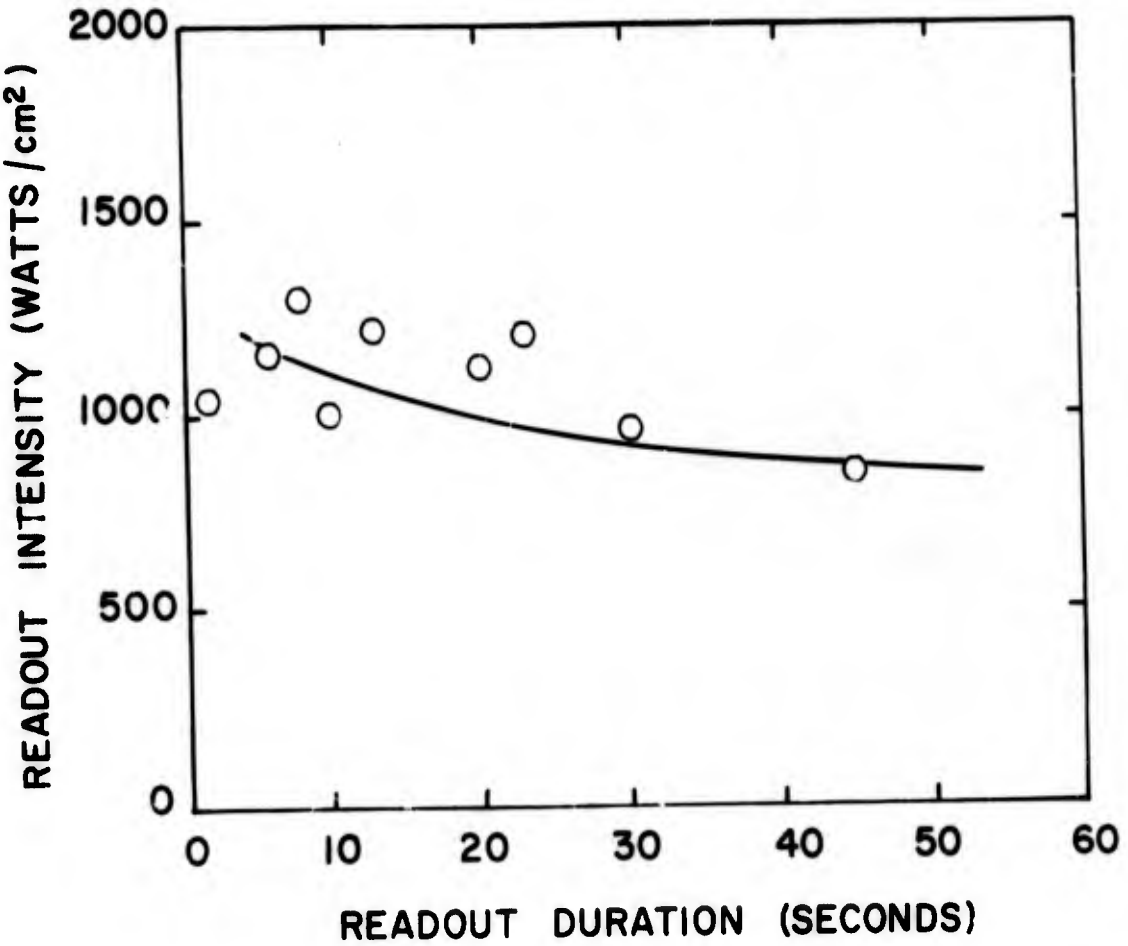

Figure 66

Destructive readout intensity as a function of readout duration for iron oxide holograms.

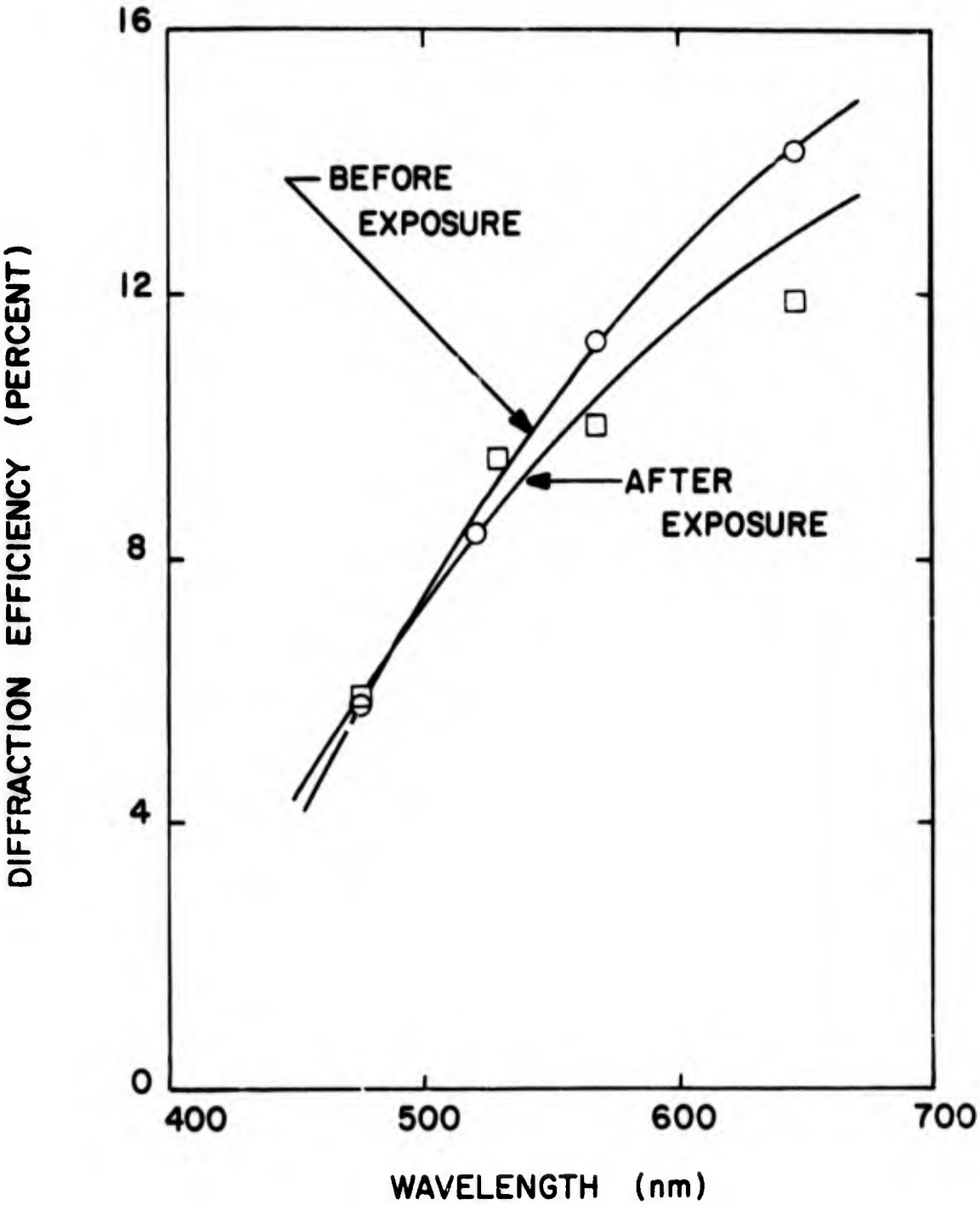

Figure 67

Readout efficiency as a function of wavelength for an iron oxide grating, before and after outdoor exposure.

3.7 Photoplastics

Photoplastic materials are photoconductive thermoplastic media on which holograms are recorded as surface deformations.[29,30,31] The materials are sensitized by a corona discharge to a positive or negative potential, exposed to visible radiation, and developed by heating to the flow temperature. Electrostatic forces produce deformations which are proportional to the light intensity used for exposure, and a stable hologram is formed if the photoplastic is cooled before surface tension of the plastic layer restores the original smooth surface. The hologram can be erased by heating the thermoplastic layer beyond the softening point. The surface forces restore the smooth surface and the materials are ready for a new recording cycle. The salient features of photoplastics which make them most attractive for general holographic applications are: (1) read/write/erase capabilities, (2) in situ recording, development, and readout, and (3) virtually real-time recording cycle (typically less than 5 seconds). For the holographic element applications, however, their attractive features include relatively high exposure sensitivities and, most important, a potential for holographic recording in the near infrared.

3.7.1 Mechanism of Hologram Formation. Photoplastic recording materials may be made with a number of different configurations on various substrates. We shall be concerned only with the configuration shown in Figure 68 which can be conveniently prepared. The substrate is an optical grade glass onto which a thin film of transparent conductor (generally tin oxide or indium oxide) has been deposited. The conductive layer is used for electrical heating and also for a ground plane for the charges deposited on the surface of the thermoplastic. An organic photoconductor layer is then coated on the transparent conductor, and the top layer consists of a deformable thermoplastic layer.

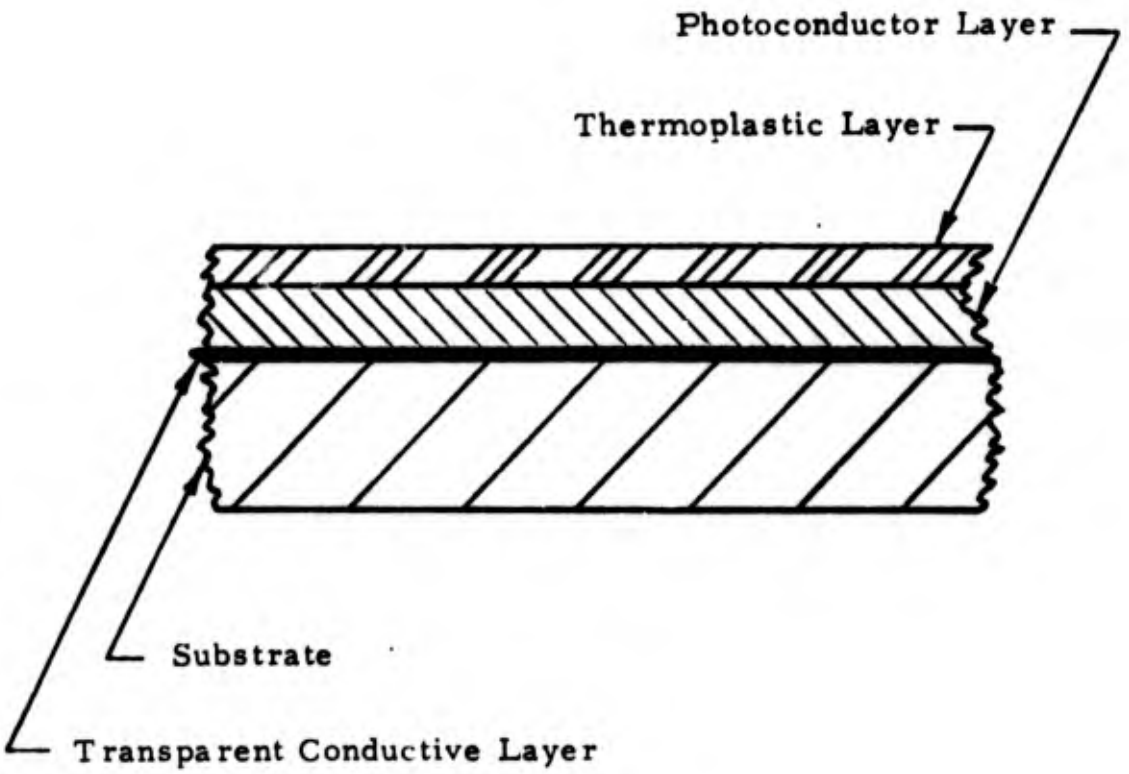

Figure 68

Configuration of photoplastic device.

A hologram is recorded in the photoplastic material as surface deformations corresponding to the spatial variations of the exposure pattern. The photoplastic holography process, which can be described with the aid of Figure 69 consists of four basic steps:

1. The recording medium is charged (in darkness) to a uniform potential by a corona discharge device.

2. The medium is exposed to light, causing a variation of the charge pattern on the photoconductor which corresponds to the variation in illumination. In the illuminated regions, displacement of charges from the transparent electrode to the photoconductor-thermoplastic interface reduces the electrostatic surface potential at the free surface of the thermoplastic.

3. The medium is recharged by the corona discharge to the original uniform surface potential.

4. The medium is developed by raising its temperature to near the plastic point and then rapidly lowering the temperature to the ambient level; surface deformations proportional to the light intensity are produced.

In the first step the medium is prepared for subsequent recording. The corona discharge device, consisting of a thin wire (approximately 4 mils diameter) at a voltage of 3 to 10 KV and an electrically grounded shield, deposits a uniform charge distribution on the thermoplastic. After this sensitization step the recording material must be handled or stored in darkness. After the exposure, additional surface charge is added to the optically exposed areas only; the amount of additional charge is proportional to the change in the internal field during exposure and, therefore, to the impinging light pattern. Varying surface charge densities corresponding to the holographic light intensity pattern are thereby formed, creating variations in the attractive electrostatic forces across the thermoplastic layer.

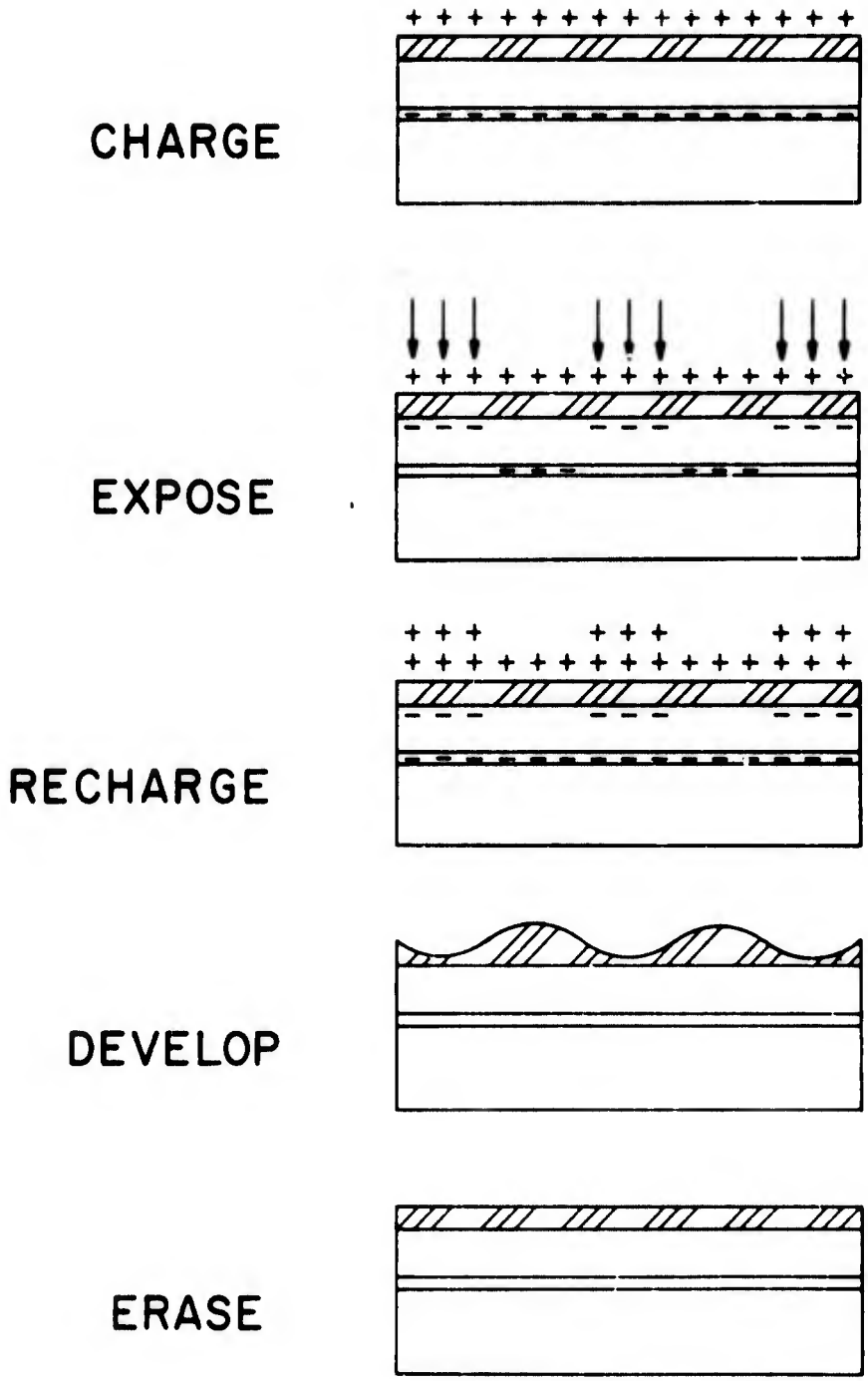

Figure 69

Steps of hologram formation in Kotoplastic.

In the fourth step, the photoplastic medium can be developed, even in ambient light, by lowering the viscosity of the thermoplastic layer. The material then deforms in a manner related to the surface charge density distribution. To lower its viscosity, the temperature is raised to approximately 80°C. Rapid cooling to room temperature will result in a deformation which remains stable until intentional erasure. Heating is achieved by applying a voltage pulse across the conductive layer.

One of the attractive features of photoplastic holograms is that they can be erased and rewritten. More heat than that used for developing is applied to the thermoplastic either by increasing the current in the pulse or by applying the same pulse for a longer period. Erasure usually neutralizes the electrostatic charges after which the recording process can be repeated.

Recently it has been shown that holograms can be recorded by simultaneously charging and exposing the photoplastic during and immediately following heating.[32] The continuous application of charge while the hologram is deforming increases the ultimate amount of deformation. This is because charging the surface to a uniform potential once deformation has begun places more charge in the thermoplastic grooves, since the grooves are closer to the ground plane than the peaks are. This technique is reported to produce holograms with high diffraction efficiences and good SNR.

3.7.2 Method of Use. — The holographic technique for recording information places a number of requirements on the photoplastic material. First, it must be sensitive to laser radiation. Second, it must scatter very little of the laser light. Third, it should have sufficient

electrical resistance to prevent dissipation of the electro-static charges before deformations can occur. Finally, the glass transition temperature must be reasonably low to enable deformation with practical resistive heating but high enough to prevent loss of deformation during storage.

A number of materials satisfy most of these requirements, including poly-n-vinyl carbazole (PVK) sensitized with trinitrofluorenone (TNF) photoconductor and Staybelite wood resin thermoplastics. Recently we have been using an ester resin thermoplastic with improved chemical stability. It also has a softening temperature about 20°C higher than that of Staybelite, making holograms more resistant to unintentional erasure due to high ambient temperature.

The substrate for the photoplastic device is typically a glass plate, coated with transparent tin oxide having a resistivity of 50 ohms per square. The substrate is etched with zinc powder and hydrochloric acid to leave isolated squares; we have used squares that range in size from 1 mm x 1 mm to 100 mm x 100 mm. Two silver electrodes along opposite edges of each square are used to connect the tin oxide squares to an electrical source which supplies the necessary current pulses to heat the squares. Development and erasure of a hologram is achieved by resistive heating; a voltage pulse is applied across each square. We use pulse lengths of 150 milliseconds and an average power of 30 watts for developing a 10 mm x 10 mm square.

After chemical cleaning, the substrate is coated with a layer of organic photoconductor and a layer of thermoplastic; conventional dip coating techniques are used. To obtain a photoconductive solution suitable for coating, we mix the PVK polymer sensitized with TNF in a tetrahydrofuran solvent. The concentration of the solution and the rate of pulling are adjusted to give a coating thickness of 3 microns. The thermoplastic is dissolved in naphtha; the concentration and pulling rates are adjusted to give thermoplastic layer thicknesses ranging from 0.5 to 2 microns.

The substrate and component layers are then baked in an oven at 60°C for an hour to evaporate the solvents. The coated plates are removed, cooled, and stored in dust-free containers until used.

Holograms are recorded as outlined in the previous section. Charging is usually accomplished by moving the corona discharge device over the surface of the photoplastic device. If the hologram area is small (1 cm^2 or less), the corona can be applied during the entire second cycle with a stationary corona device, simplifying the cycle somewhat.

Because the PVK-TNF charge complex has a panchromatic response, holograms can be recorded throughout the visible spectrum. The exposure sensitivity is relatively high, at about 100 $\mu J/cm^2$. The high exposure sensitivity and broad spectral response are comparable to those of 649F.

Photoplastic recording materials show a bandpass response to the spatial frequencies in the recording light.[29] The reasons for this behavior can be seen from the following simple arguments: the low frequency response is limited by the distance over which the electrostatic forces can move material and by the amount of material they can transport. At high frequencies, the response is limited by increased surface tension forces and reduced resolution in the surface potential variation caused by the exposure. It can be seen from these arguments that the center frequency of the passband will vary inversely with the thickness of the thermoplastic layer. Thus the thickness of the thermoplastic must be adjusted to the band of spatial frequencies to be recorded in the hologram.

3.7.3 Experimental Results. — Most of our measurements were made on 1 cm^2 photoplastic devices using the highly stabilized ester resin as thermoplastic. Because of the small sample area, we used a stationary corona device. Except where noted, all holograms were recorded and read out at 633 nm.

3.7.3.1 Holographic Parameters. — Figure 70 shows diffraction efficiency as a function of exposure for plane wave gratings recorded with K-ratios of 1, 4, 10, and 40. The peak diffraction efficiency is 10% occurring at an exposure of about 60 microjoules/cm^2. At K = 1, the material has a very broad response, with a nearly constant efficiency over four orders of magnitude of exposure.

Figure 71 shows curves of diffraction efficiency and SNR for holograms recorded with the diffuse signal at K = 5. The SNR peaks at 45 (16.5 dB) at an exposure of 40 microjoules/cm^2. The diffraction efficiency at this exposure was about 2%. These parameters are very similar to those measured for bleached 649F at a K-ratio of 4. Although both photoconductor and thermoplastic materials are grainless, photoplastic holograms can suffer from some noise due to scattering. This is noise due to a quasi-random surface deformation, referred to as "frost", that is created by the action on the thermoplastic of charging and heating alone. Careful adjustment of the recording parameters suppresses most of the frost deformation; residual frost acts as a source of noise in the hologram.

The frequency response of a typical photoplastic device is shown in Figure 72. This curve of diffraction efficiency as a function of spatial frequency was made with plane wave gratings at 488 nm. The center frequency of the response can be taken as about 850 lines/mm, with a passband of nearly 600 lines/mm.

Figure 73 shows the spectral variation of readout efficiency and intensity transmittance for a typical photoplastic grating. In the visible portion of the spectrum, the efficiency variation is dominated by the transmittance of the PVK-TNF complex. At longer wavelengths, where the transmittance is nearly contant, the λ^{-1} term in Kogelnik's expression for efficiency dominates, and the diffraction efficiency decreases from 11% to 4.5%. We attempted to record plane wave gratings in photoplastic at 1150 nm but were unsuccessful even with exposures as great as 50 J/cm^2.

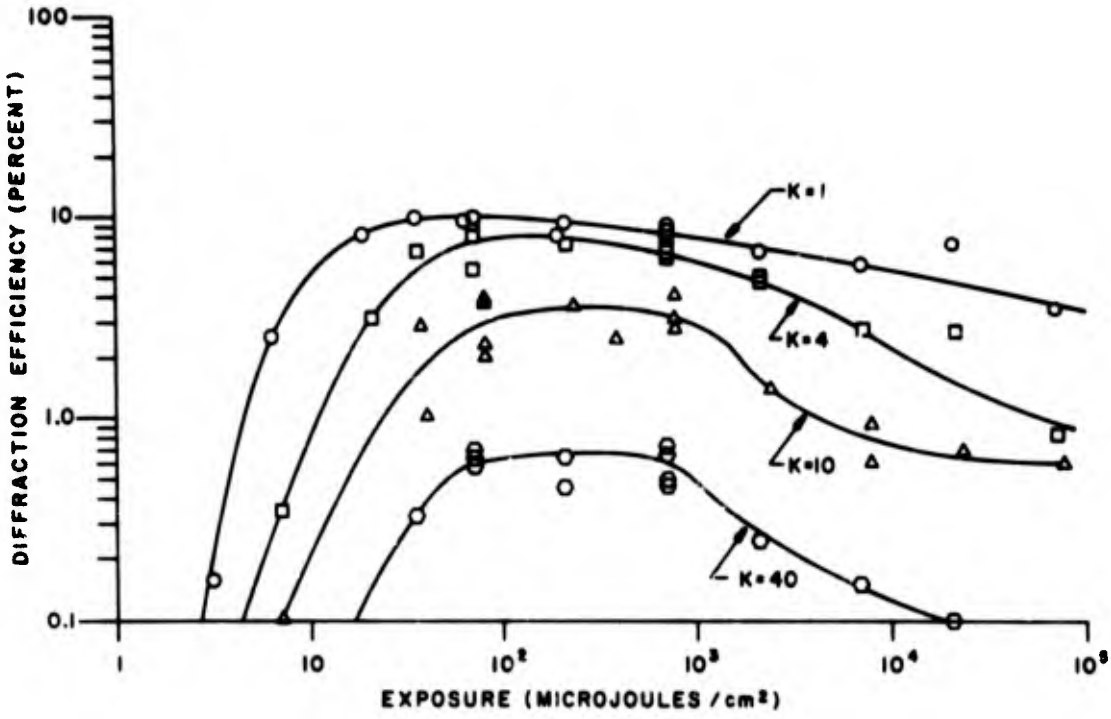

Figure 70

Diffraction efficiency as a function of exposure for plane wave gratings recorded in photoplastic.

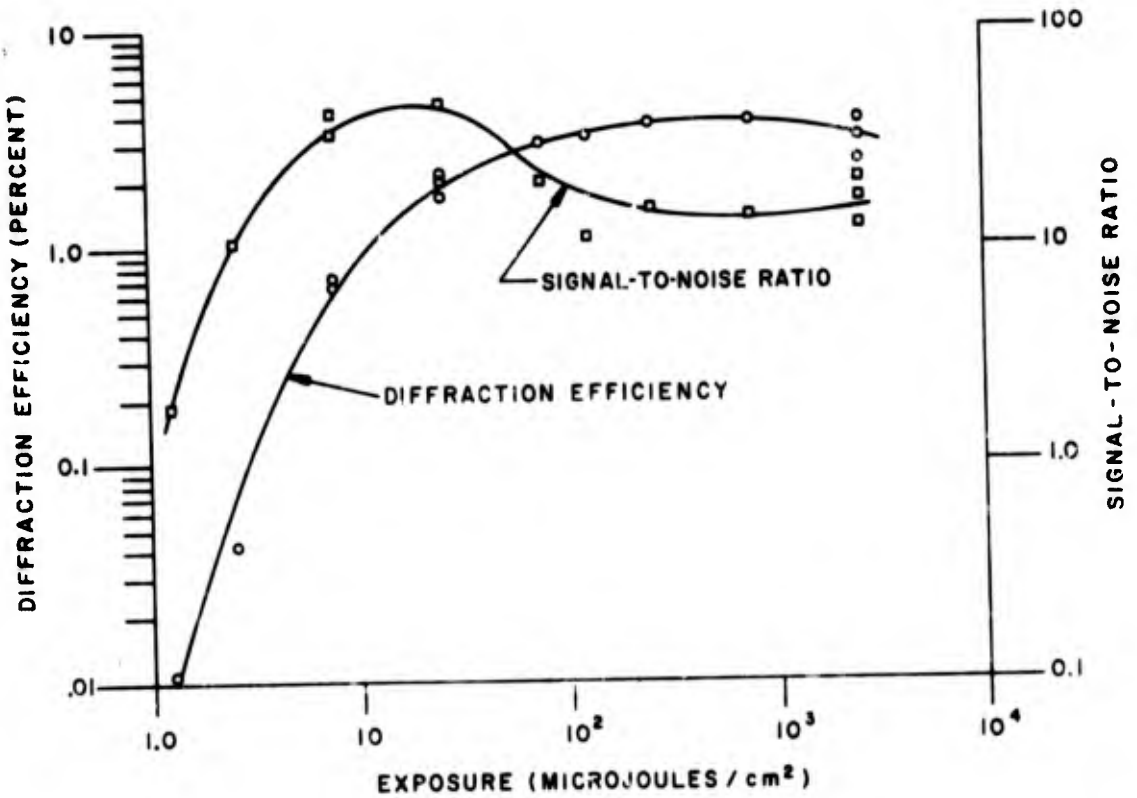

Figure 71

Diffraction efficiency and S/N as functions of exposure for holograms recorded in photoplastic at K=5.

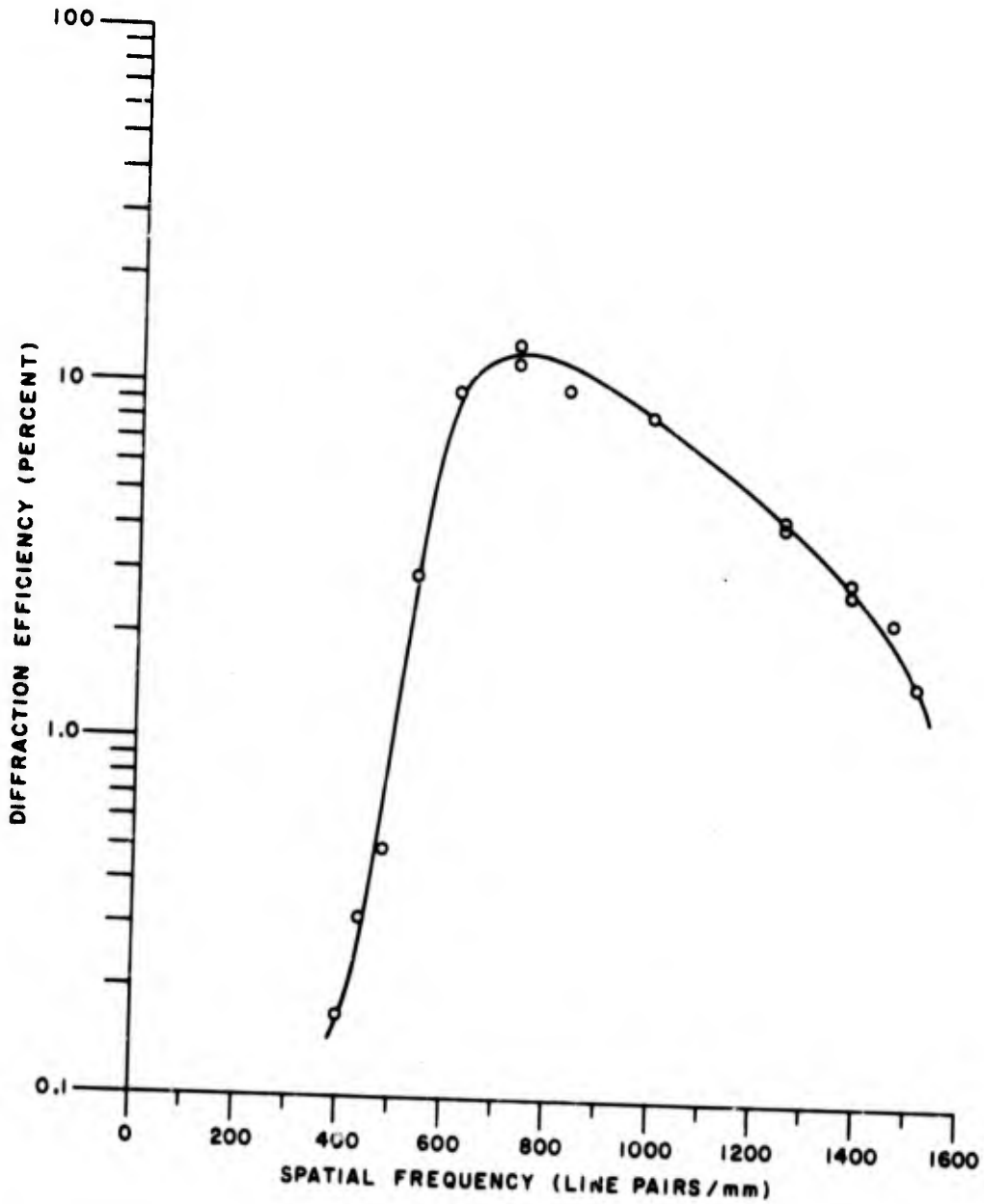

Figure 72

Spatial frequency response of photoplastic.

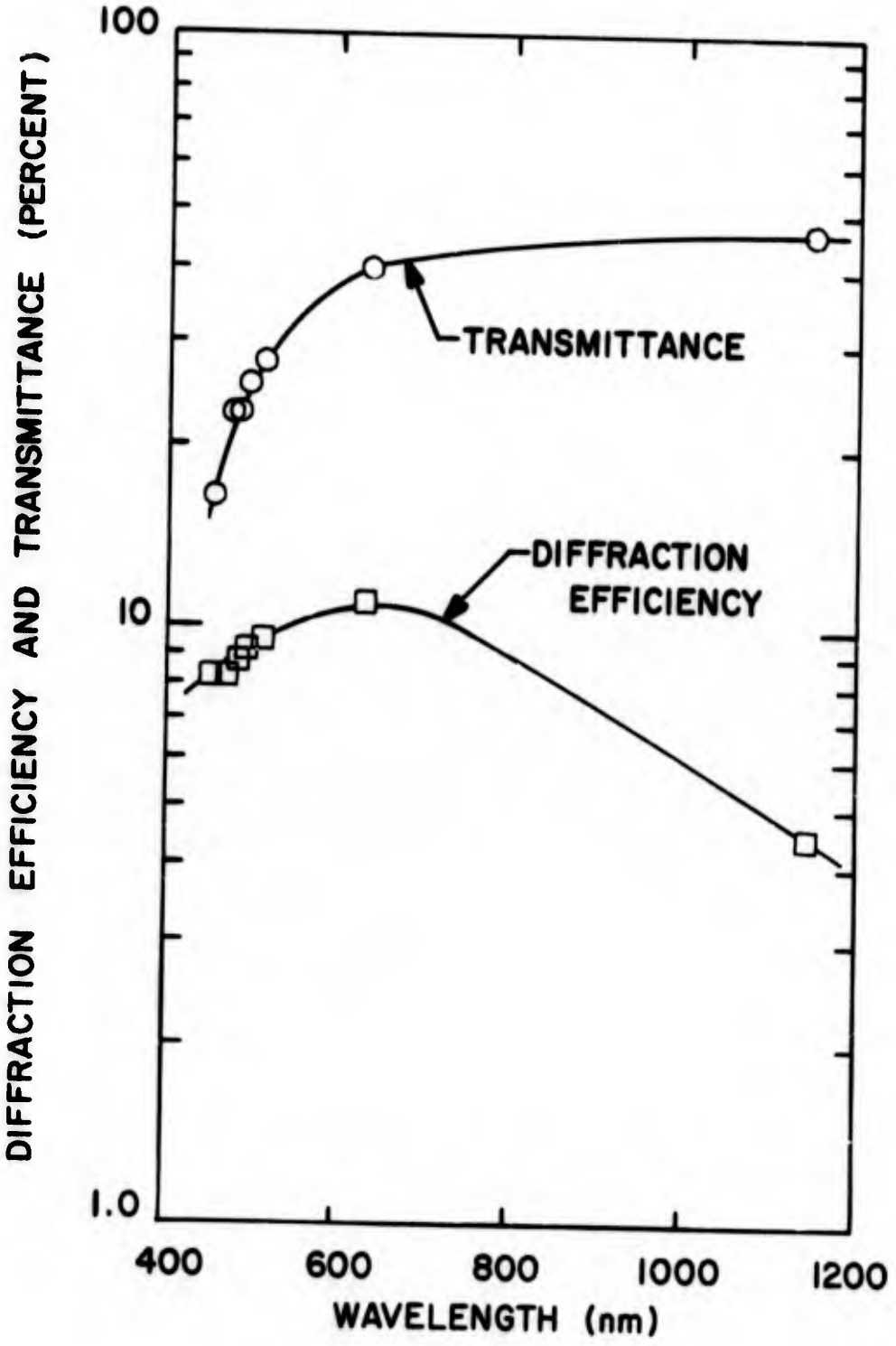

Figure 73

Spectral variation of transmittance and readout efficiency for a photoplastic grating.

3.7.3.2 Environmental Testing. — Photoplastic holograms withstood the humidity and temperature range well except that at 140°F they gradually erased due to cold flow of the thermoplastic. This is illustrated in Figure 74. At 112°F, the diffraction efficiency is not affected by humidity. The curve at 140°F turns downward due to the temperature rather than humidity. The test began at low humidity; temperature was maintained at 140°F while the relative humidity was gradually increased to 90%. During the time required for the test, the thermoplastic deformations flowed sufficiently to erase the hologram. This was confirmed by monitoring the efficiency of a photoplastic hologram maintained at 140°F with low humidity. Unintentional erasure due to cold flow at high ambient temperature can be prevented by choosing a thermoplastic with a sufficiently high softening temperature. The nominal softening temperature of the thermoplastic we tested is about 210°F (35 degrees higher than the conventional Staybelite resin). We would expect thermoplastics with a nominal softening temperature on the order of 300°F to be resistant to cold flow at 140°F. (Unlike substances such as ice, thermoplastics soften gradually with increasing temperature in the manner of glass. The softening temperature is arbitrarily defined by one of several standard measurements.)

Twenty six hours exposure to UV radiation did not affect either the SNR or diffraction efficiency of photoplastic holograms.

Figure 75 shows the readout intensity required to damage photoplastic holograms. The lower curve represents the intensity level that heats the material (actually the photoconductor) enough to erase the hologram. The level of this curve will also depend on the softening temperature of the thermoplastic. The upper curve represents the intensity level that actually destroys the material (again the photoconductor). The minimum destructive intensity is approximately 100 watts/cm^2; the minimum erasure intensity is about 12 watts/cm^2. Both curves should be higher

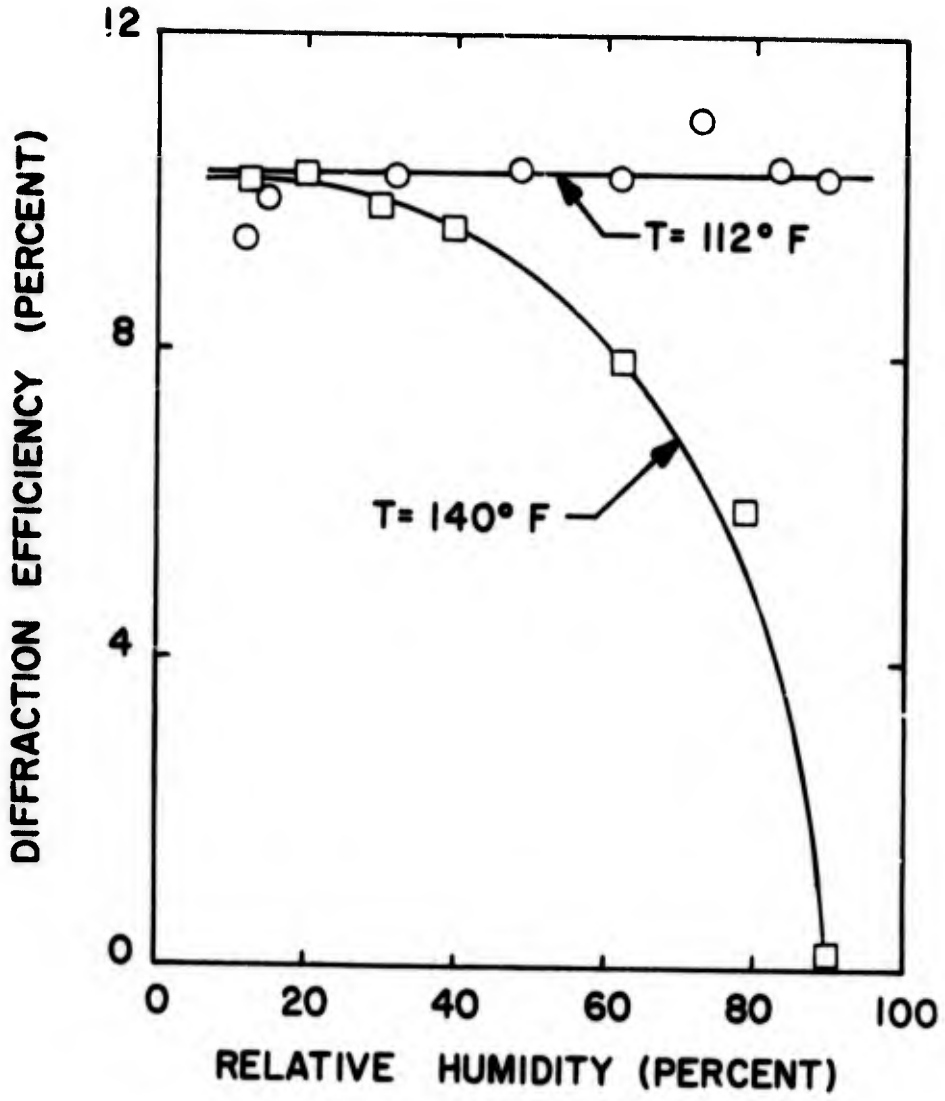

Figure 74

Diffraction efficiency as a function of relative humidity for photoplastic holograms (degradation shown by lower curve is due to high temperature).

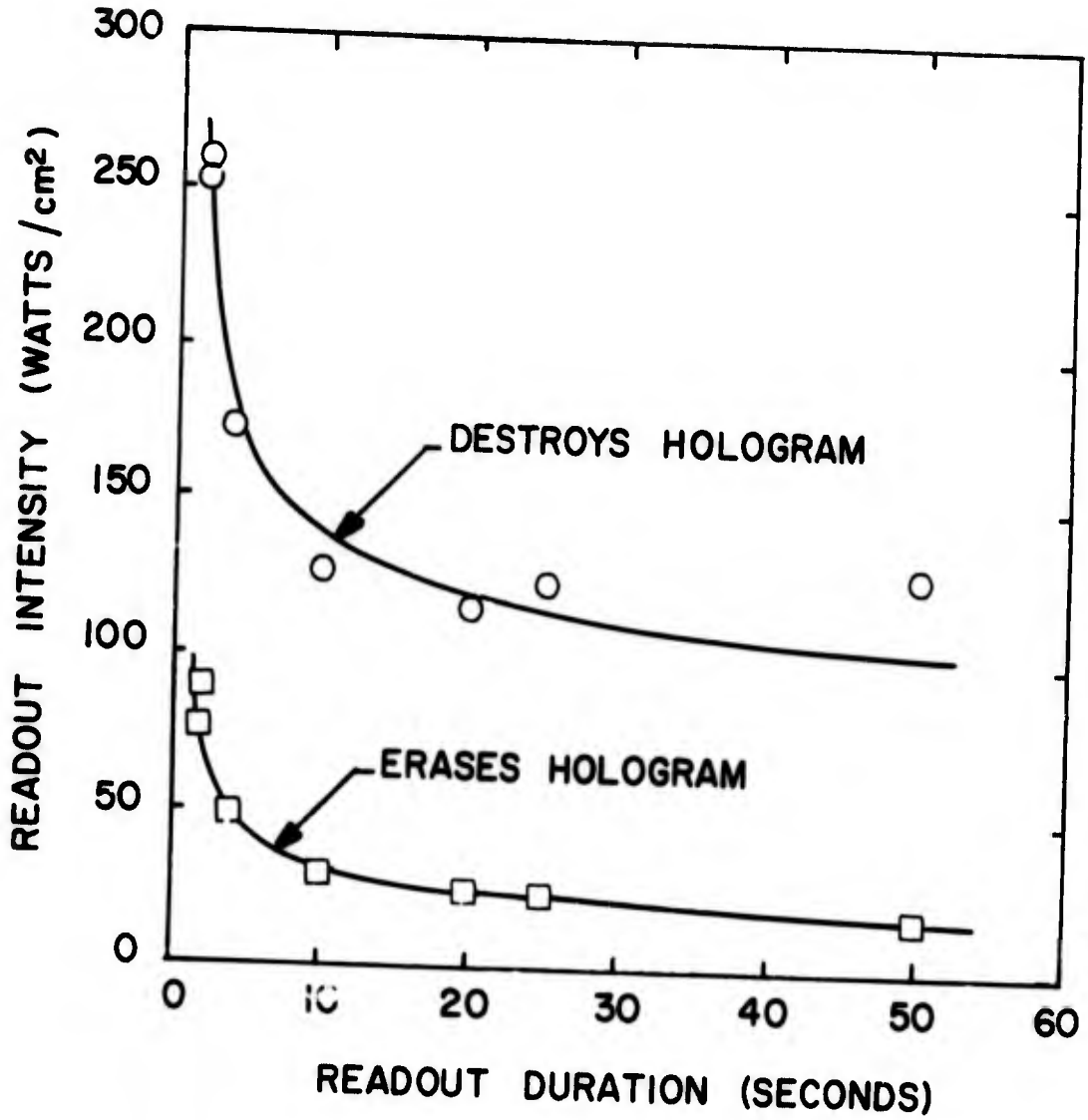

Figure 75

Destructive readout intensity as a function of readout duration for photoplastic holograms.

for readout with red light since the absorption of long wavelengths by the PVK-TNF complex is less by a factor of at least two. Alternatively, the TNF can be omitted from the photoconductor which is then colorless. Reduced absorption in this case is gained at the price of three orders of magnitude in exposure sensitivity as well as the loss of sensitivity to red light.

SECTION IV

SUMMARY OF MATERIALS

In the course of this program we tested seven holographic recording materials; four of the materials form volume phase holograms and three form thin phase holograms. Each material had certain outstanding characteristics; none was outstanding in all respects.

Photographic emulsions have relatively high exposure sensitivity and panchromatic spectral response. Although the entire process required to develop and bleach holograms is lengthy, it is straightforward and gives consistent results. The diffraction efficiency and SNR of bleached holograms is limited by relatively strong absorption and scattering caused by silver halide grains. Because of the gelatin emulsion, bleached photographic plates must be protected from the effects of humidity. Finally, exposure to blue or UV light tends to cause the bleached holograms to darken.

Dichromated gelatin forms holograms of high efficiency and good SNR; it was perhaps the best of the materials in this respect. Exposure sensitivity is moderate, but is limited to the blue region of the spectrum. Although consistency was once a problem, recent improvements in the processing technique have led to generally consistent results. Because of the nature of the dichromated gelatin holograms, they are extremely sensitive to the effects of humidity. The only means by which we could give them complete protection was to cement a glass cover plate over the holograms.

The DuPont photopolymer is also capable of recording holograms of high efficiency and good SNR. In addition, it is a self-developing material, and it can be cast to any reasonable thickness. The spectral response is limited to the UV and blue region of the spectrum. With UV light, the exposure sensitivity is moderate; with blue light the

exposure sensitivity is low unless a special dye is added which may tend to cause some scattering noise. Continued exposure to UV radiation appears to cause some degradation to photopolymer holograms. The combination of high temperature and humidity also degrades holograms recorded in the photopolymer.

Thick thermoplastics are also capable of recording holograms of high efficiency and good SNR. Like the photopolymer, they are self-developing and can be cast to any reasonable thickness. Their exposure sensitivity is low, and is limited to the blue and UV region of the spectrum. They are affected somewhat by high temperature and humidity. Holograms recorded in thick thermoplastics have the lowest nondestructive readout intensity limit of the seven materials.

Photoresist can record efficient holograms with good SNR. Blazed gratings with very high efficiencies can be formed in certain cases. Processing is relatively simple, but requires careful control. Exposure sensitivity is low to moderate, with a spectral sensitivity that limited to the blue and UV region of the spectrum. Photoresist holograms are darkened by prolonged exposure to UV and cracked by high humidity. Unlike the thick phase holograms, photoresist holograms can be overcoated with a reflective metallic layer and read out in reflection. Finally it is possible to carry out large scale replication of photoresist holograms through pressing techniques.

Iron oxide holograms are unaffected by the range of environmental testing we carried out; iron oxide is the best material in this respect. Since it forms thin phase holograms with considerable absorption, the diffraction efficiency is relatively low. The exposure and spectral sensitivity are determined by the photoresist in which the holograms are initially recorded. Processing of iron oxide holograms is relatively complicated and requires very careful control; due to the nature of the etching step, the holograms are very sensitive to variations in exposure.

Photoplastic recording material was the most sensitive of the seven materials. It was the only material in addition to 649F to be sensitive to red light. Since the photoconductor is readily modified, photoplastic material has the greatest potential for being sensitized to the near infrared region of the spectrum. In addition, processing is fast, in situ and reversible. Photoplastic materials stand up well against exposure to UV radiation and the effects of humidity. Holograms are unaffected by temperature below the temperature at which cold flow begins. Diffraction efficiency of photoplastic holograms was the lowest of the seven materials.

Figure 76 shows curves of diffraction efficiency as a function of exposure for plane wave gratings recorded in each of the seven materials. These gratings were all recorded at K = 1 at a spatial frequency near 1000 lines/mm. Gratings recorded in dichromated gelatin, photopolymer, thick thermoplastics, and blazed photoresist reached efficiencies of 60% or better. Table 9 gives the peak diffraction efficiency of each material and the exposure required to reach that efficiency.

	Maximum Diffraction Efficiency	Exposure
Bleached 649F	46%	6.7×10^{-4} J/cm^2
Dichromated gelatin	85	3.7×10^{-2}
Photopolymer	83	2.1
Thick Thermoplastics	60	12
Photoresist (blazed)	79 (at 633 nm)	0.2
Iron Oxide	20	0.15
Photoplastics	10	6.0×10^{-5}

TABLE 9. Maximum Diffraction Efficiency and Corresponding Exposure for Plane Wave Gratings Recorded in Each Material.

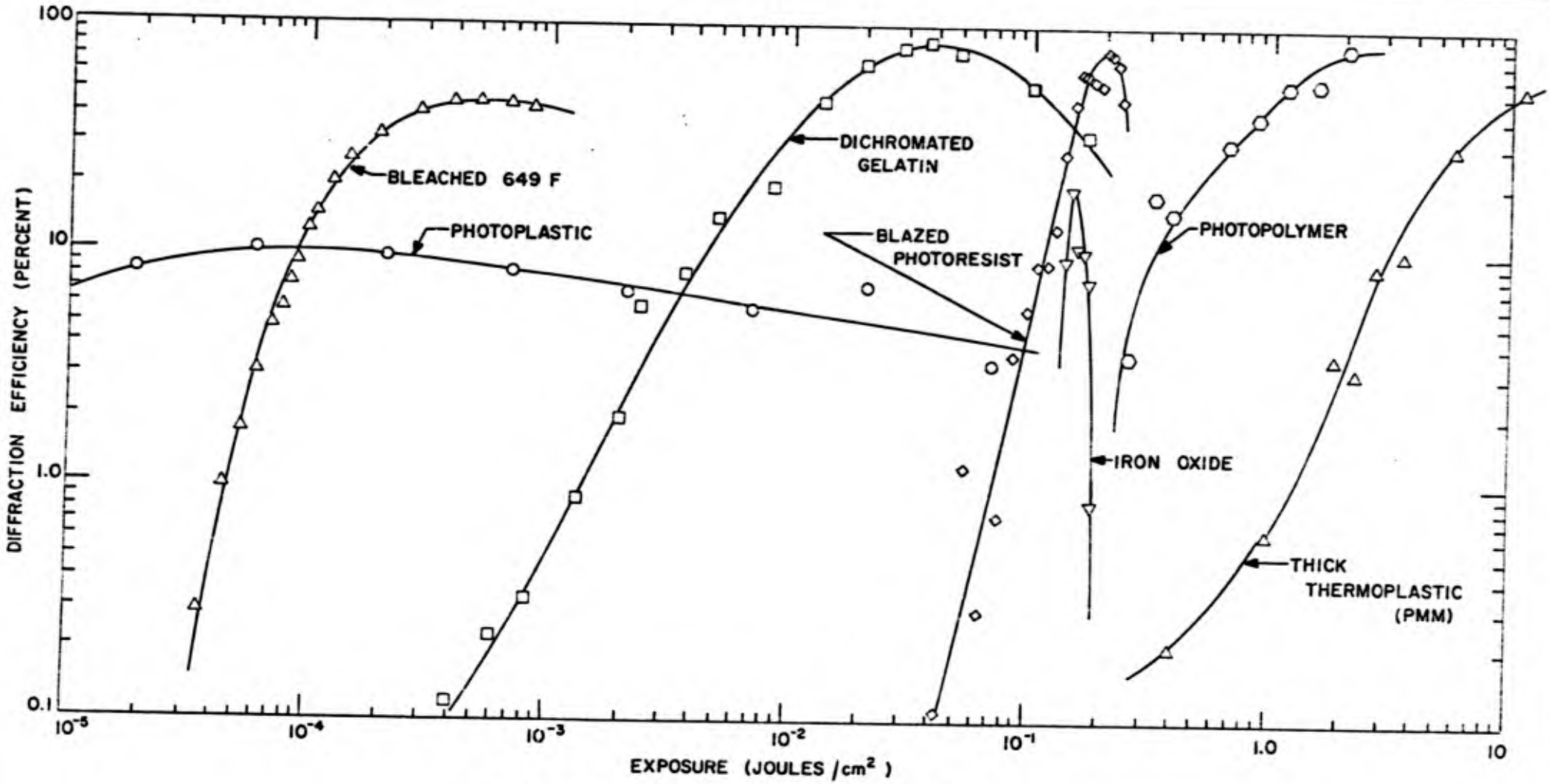

FIGURE 76. Diffraction efficiency as a function of exposure for plane wave gratings recorded in each material at K=1.

With the exception of bleached photographic emulsions and, to some extent photoplastics, the materials were grainless; scattering noise was very low. Most of the noise was due to nonlinearities, both from the phase recording process and from the nonlinear response of the materials themselves. In most cases, the noise due to nonlinearities severely limited the diffraction efficiency that could be reached with good SNR. This is illustrated by Table 10 where we give the peak SNR we measured for each material and the corresponding diffraction efficiency; for comparison we also show the best SNR we measured at a diffraction efficiency of 10%. It should be recalled that these measurements are from holograms recorded with the relatively high information packing density of 10^6 bits/cm^2.

	Max SNR	Diff. Eff.	Max SNR at 10% Eff.
Bleached 649F	2? dB	1.0%	18 dB
Dichromated Gelatin	27	1.0	23
Photopolymer	28	1.4	24
Thick Thermoplastics	19	0.5	17
Photoresist	24	0.33	16
Iron Oxide	11	2.5	-
Photoplastic	17	1.5	-

Table 10. Maximum SNR with corresponding diffraction efficiency and maximum SNR at 10% diffraction efficiency for each material.

Figure 77 shows representative curves of SNR as a function of exposure for holograms recorded in each of the seven materials.

For comparison, the maximum SNR we measured for unbleached 649F holograms was 25 dB with a diffraction efficiency of 1.0%. This was the SNR of a hologram recorded at 633 nm with K = 4. The maximum efficiency, however was only 2.3% (for a hologram recorded on High Resolution plates at 488 nm).

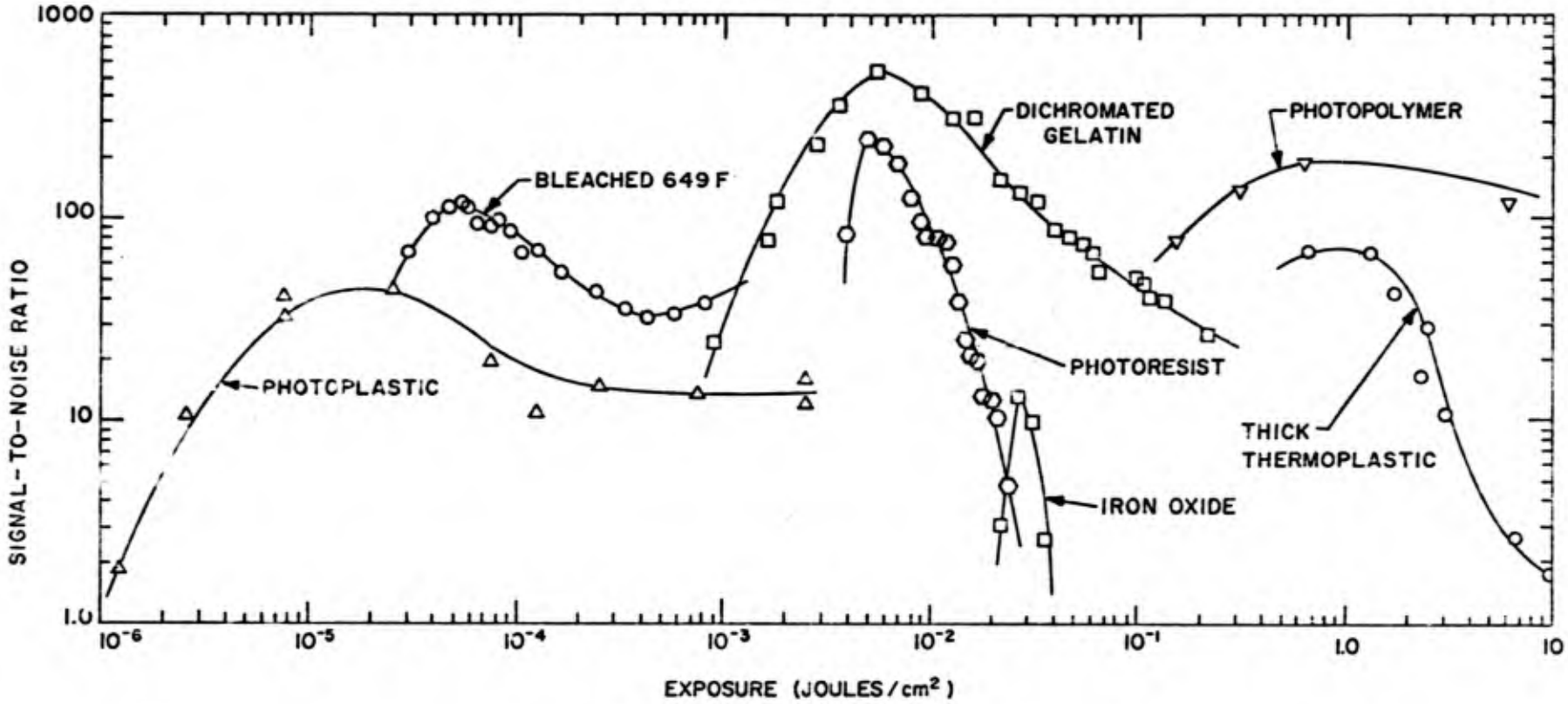

FIGURE 77. Signal-to-noise ratio as a function of exposure for each of the seven materials.

The spectral sensitivity of most of the materials we tested was restricted to the UV and blue-green regions of the spectrum. In general these materials are more sensitive to UV radiation and are rapidly decreasing in sensitivity with increasing wavelength in the blue-green region of the visible spectrum. Only photographic emulsions and photoplastics are sensitive to light throughout the visible spectrum. None of the materials we tested showed any sensitivity to near infrared radiation at 1150 nm. The development of materials sensitive to the near infrared will be the subject of a continuing effort, which will concentrate initially on finding an infrared sensitive photoconductor for photoplastics, synthesizing a new photodegradable material which is sensitive to infrared radiation, and investigating experimental photographic emulsions.

All of the materials were of good optical quality. In general the optical quality is a function of the care and technique followed in preparing the material in its final form, whether it be dipping, coating, or casting. With proper care and technique, we were able to prepare samples of all of the materials with good uniformity and flatness and low distortion. The most difficult samples to prepare were the thick castings of thermoplastic; we obtained high quality castings with the technique outlined in Section 3.4.2.

The transmission of the materials varied. Dichromated gelatin and photopolymer (without the blue-green sensitizing dye) had very high transmission throughout the visible spectrum and at 1150 nm. The remaining materials showed relatively strong absorption of blue and green light so that the transmission increased throughout the visible spectrum, with about the same transmission at 1150 nm as at 647 nm.

Most of the materials were affected by high relative humidity or by the combination of high humidity and high temperature. Only iron oxide was completely unaffected by any combination of temperature and humidity throughout the range of test conditions. Holograms recorded in gelatin based materials are seriously affected by high humidity; dichromated gelatin holograms are essentially destroyed by high humidity, although they can be restored by reprocessing. The sensitivity of dichromated gelatin holograms to humidity is so great that they can only be considered practical with a protective cover plate. Indeed, with a glass plate cemented to the gelatin, they are unaffected by temperature and humidity. Photoplastic holograms were affected only because the thermoplastic we used tends to cold flow at 140°F; with the proper thermoplastic they would also be unaffected throughout the temperature-humidity range. Thick thermoplastics are affected by the combination of high temperature and humidity; in certain cases these cause distortions of the thermoplastic itself, such as shrinkage, or lifting off the substrate. High humidity causes fine cracks to develop in photoresist holograms, seriously affecting the SNR.

We simulated exposure to direct sunlight with a 100 watt UV lamp. Four materials, dichromated gelatin, thick thermoplastics, iron oxide, and photoplastics showed no ill effects due to the UV exposure. Holograms recorded in bleached photographic emulsions and photoresist are darkened by long exposure to the UV radiation; the diffraction efficiency of photopolymer holograms decreases after long UV exposure.

Table 11 summarizes the environmental stability of the seven materials. In Table 12 we give the nondestructive readout intensity limits for laser illumination at 488 nm. These figures were selected by extrapolating to 60 seconds the curves of destructive readout intensity as a function of readout duration, and, taking one half the destructive intensity to give the nondestructive intensity.

	Temperature	Humidity	UV Exposure
Bleached 649F	Degrades at high temperature and humidity		Darkens holograms
Dichromated Gelatin	Complete degradation (no effect with glass cover plate)		No effect
Photopolymer	Degrades at high temperature and humidity		Degrades with long exposure
Thick Thermoplastic	Material distorts at high temperature and humidity		No effect
Photoresist	No effect	Causes fine Cracks	Darkens holograms
Iron Oxide	No effect	No effect	No effect
Photoplastic	Holograms erased at 140°F	No effect	No effect

TABLE 11. Effects of temperature, humidity, and UV exposure on each material.

	Nondestructive Readout Intensity Limit
Bleached 649F	18 watts/cm^2
Dichromated Gelatin	1300
Photopolymer	1000
Thick Thermoplastics	1.5
Photoresist	1700
Iron Oxide	390
Photoplastic	6 (melts thermoplastic) 50 (destroys material)

TABLE 12. Nondestructive laser readout intensity for each material.

SECTION V
CONCLUSIONS

In this materials study, we have concentrated our efforts on developing recording materials that are well suited for holographic optical elements. In particular we investigated the environmental stability of the materials as well as the holographic parameters, in order to evaluate their potential for certain field applications.

As we stated in the previous section, none of the materials is outstanding in all respects. Probably the most attractive material is dichromated gelatin, because of its high diffraction efficiency and SNR, its moderate exposure sensitivity, and with a cover plate, its good environmental stability. Furthermore, its high transmission combined with high efficiency makes it attractive for use in a multiple element system. Its major disadvantage appears to be that its spectral sensitivity is limited to short wavelengths. Photopolymer holograms are similar in some respects to dichromated gelatin holograms, but further work is necessary to improve the environmental stability of photopolymer before it will be suitable for field applications. Holograms can be recorded in very thick layers of photopolymer, however, which is an advantage in those applications where greater angular orientation sensitivity or wavelength discrimination are necessary. Similar conclusions can be taken about thick thermoplastics, for which further work is also necessary to improve their environmental stability and perhaps their nondestructive readout limits.

For applications where sensitivity to red light is important, one must choose between bleached photographic emulsions and photoplastic materials. The bleached emulsions are limited somewhat by absorption and scattering losses, and, even if protected from the effects of humidity by a cover plate, they tend to darken when exposed to light

of short wavelengths. Until this last problem is overcome, the application of bleached photographic emulsions will always be limited. Photoplastic holograms have good environmental stability except at the highest temperatures although they are limited in diffraction efficiency. Their transmission tends to be relatively low at short wavelengths, but it can be increased by reducing the sensitizer concentration in the photoconductor.

The diffraction efficiency of blazed photoresist can be very high. Overcoating techniques can also be used to obtain high efficiencies with photoresist. Since it has fair environmental integrity, photoresist might be useful for certain applications. Further investigation is necessary, however, into the cause of the fine cracks that form in photoresist holograms at high humidity. Although their environmental stability is excellent, iron oxide holograms are limited to relatively low diffraction efficiency and transmission. Nevertheless, they may be useful in applications where the environmental extremes are greater than those we investigated.

REFERENCES

1. W. Kock, "Three-Color Hologram Zone Plates," Proc. IEEE, 54, 1610 (1966).

2. E. N. Leith and J. Upatnieks, "Zone Plate with Aberration Correction," J. Opt. Soc. Am. 57, 699 (1967).

3. E. B. Champagne, Ph.D. Dissertation, Ohio State University, 1967.

4. J. N. Latta, "Computer-Based Analysis of Hologram Imagery and Aberrations. 1: Hologram Types and Their Nonchromatic Aberrations," Appl. Opt., 10, 599 (1971).

5. H. W. Rose, "Holographic Lens Systems," J. Opt. Soc. Am., 61, 667A, (1971).

6. R. H. Katyl, "Part 1: Broadband Holographic Reconstruction," Appl. Opt., 11, 1241 (1972).

7. M. Chang and N. George, "Holographic Dielectric Grating: Theory and Practice," Appl. Opt., 9, 713 (1970).

8. Kodak Plates and Films for Science and Industry, First Ed., (Eastman Kodak Company, 1967), p. 23d.

9. J. Upatnieks and C. Leonard, "Efficiency and Image Contrast of Dielectric Holograms," J. Opt. Soc. Am., 60, 297 (1970).

10. A. Vander Lugt and R. H. Mitchel, "Technique for Measuring Modulation Transfer Functions of Recording Media," J. Opt. Soc. Am., 57, 372 (1967).

11. H. Kogelnik, in Proceedings of Symposium on Modern Optics, J. Fox, Ed., (Polytechnic Press, Brooklyn, N.Y., 1967), pp. 605-617.

12. A. J. Chenoweth, "Humidity Testing of Bleached Holograms," Appl. Opt., 10, 913 (1971).

13. R. K. Curran and T. A. Shankoff, "The Mechanism of Hologram Formation in Dichromated Gelatin," Appl. Opt., 9, 1651 (1970).

14. M. S. Chang, "Dichromated Gelatin of Improved Optical Quality," Appl. Opt., 10, 2550 (1971).

15. L. H. Lin, "Hologram Formation in Hardened Dichromated Gelatin Films," Appl. Opt. 8, 963 (1969).

16. D. H. Close, A. D. Jacobson, J. D. Margerum, R. G. Brault, and F. J. McClung, "Hologram Recording on Photopolymer Materials," Appl. Phys. Letters, 14, 159 (1969).

17. J. A. Jenney, "Holographic Recording with Photopolymer," J. Opt. Soc. Am., 60, 1155 (1970).

18. R. H. Wopschall, "Dry Photopolymer Film for Recording Holograms," J. Opt. Soc. Am., 61, 649A (1971).

19. W. S. Colburn and K. A. Haines, "Volume Hologram Formation in Photopolymer Materials," Appl. Opt., 10, 1636 (1971).

20. F. P. Laming, "Holographic Grating Formation in Photopolymers-Poly (Methyl-methacrylate)," Society of Plastic Engineers Technical Meeting, October, 1970.

21. V. J. Vanhuyse, Nature, 191, 595 (1961).

22. W. J. Tomlinson, I. P. Kaminow, E. A. Chandross, R. L. Fork and T. Silvast, "Photoinduced Refractive Index Increase in Poly (Methyl Methacrylate) and its Applications," Appl. Phys. Lett., 16, 486 (1970).

23. N. K. Sheridan, "Production of Blazed Holograms," Appl. Phys. Lett. 12, 316, (1968).

24. R. Bartolini, W. Hannan, D. Karlsons, and M. Lurie, "Embossed Hologram Motion Pictures for Television Playback," Appl. Opt. 9, 2283 (1970).

25. R. A. Bartolini, "Improved Development for Holograms Recorded in Photoresist," Appl. Opt. 11, 1275 (1972).

26. M. J. Beesley and J. G. Castledine, "The Use of Photoresist as a Holographic Recording Medium," Appl. Opt., 9, 2?20 (1970).

27. R. A. Bartolini, "Recording of Relief-Phase Holograms in Photoresist," J. Opt. Soc. Am., 62 1397A (1972).

28. W. R. Sinclair, M. V. Sullivan, and R. A. Fastnacht, "DC Sputtered Films," J. Electrochem. Soc. 118, 341 (1971).

29. J. C. Urbach and R. W. Meier, "Thermoplastic Xerographic Holography," Appl. Opt. 5, 666 (1966).

30. L. H. Lin and M. L. Beauchamp, "Write-Read-Erase in Situ Optical Memory Using Thermoplastic Holograms", Appl. Opt., 9, 2088 (1970).

31. A. A. Friesem and E. N. Tompkins, "Photoplastic Recording Materials in Holographic Memories," Conf. on Holography and Optical Filtering, Huntsville, Ala., May 1971.

32. T. L. Credelle and F. W. Spong, "Thermoplastic Media for Holographic Recording," RCA Review, 33, 206 (1972).